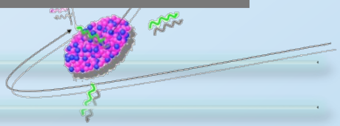

Heavy Ion Reactions

Collisions at the Coulomb barrier

Dieter Ackermann

Grand Accélérateur National d'Ion Lourdes – GANIL, Caen, France

Pisa, 25th July 2017

Heavy Ion Reaction

collisions at the Coulomb barrier

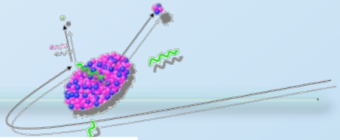

OUTLINE

- Introduction
  – competing channels in heavy ion collisions around the Coulomb barrier

- The nuclear potential

- Tunneling through a potential well

- Compound nucleus formation and de-excitation (statistical model)

- The concept of the distribution of barriers
  - Inelastic excitations of nuclear degrees of freedom
  - Deformation
  - Fusion-fission competition
  - Experimental access to the barrier distribution – alternative methods
  - Theoretical description – the coupled channels approach

- Applications
  - The synthesis of the heaviest elements
  - Stellar nucleo-synthesis

elastic scattering

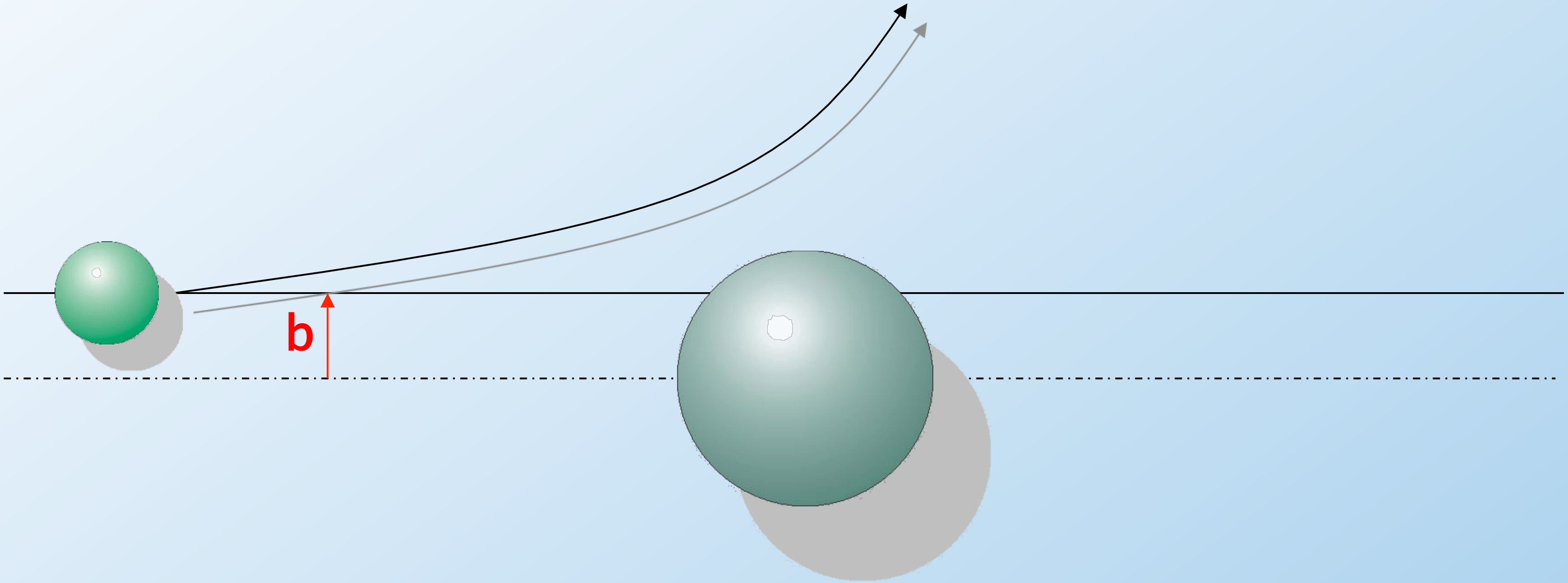

Heavy Ion Reactions @ the Coulomb Barrier

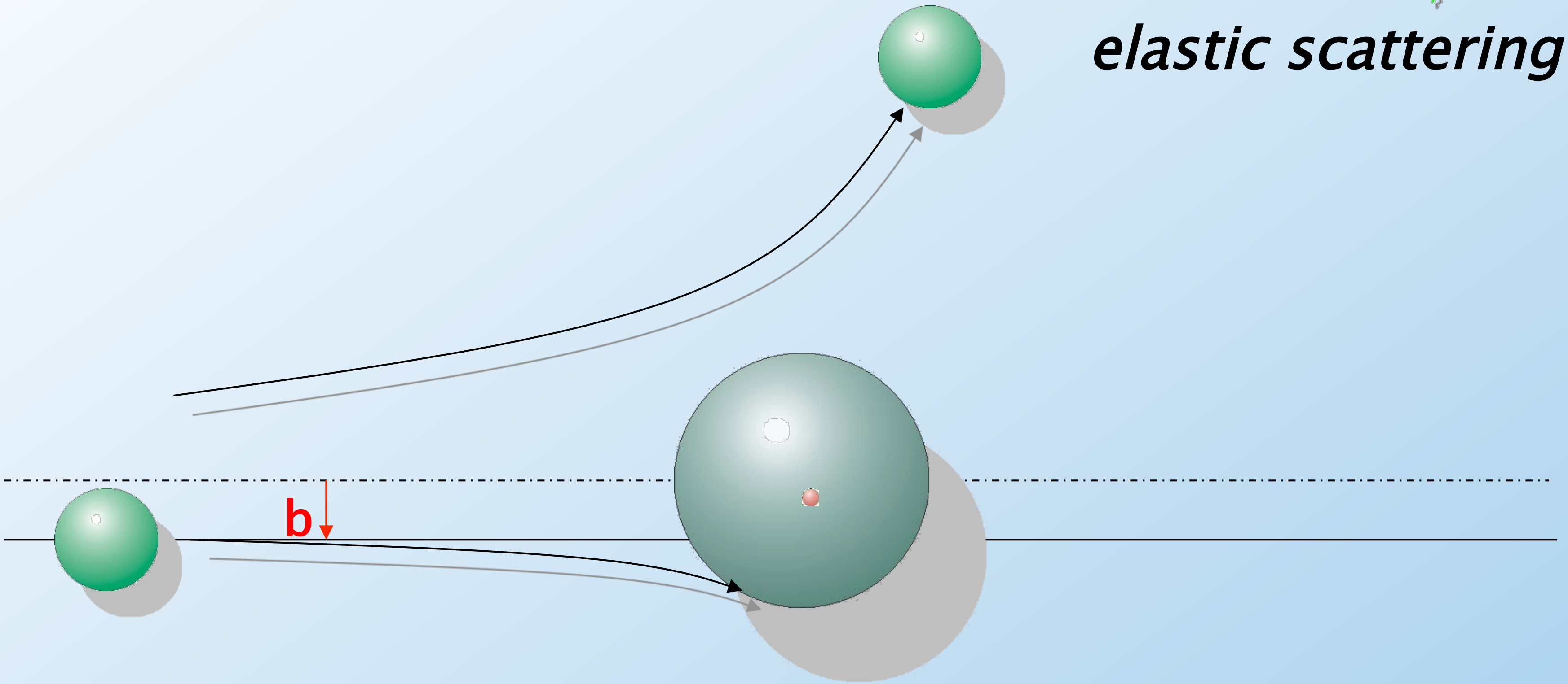

elastic scattering

Heavy Ion Reactions @ the Coulomb Barrier

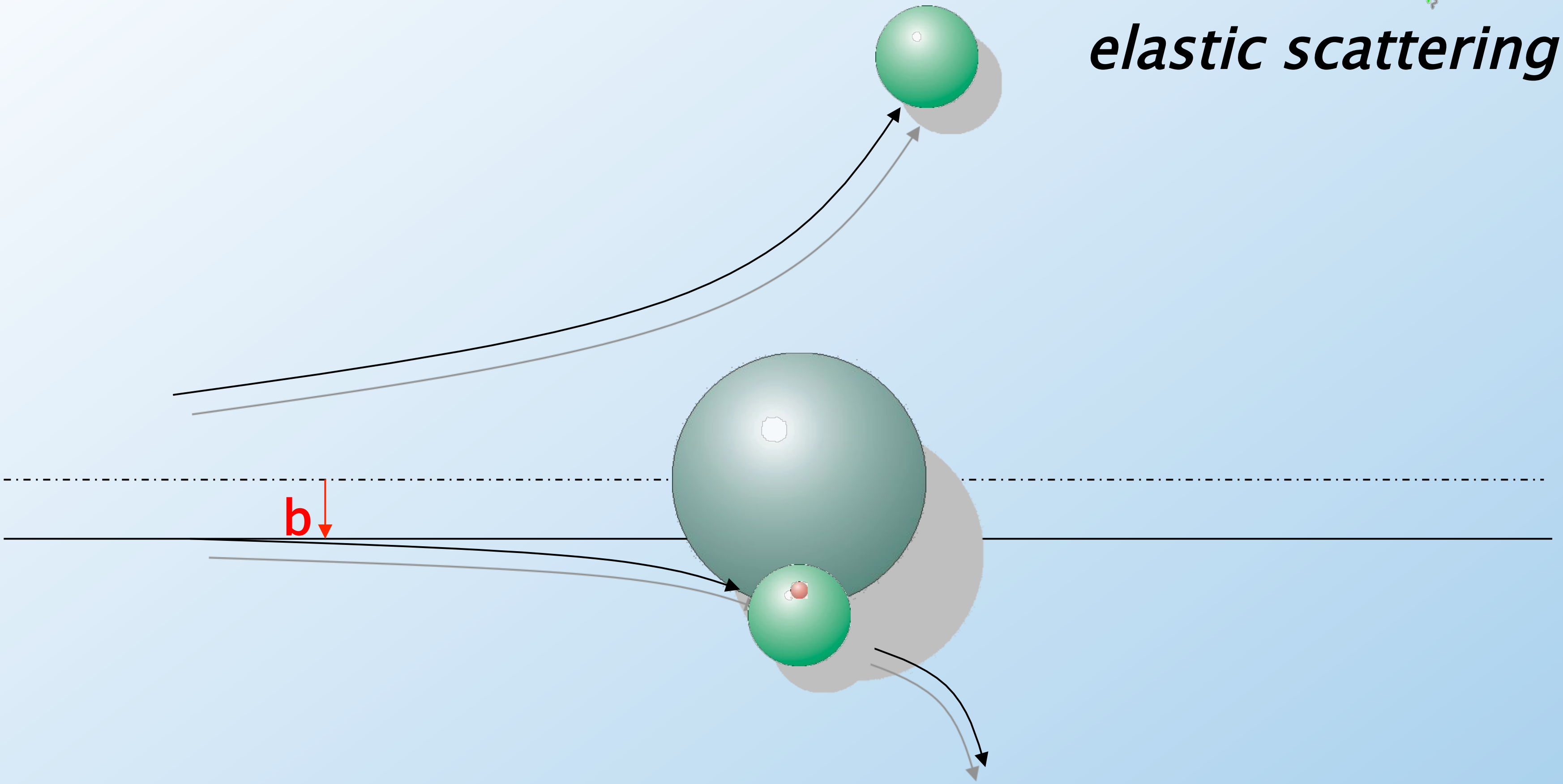

elastic scattering

nucleon transfer

Heavy Ion Reactions @ the Coulomb Barrier

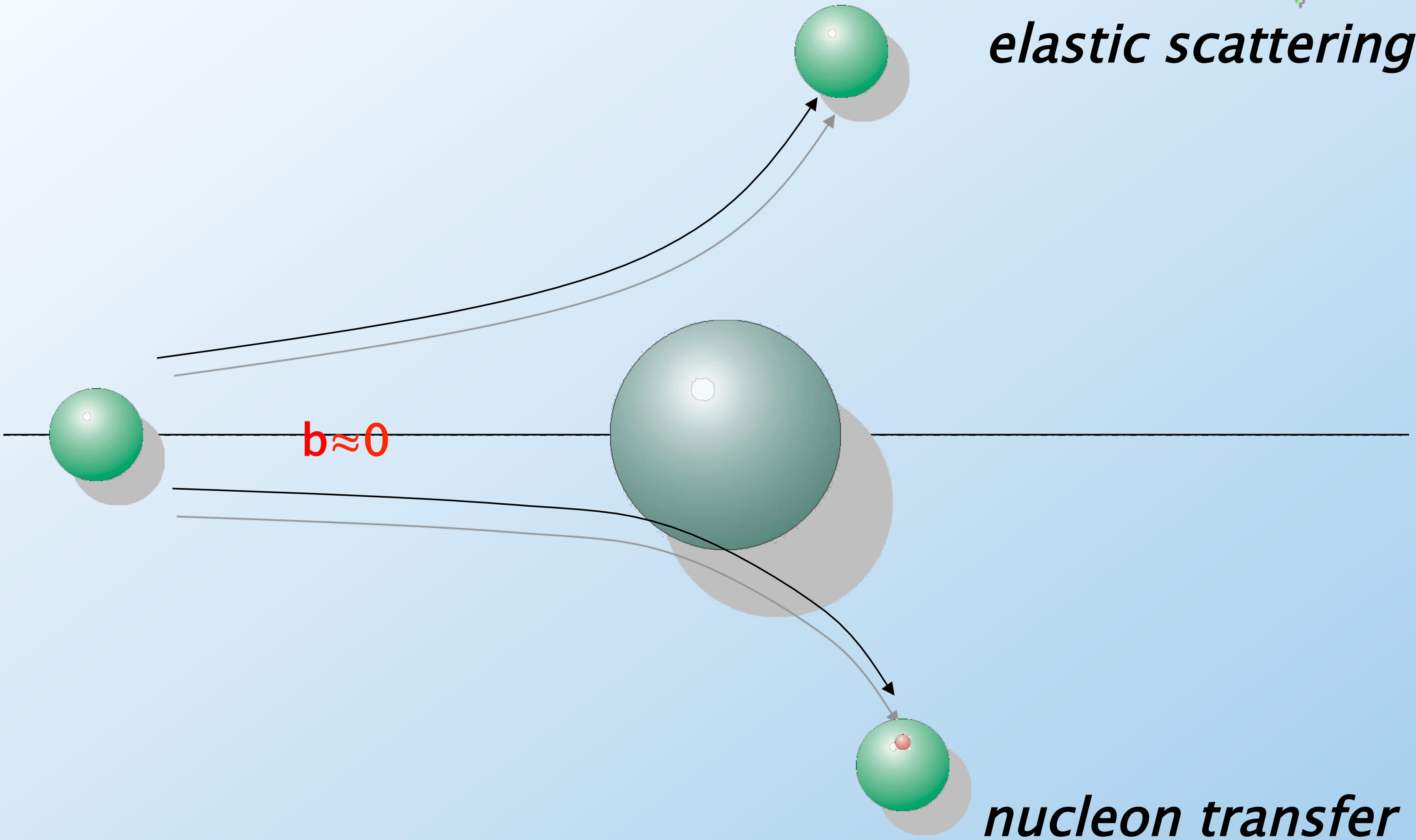

Heavy Ion Reactions @ the Coulomb Barrier

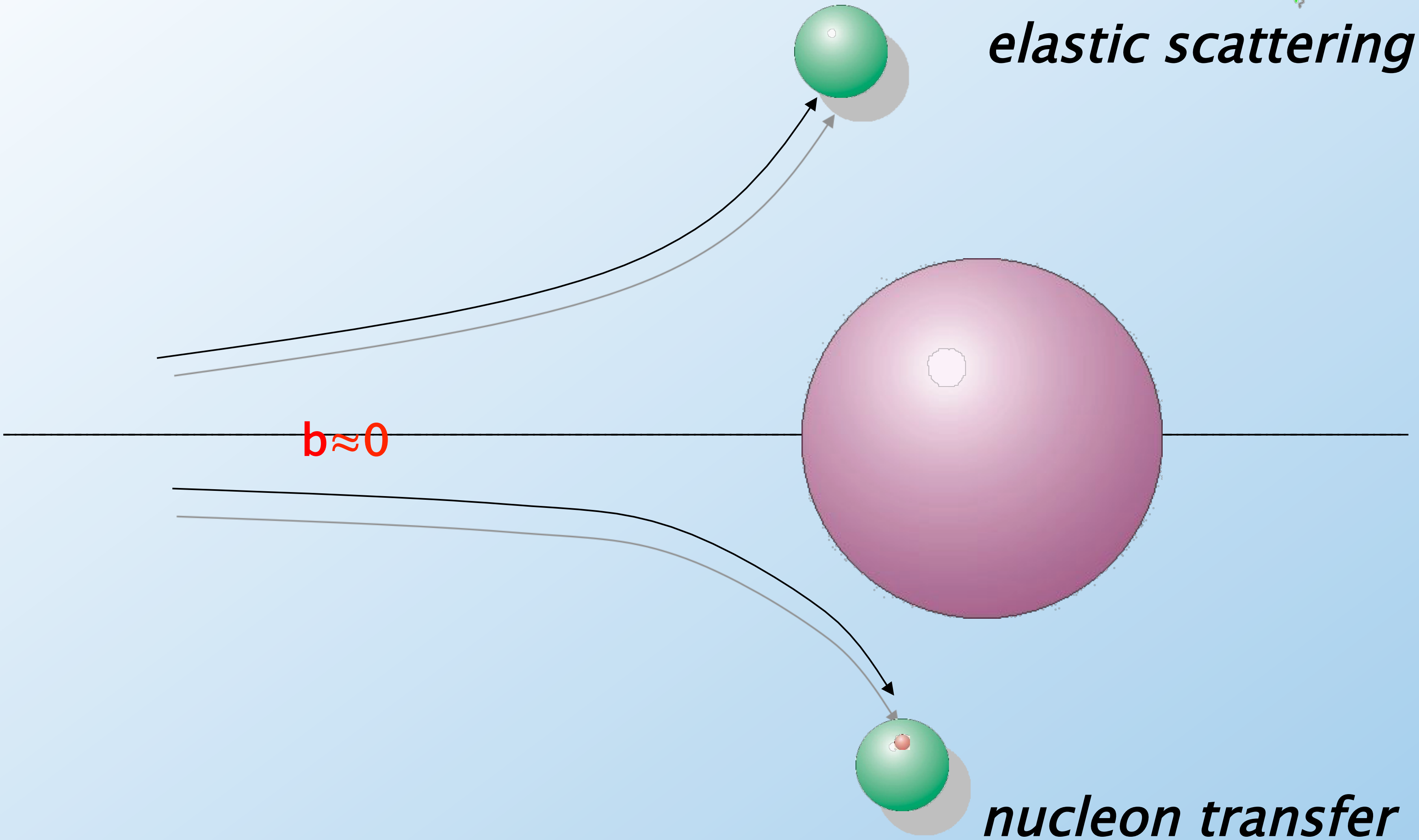

Heavy Ion Reactions @ the Coulomb Barrier

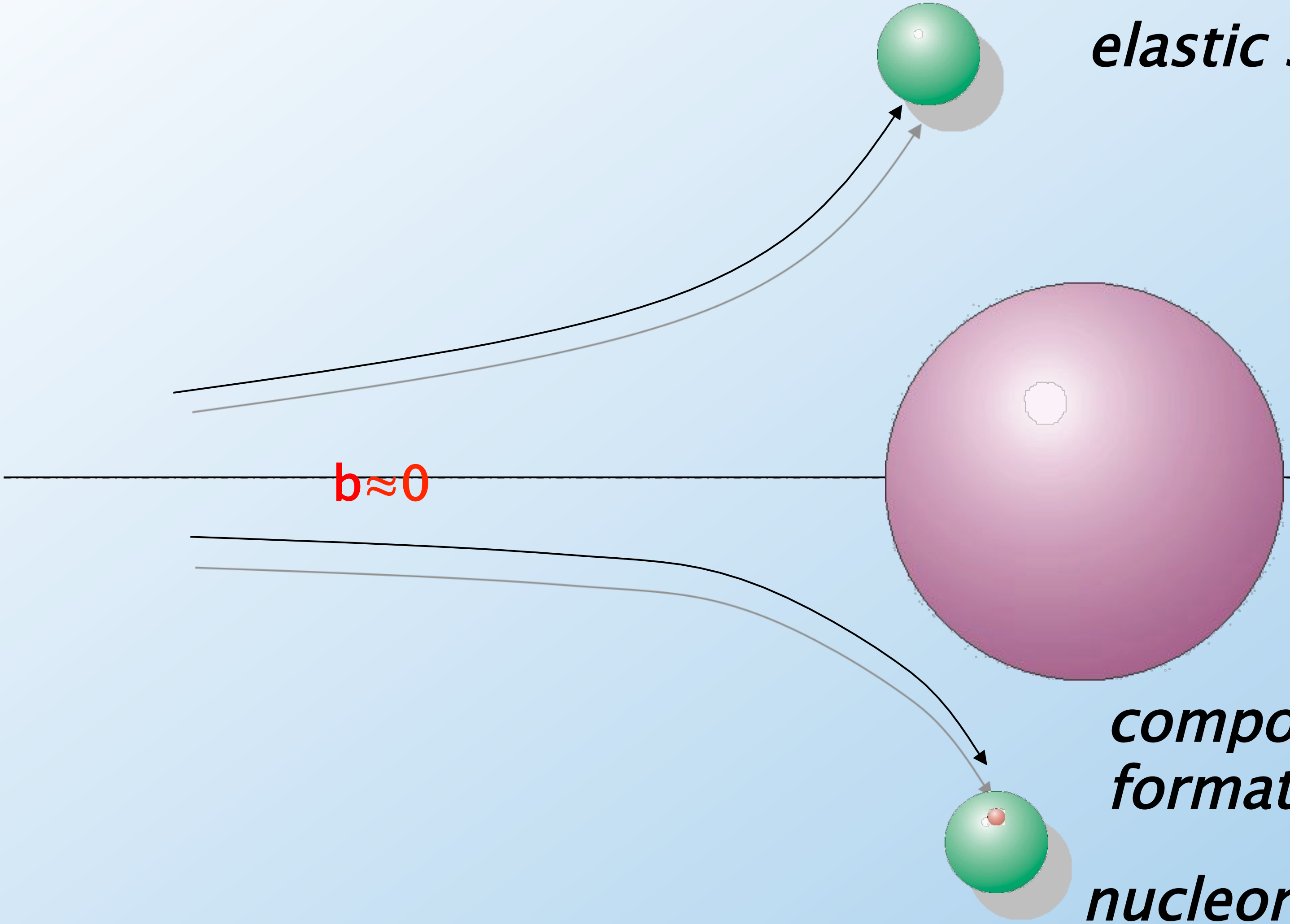

elastic scattering

compound nucleus formation

nucleon transfer

The Nuclear Potential

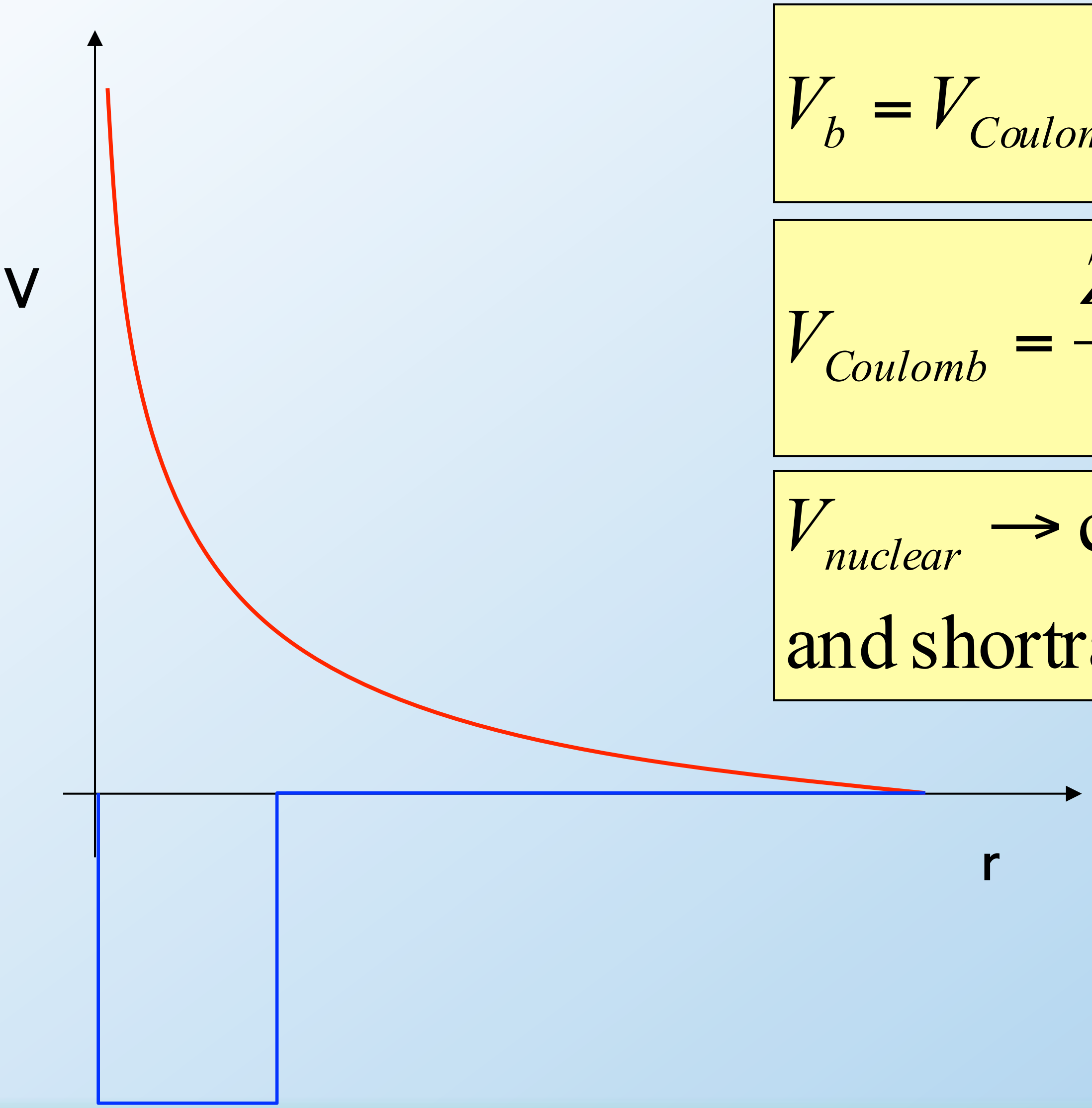

$$V_b = V_{Coulomb} \propto \frac{1}{r} + V_{nuclear} + V_{rotational}$$

$$V_{Coulomb} = \frac{Z_p Z_t e^2}{R_b} \propto \frac{1}{r}$$

$V_{nuclear}$ → constant, attractive and shortrange → rectangular

The Nuclear Potential

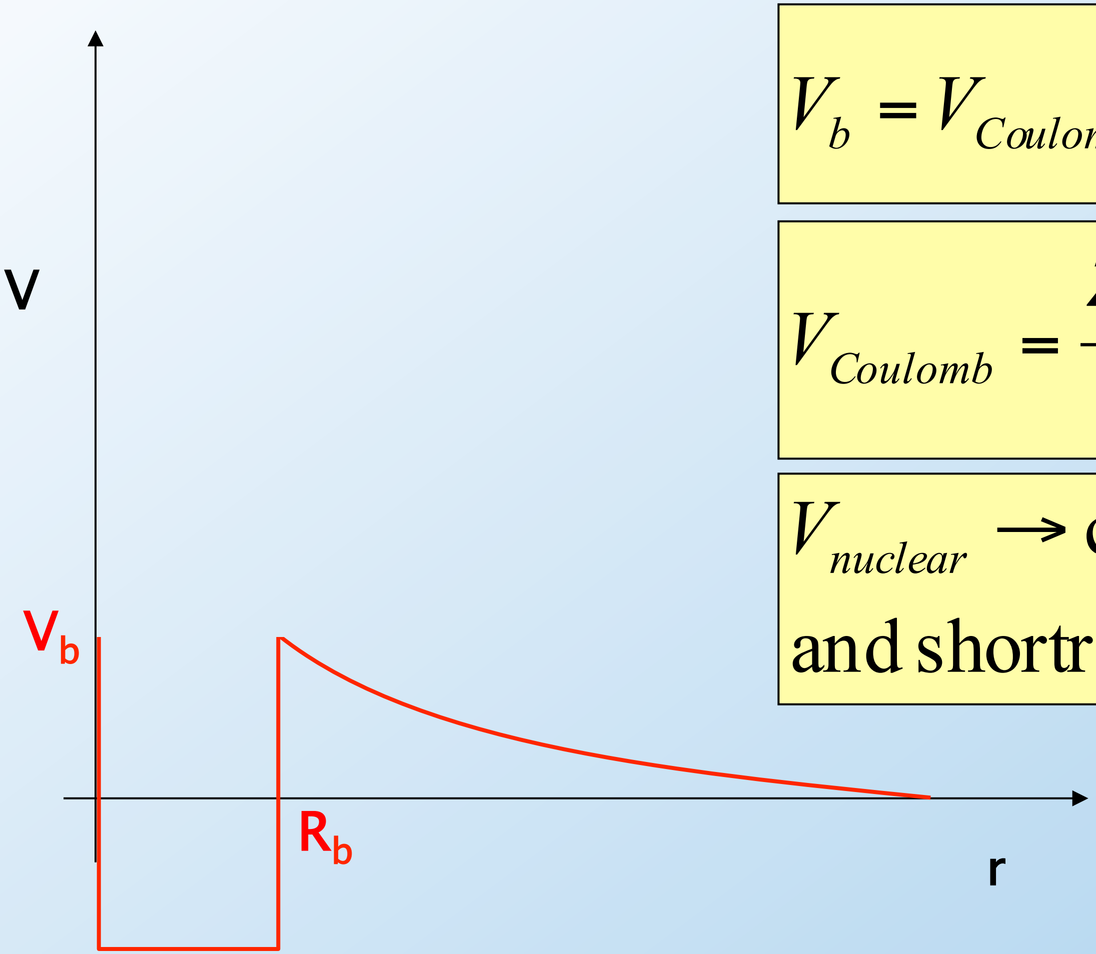

$$V_b = V_{Coulomb} \propto \frac{1}{r} + V_{nuclear} + V_{rotational}$$

$$V_{Coulomb} = \frac{Z_p Z_t e^2}{R_b} \propto \frac{1}{r}$$

$V_{nuclear}$ → constant, attractive and shortrange → rectangular

The „tunnel“ effect

– a fondamental concept of quantum mechanics

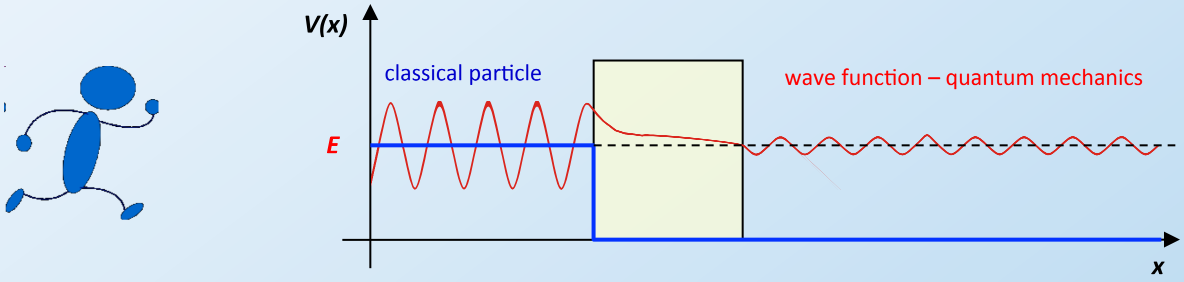

Tunneling across a one-dimensional barrier

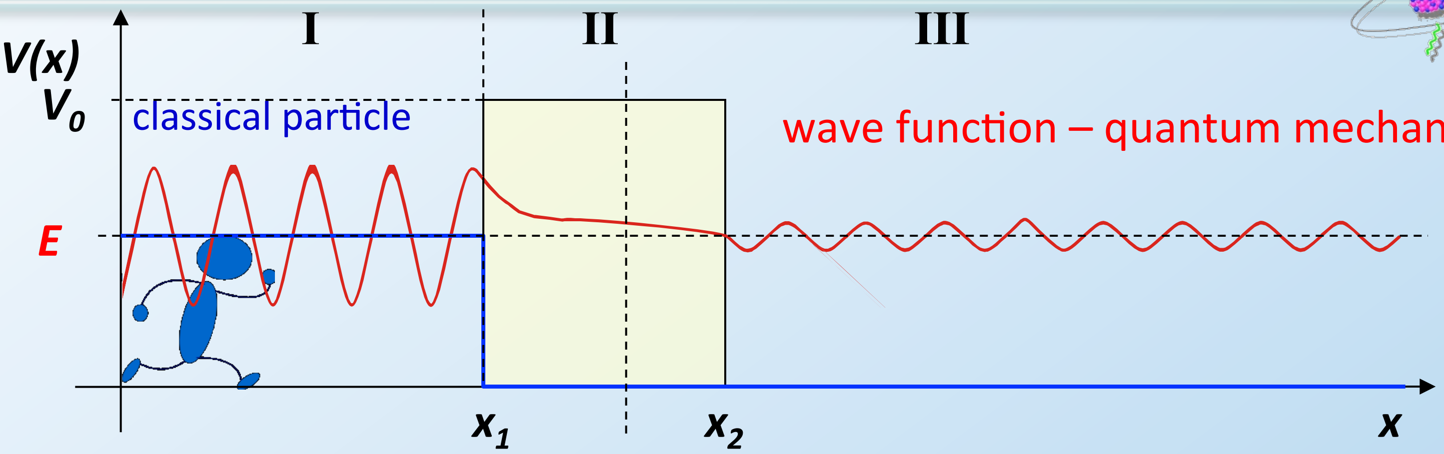

- Schrödinger equation
  - stationary
  - one-dimensional

$$\boxed{-\frac{\hbar^2}{2m}\Delta\varphi(x)+\boldsymbol{V}(x)\varphi(x)=\boldsymbol{E}\varphi(x)}$$

incoming ave before the barrier

$$\boxed{\mathrm{I}:\quad \varphi(x)=Ae^{ikx}+Be^{-ikx};\qquad k=\sqrt{\frac{2m}{\hbar^2}E}}$$

in the barrier region

$$\boxed{\mathrm{II}:\quad \varphi(x)=Ce^{-ilx}+De^{ilx};\qquad l=\sqrt{\frac{2\mathrm{m}}{\hbar^2}(V-E)}}$$

out coming wave after the barrier

$$\boxed{\mathrm{III}:\quad \varphi(x)=A'e^{ikx}\ \rightarrow\ \text{no reflection}}$$

Tunneling across a one-dimensional barrier

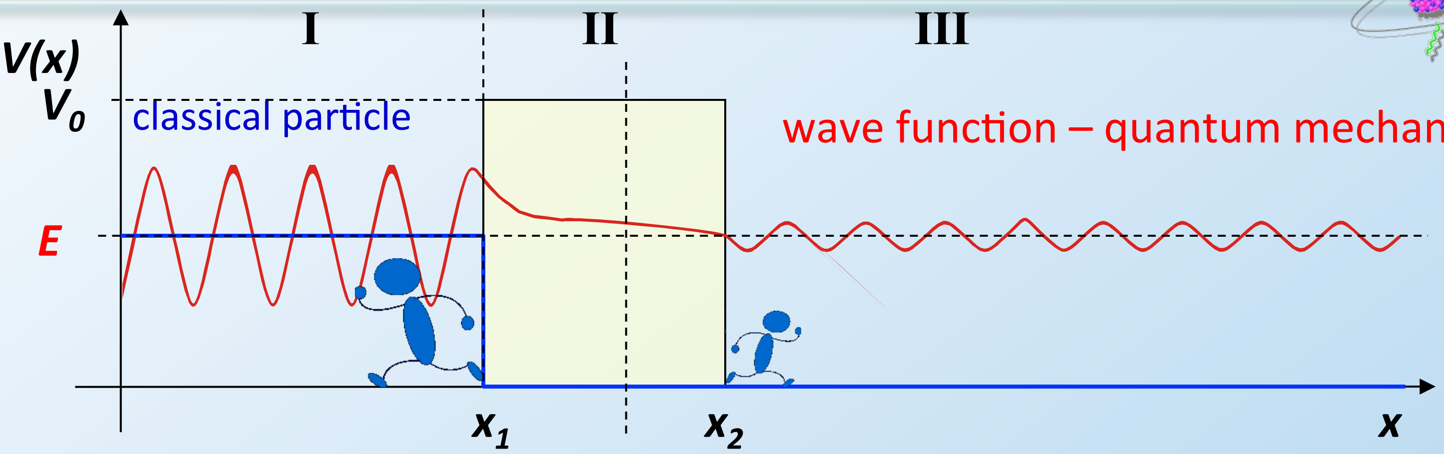

- Schrödinger equation
  - stationary
  - one-dimensional

$$-\frac{\hbar^2}{2m}\Delta\varphi(x)+\boldsymbol{V}(x)\varphi(x)=\boldsymbol{E}\varphi(x)$$

incoming ave before the barrier

$$\mathrm{I}:\quad \varphi(x)=Ae^{ikx}+Be^{-ikx};\qquad k=\sqrt{\frac{2m}{\hbar^2}E}$$

in the barrier region

$$\mathrm{II}:\quad \varphi(x)=Ce^{-ilx}+De^{ilx};\qquad l=\sqrt{\frac{2\mathrm{m}}{\hbar^2}(V-E)}$$

out coming wave after the barrier

$$\mathrm{III}:\quad \varphi(x)=A'e^{ikx}\quad\rightarrow\ \text{no reflection}$$

Tunneling across a one-dimensional barrier

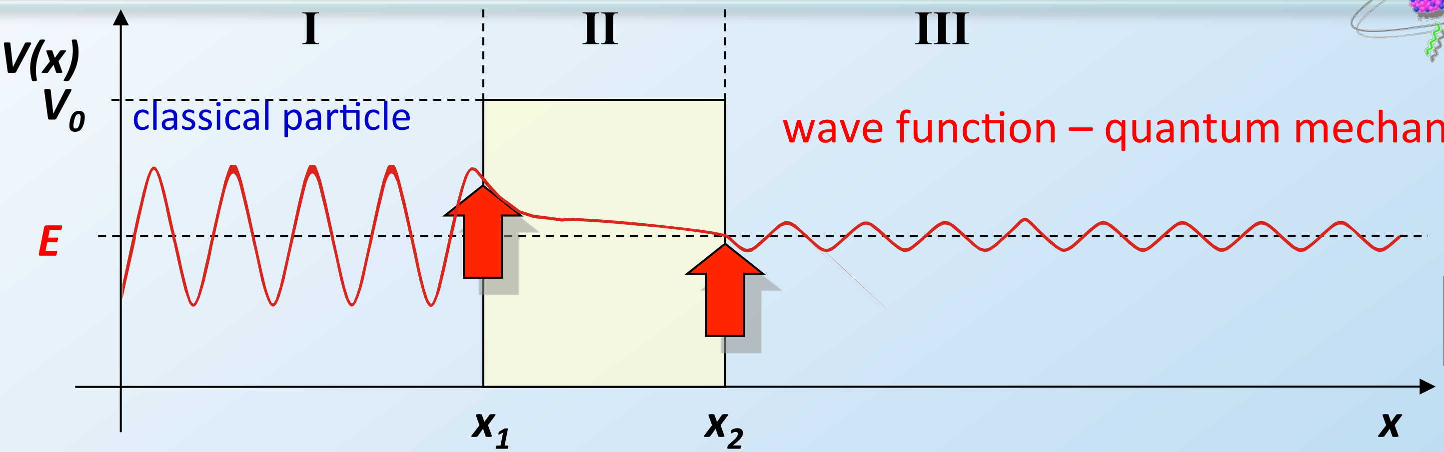

$$k = \sqrt{\frac{2m}{\hbar^2}E}$$

$$l = \sqrt{\frac{2\mathrm{m}}{\hbar^2}(V - E)}$$

$\mathrm{I}: \quad \varphi(x) = Ae^{ikx} + Be^{-ikx}$

$\varphi(x) = Ce^{ilx} + De^{-ilx}$

$\varphi(x) = A'e^{ikx}$

border conditions: continuous connection

- **I → II**

$$1. \quad \varphi_{\mathrm{I}}(x_1) = \varphi_{II}(x_1)$$

$$2. \quad \frac{d\varphi_{\mathrm{I}}(x_1)}{dx} = \frac{\varphi_{II}(x_1)}{dx}$$

- **II → III**

$$3. \quad \varphi_{\mathrm{II}}(x_2) = \varphi_{III}(x_2)$$

$$4. \quad \frac{d\varphi_{\mathrm{II}}(x_2)}{dx} = \frac{\varphi_{III}(x_2)}{dx}$$

Tunneling across a one-dimensional barrier

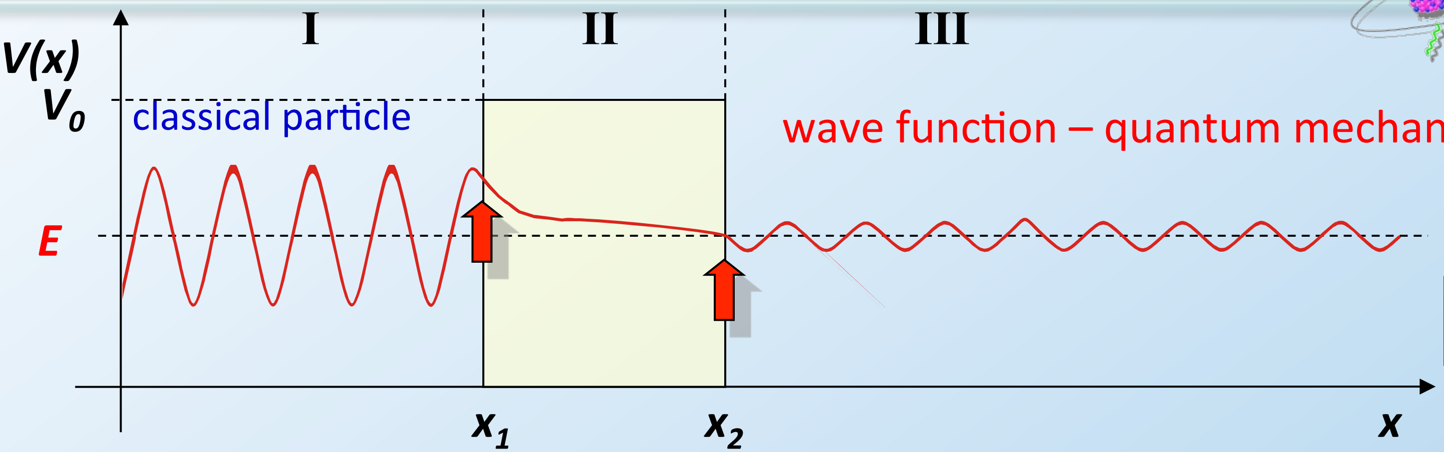

$$k = \sqrt{\frac{2m}{\hbar^2}E}$$

$$l = \sqrt{\frac{2\mathrm{m}}{\hbar^2}(V-E)}$$

$$\mathrm{I:}\quad \varphi(x) = Ae^{ikx} + Be^{-ikx}$$

$$\varphi(x) = Ce^{ilx} + De^{-ilx}$$

$$\varphi(x) = A'e^{ikx}$$

solution of the system of equations

$$1.\ A(x_1) + B(x_1) = C(x_1) + D(x_1)$$

$$2.\ ikA - ikB = -ilC + ilD$$

$$3.\ C(x_2)e^{-il(x_2-x_1)} + D(x_2)e^{il(x_2-x_1)} = A'e^{ik(x_2-x_1)}$$

$$4.\ -lCe^{-l(x_2-x_1)} + lDe^{l(x_2-x_1)} = ikA'e^{-k(x_2-x_1)}$$

con :

$$\cosh x = \frac{e^x + e^{-x}}{2}$$

$$\sinh x = \frac{e^x - e^{-x}}{2}$$

$$\Rightarrow A'e^{k(x_2-x_1)} = \left[\cosh l(x_2-x_1) + i\frac{k}{l}\sinh l(x_2-x_1)\right]A + \left[\cosh l(x_2-x_1) + i\frac{k}{l}\sinh l(x_2-x_1)\right]B$$

$$\Rightarrow i\frac{k}{l}A'e^{k(x_2-x_1)} = \left[\sinh l(x_2-x_1) + i\frac{k}{l}\cosh l(x_2-x_1)\right]A + \left[\sinh l(x_2-x_1) + i\frac{k}{l}\cosh l(x_2-x_1)\right]B$$

Tunneling across a one-dimensional barrier

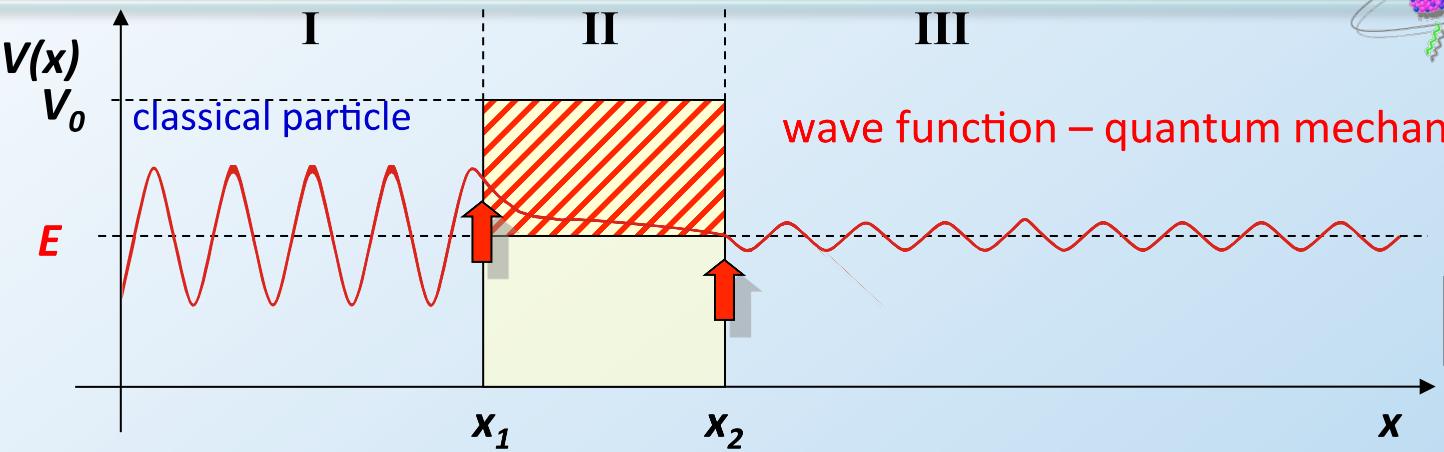

$$k=\sqrt{\frac{2m}{\hbar^2}E}$$

$$l=\sqrt{\frac{2\mathrm{m}}{\hbar^2}(V-E)}$$

$$\mathrm{I}:\quad \varphi(x)=Ae^{ikx}+Be^{-ikx}$$

$$\varphi(x)=Ce^{ilx}+De^{-ilx}$$

$$\varphi(x)=A'e^{ikx}$$

transmission and transmission probability

$$\tau=\frac{A'}{A}\quad\rightarrow\quad T=\left|\tau^2\right|$$

$$T\approx e^{-\frac{2(x_2-x_1)}{\hbar}\sqrt{2m(V_0-E)}}$$

→transmission probability depends on barrier hight and width

→ area x_2-x_1 ·V_0-E

Tunnel effect – example: α-decay
- the nuclear potential

α-Zerfall:
emission of a
α-particle (=2p+2n)

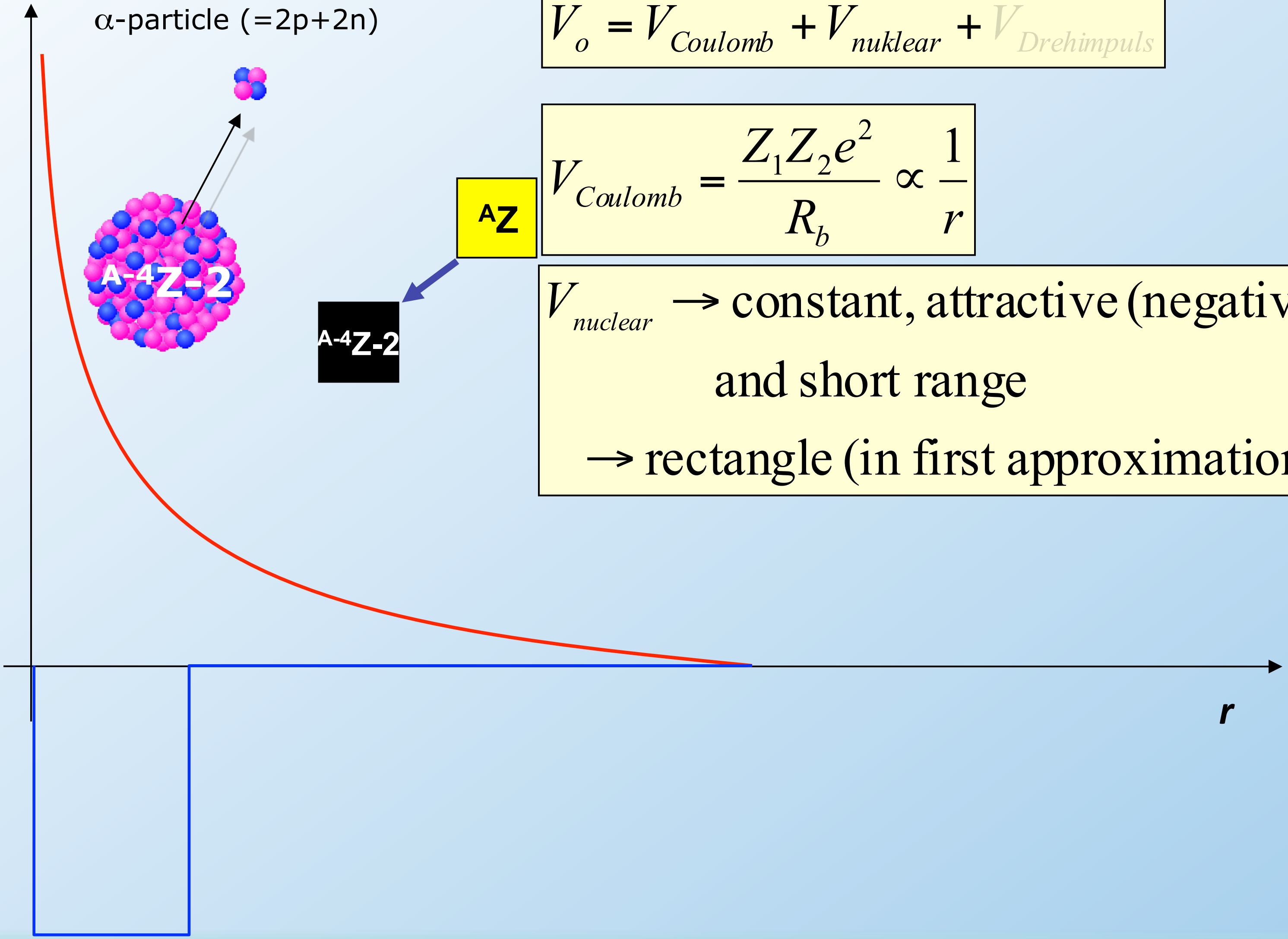

$$V_o = V_{Coulomb} + V_{nuklear} + V_{Drehimpuls}$$

$$V_{Coulomb} = \frac{Z_1 Z_2 e^2}{R_b} \propto \frac{1}{r}$$

$V_{nuclear}$ → constant, attractive (negative) and short range

→ rectangle (in first approximation)

Tunnel effect – example: α-decay
- the nuclear potential

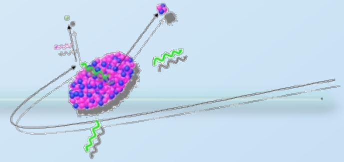

α-Zerfall:
emission of a
α-particle (=2p+2n)

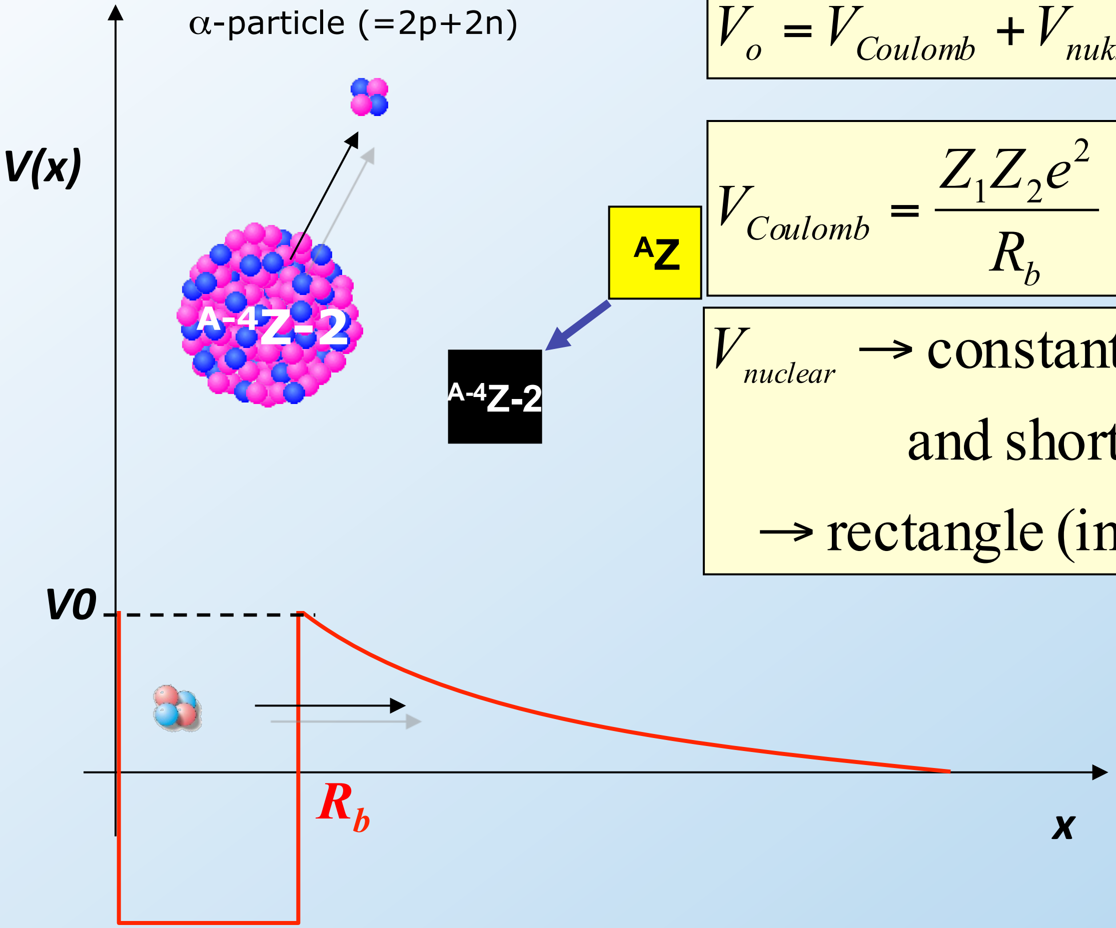

$$V_o = V_{Coulomb} + V_{nuklear} + V_{Drehimpuls}$$

$$V_{Coulomb} = \frac{Z_1 Z_2 e^2}{R_b} \propto \frac{1}{r}$$

$V_{nuclear}$ → constant, attractive (negative)
and short range
→ rectangle (in first approximation)

Tunnel effect – example: α-decay
- transmission probability

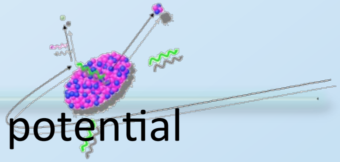

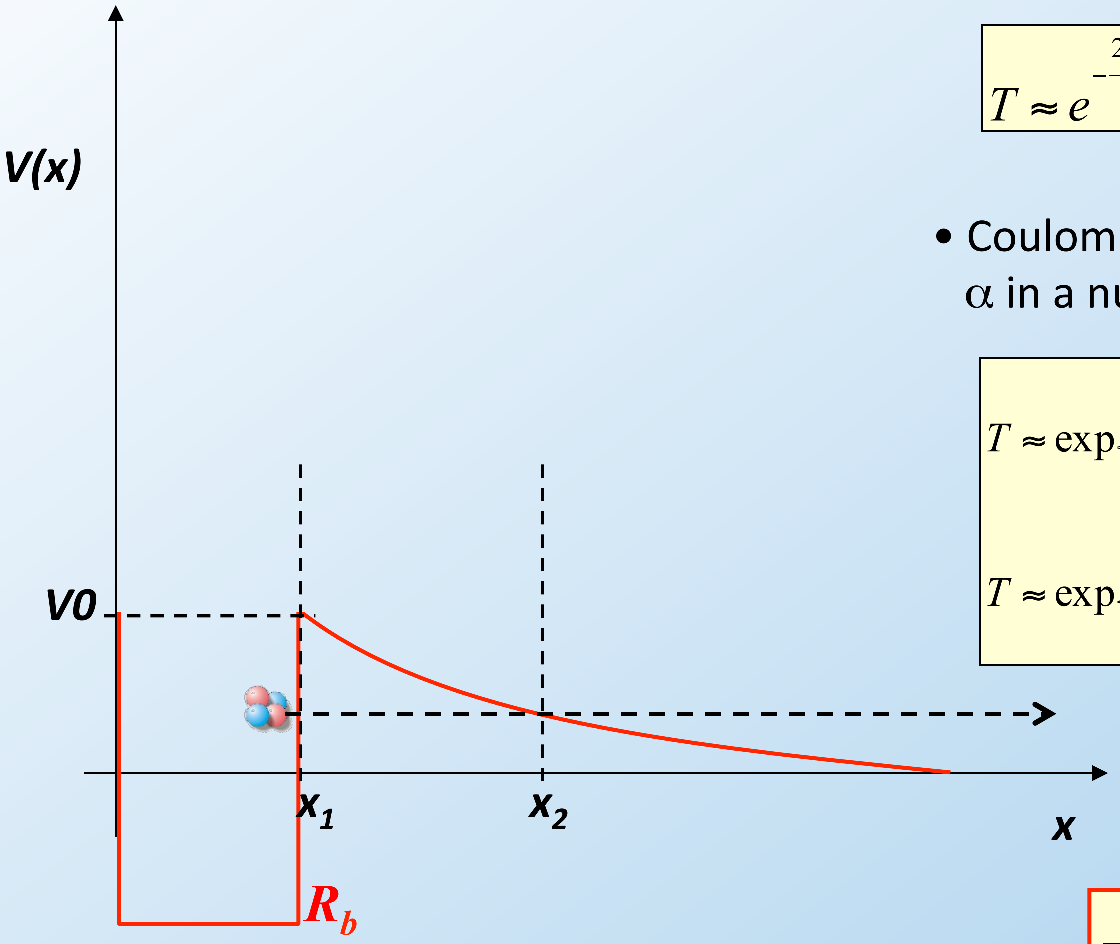

- one-dimensional rectangular potential

$$T \approx e^{-\frac{2(x_2-x_1)}{\hbar}\sqrt{2m(V_0-E)}}$$

- Coulomb potential
  α in a nucleus with atomic charge Z

$$T \approx \exp\left\{-\frac{2}{\hbar}\sqrt{2m_\alpha}\int_{r_1}^{r_2}\sqrt{\left(\frac{2Ze^2}{x}-E_\alpha\right)}dr\right\}$$

$$T \approx \exp\left\{-\frac{2\pi e^2 Z}{\hbar}\sqrt{\frac{2m_\alpha}{E_\alpha}}+\frac{8}{\hbar}\sqrt{e^2 Z R_b m_\alpha}\right\}$$

Gammow-factor ***G***

$$\boxed{T \approx e^{-G}; \quad \text{with} \quad G \propto \frac{Z}{\sqrt{E_\alpha}}}$$

Tunnel effect – example: α-decay
- transmission probability

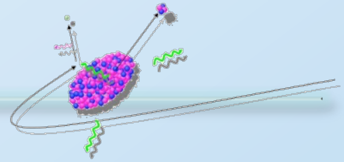

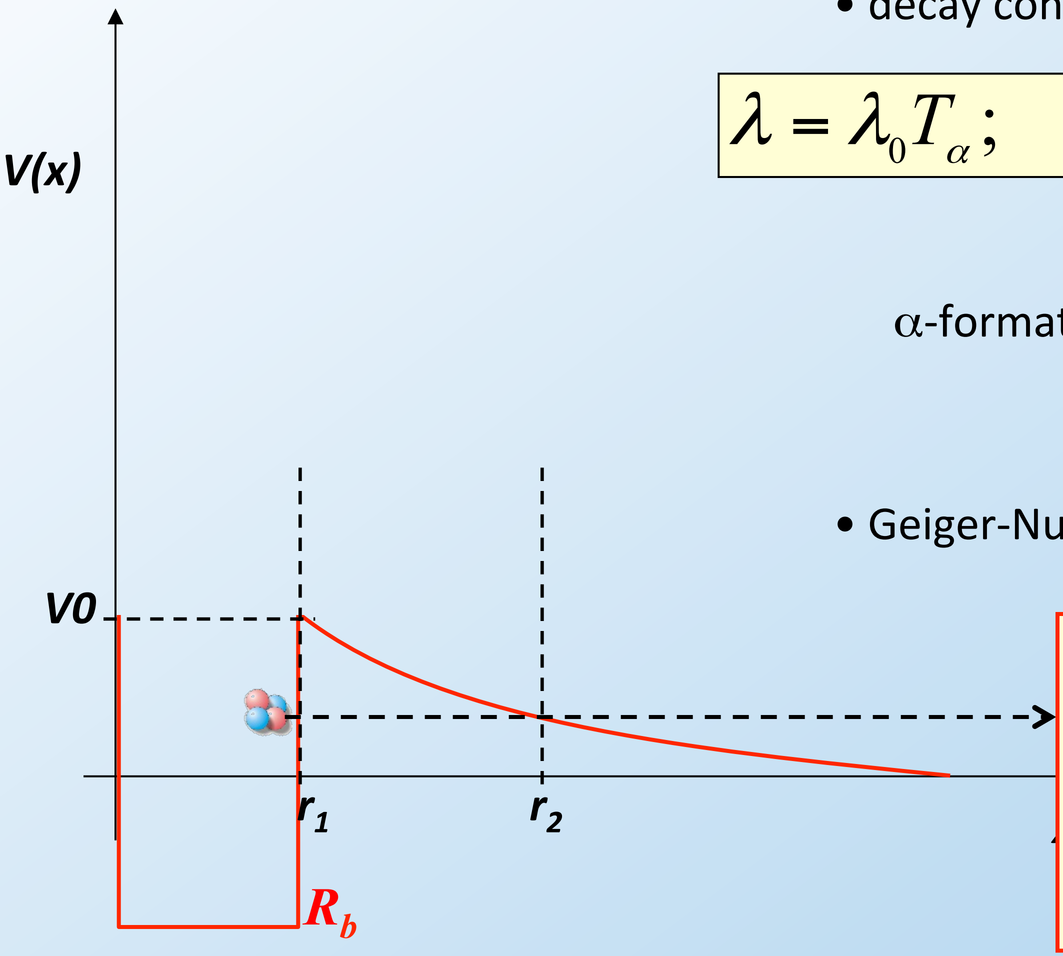

- decay constant

$$\lambda = \lambda_0 T_\alpha ; \quad \text{with} \quad \lambda_0 = w_\alpha \nu_\alpha$$

α-formation probability

„knocking rate“

- Geiger-Nuttal rule: α-decay probability

$$T \approx e^{-G} \text{ and } G \propto \frac{Z}{\sqrt{E_\alpha}}$$

$$\ln \lambda = \ln \lambda_0 - G = a - \frac{bZ}{\sqrt{E_\alpha}}$$

a and ***b***: constant

Tunnel effect – example: α-decay
- application: Geiger-Nuttal rule

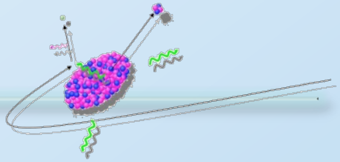

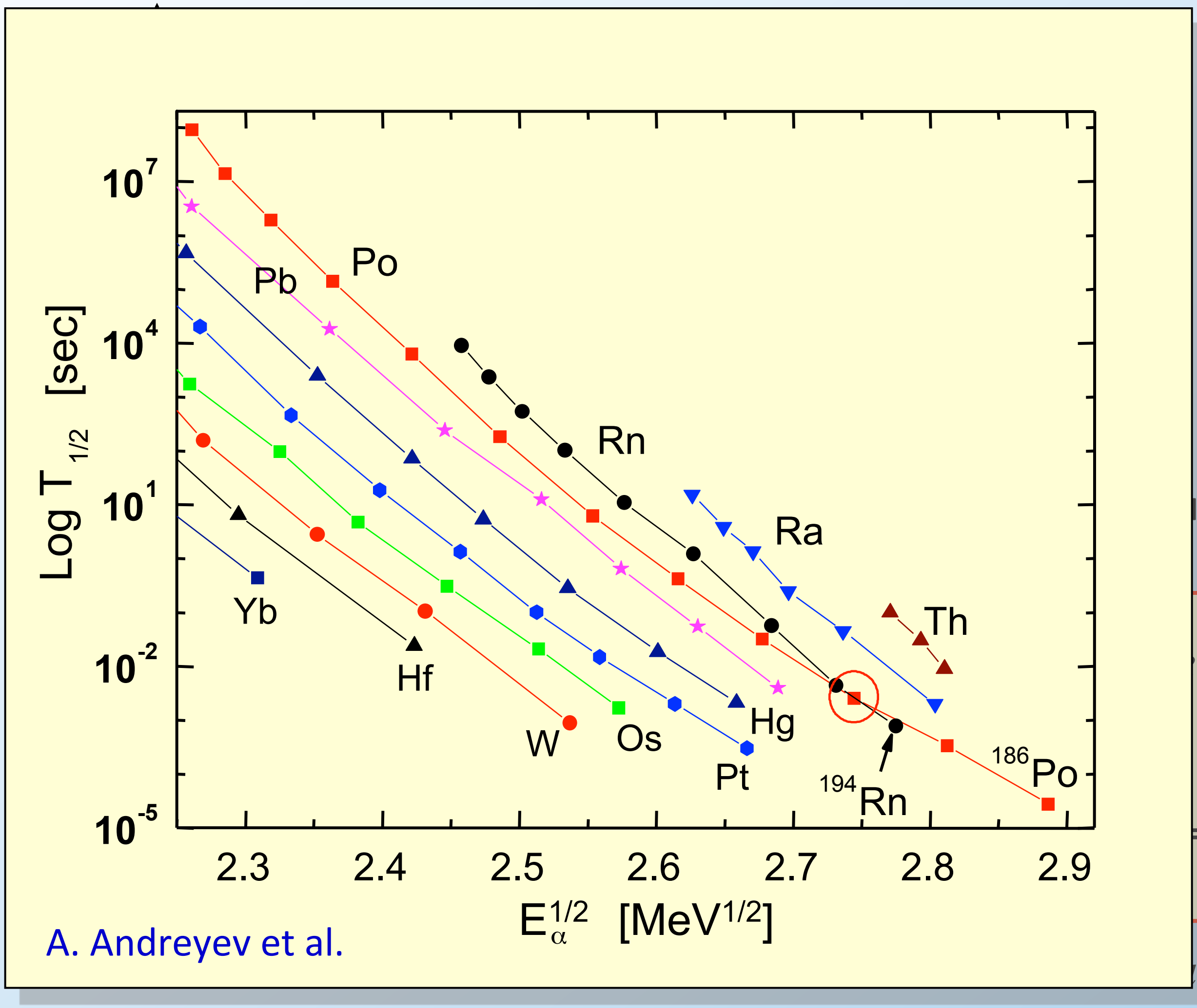

A. Andreyev et al.

le: α-decay probability

$^{-G}$ and $G \propto \dfrac{Z}{\sqrt{E_\alpha}}$

$= \ln\lambda_0 - G = a - \dfrac{bZ}{\sqrt{E_\alpha}}$

and ***b***: constant

Tunnel effect – example
- Gamow-Peak and astrophysics

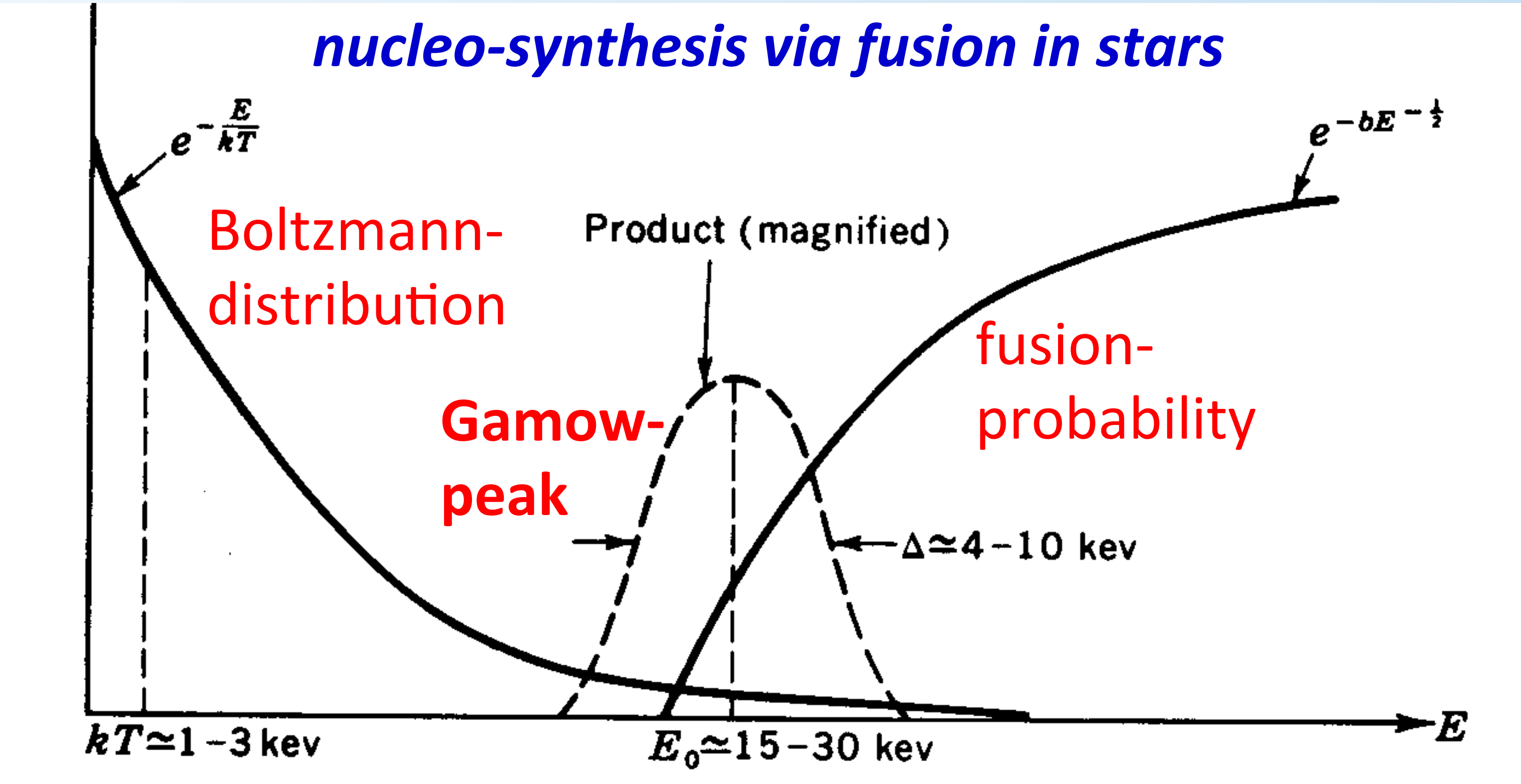

The concept of multiple barriers
– the model of coupled channels

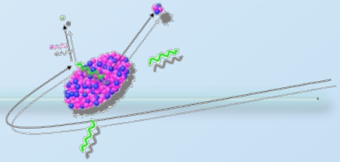

single barrier

$$T = \begin{cases} 1, & E > V_B^{\mathrm{eff}} \\ 0, & E < V_B^{\mathrm{eff}} \end{cases}$$

2 barriers

$$T = \begin{cases} 1, & E > V_B^{\mathrm{eff}} + \sqrt{N}\, V_B^{\mathrm{cpl}} \\ \frac{1}{2}, & V_B^{\mathrm{eff}} - \sqrt{N}\, V_B^{\mathrm{cpl}} < E < V_B^{\mathrm{eff}} + \sqrt{N}\, V_B^{\mathrm{cpl}} \\ 0, & E < V_B^{\mathrm{eff}} - \sqrt{N}\, V_B^{\mathrm{cpl}}. \end{cases}$$

classical limit

quantum smearing

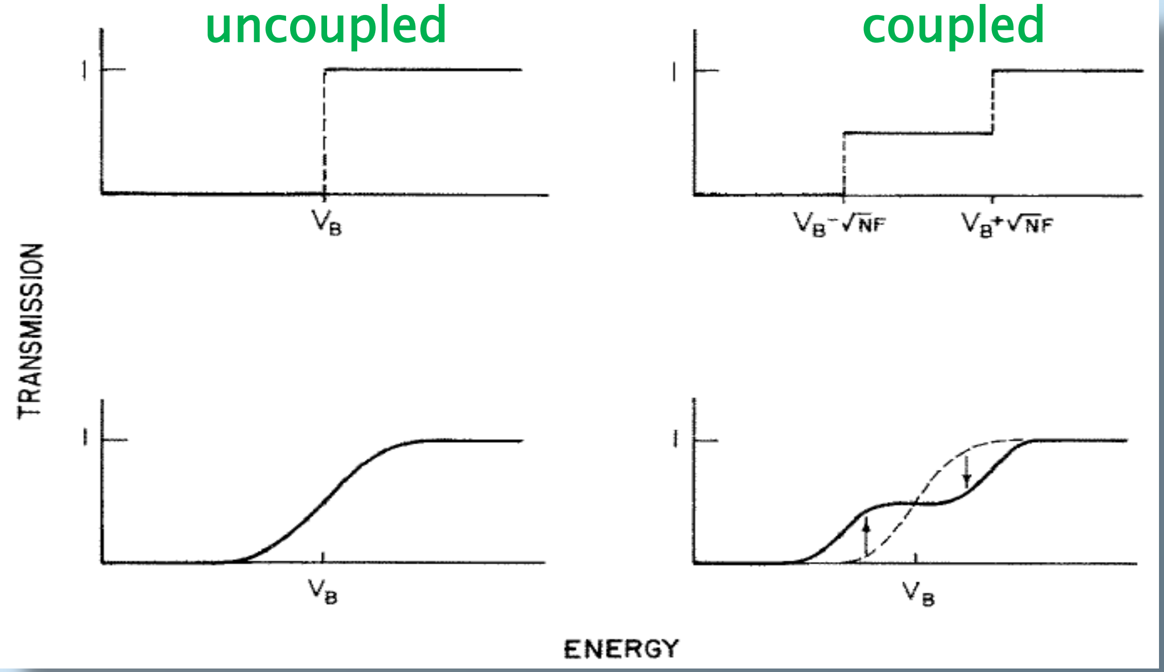

at E< E_B fusion increases

C.H. Dasso and S. Landowne, NPA405(1983)381

The concept of multiple barriers
– coupling to competing channel

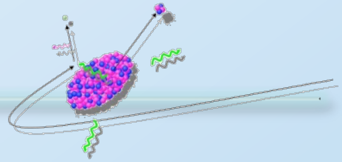

Competing reaction channels modify the interaction barrier

- inelastic excitation of either reaction partner
  vibrational nuclear excitation → barrier fluctuations

- nucleon transfer between the reaction partners
  proton-neutron ratio is modified
  Q-value effects
  <u>problem:</u> form factor

- deformation of either reaction partner
  Coulomb repulsion ∝ 1/r
  short range nuclear force → sudden onset
  → range of barriers

Fusion Barrier Distribution
- Deformed Nuclei

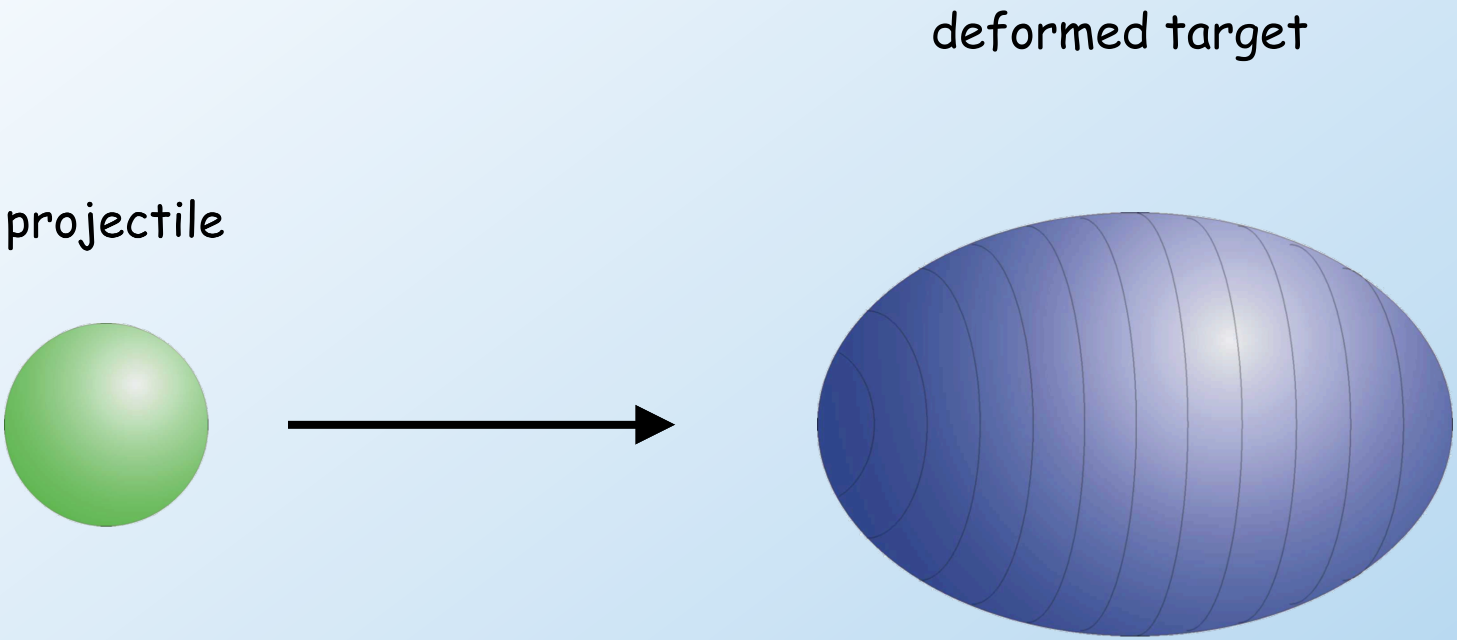

Fusion Barrier Distribution

- Deformed Nuclei

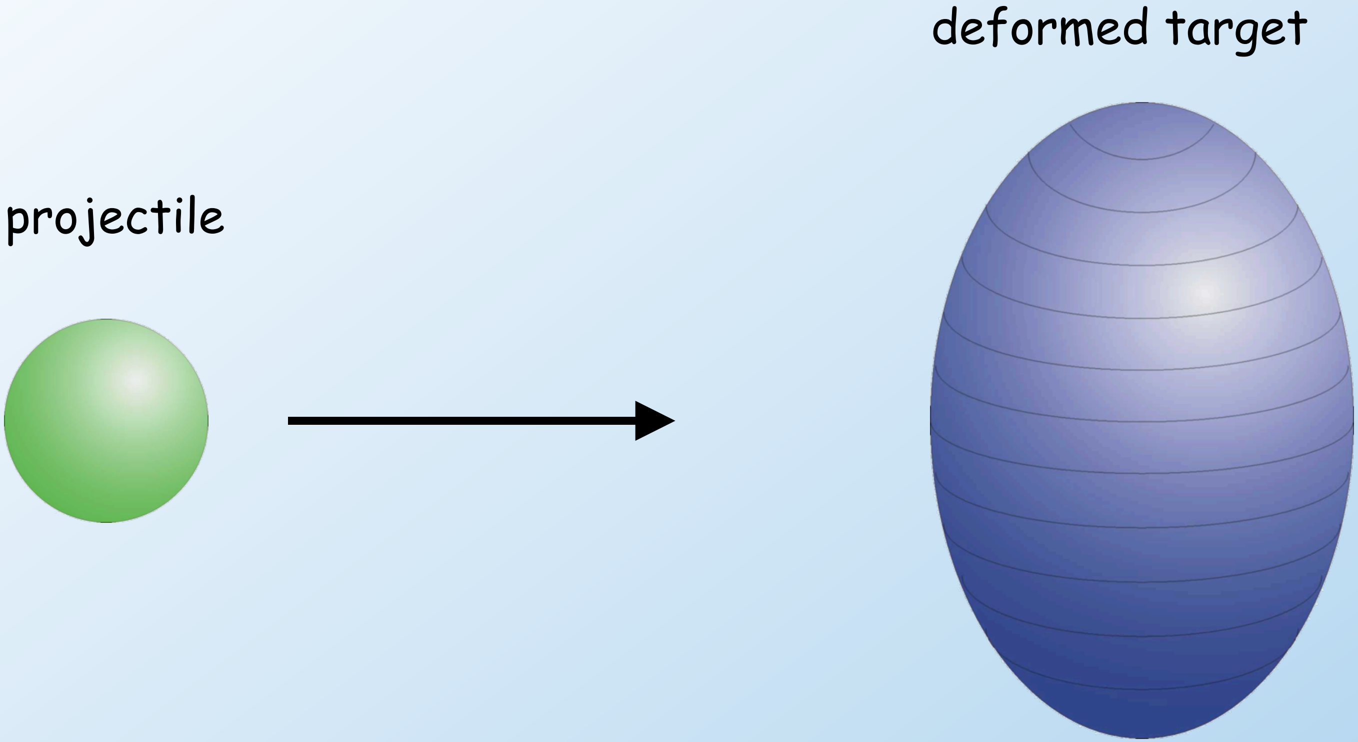

deformed target

projectile

Fusion Barrier Distribution

- Deformed Nuclei and the Potential

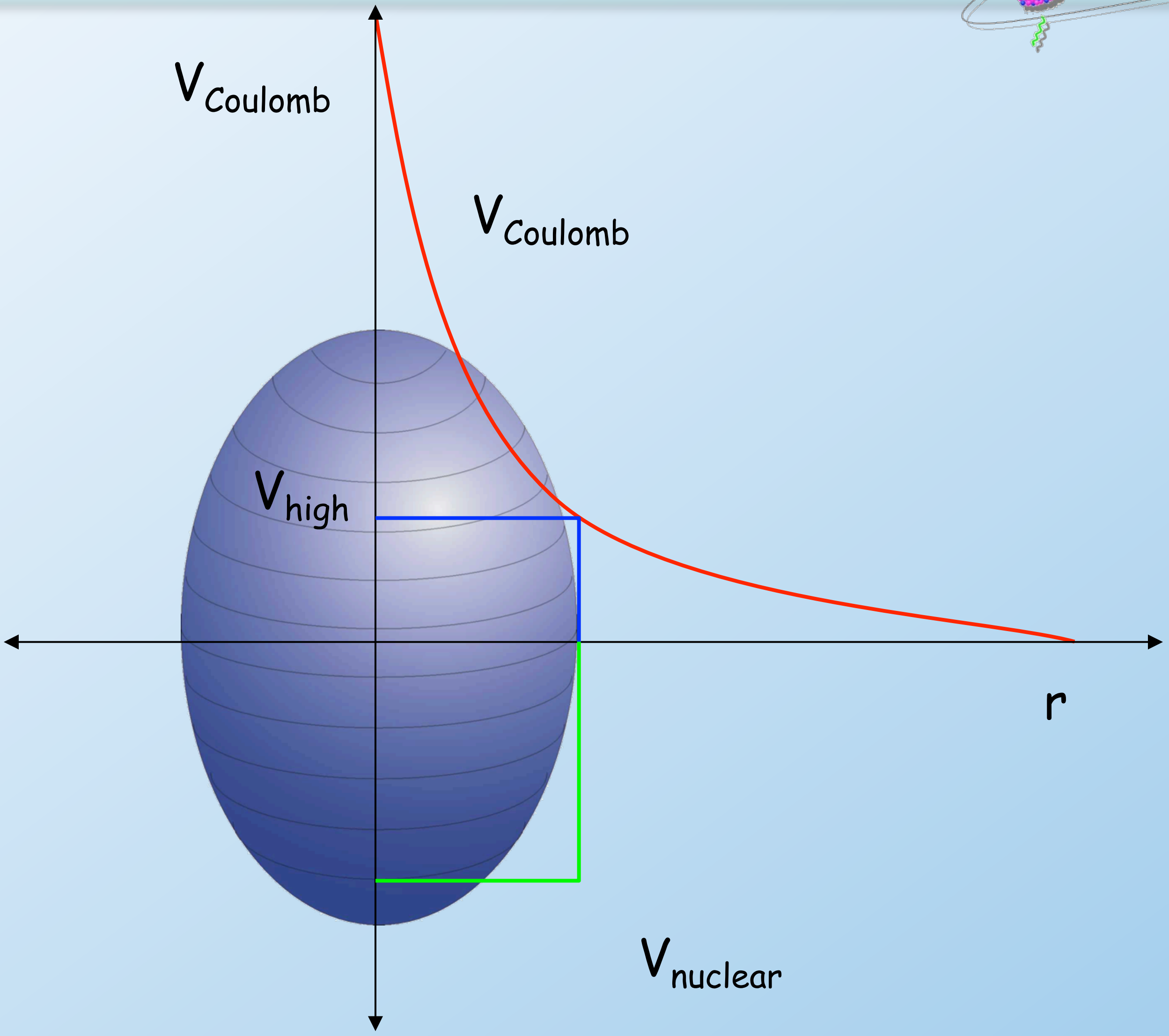

Fusion Barrier Distribution
- Deformed Nuclei and the Potential

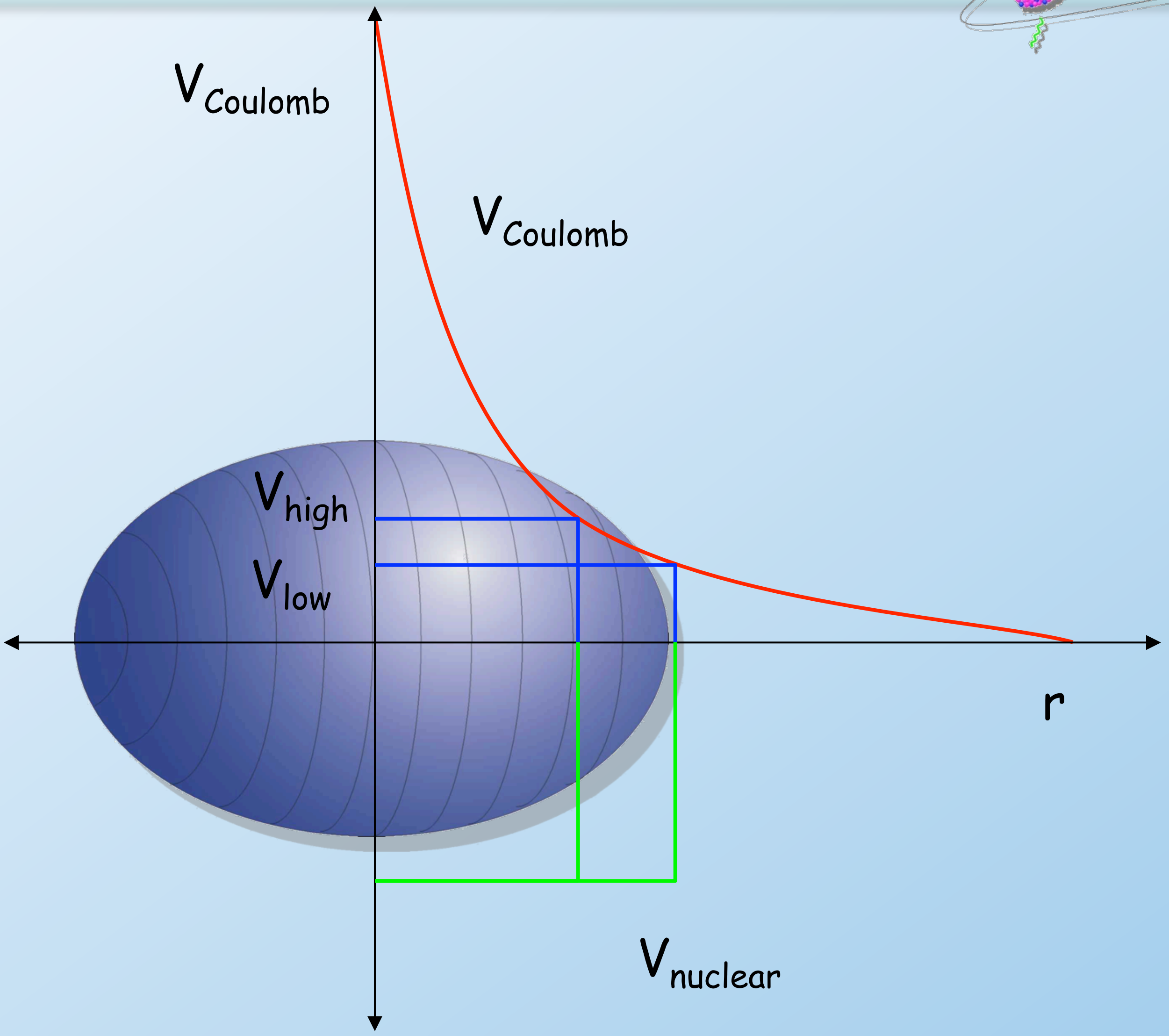

Fusion Barrier Distribution

- Deformed Nuclei: prolate and oblate

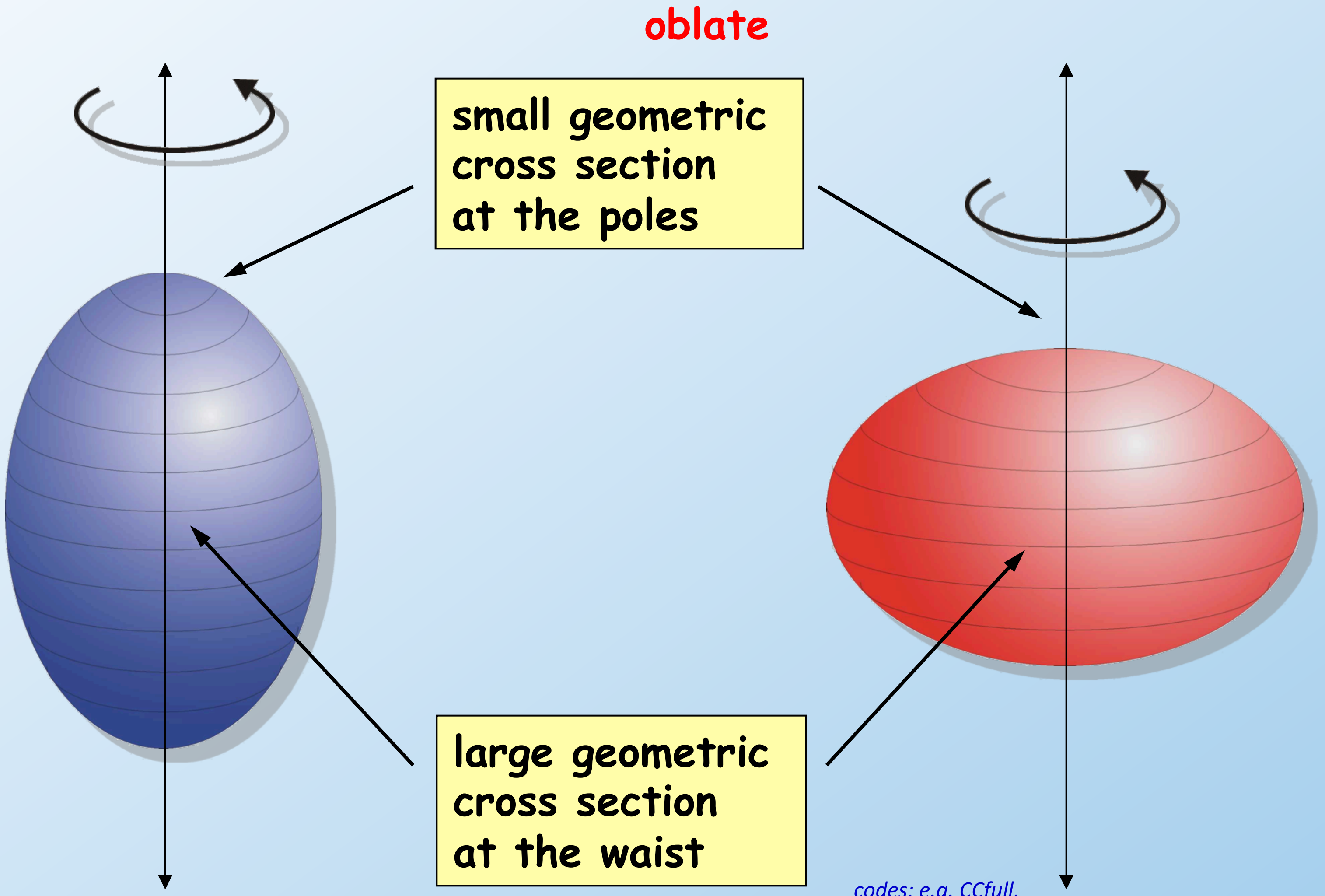

small geometric cross section at the poles

large geometric cross section at the waist

codes: e.g. CCfull,
Hagino et al. Comp.Phys. Comm. 123 (1999),p. 143–152

Fusion Barrier Distribution

- the Concept

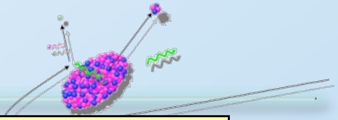

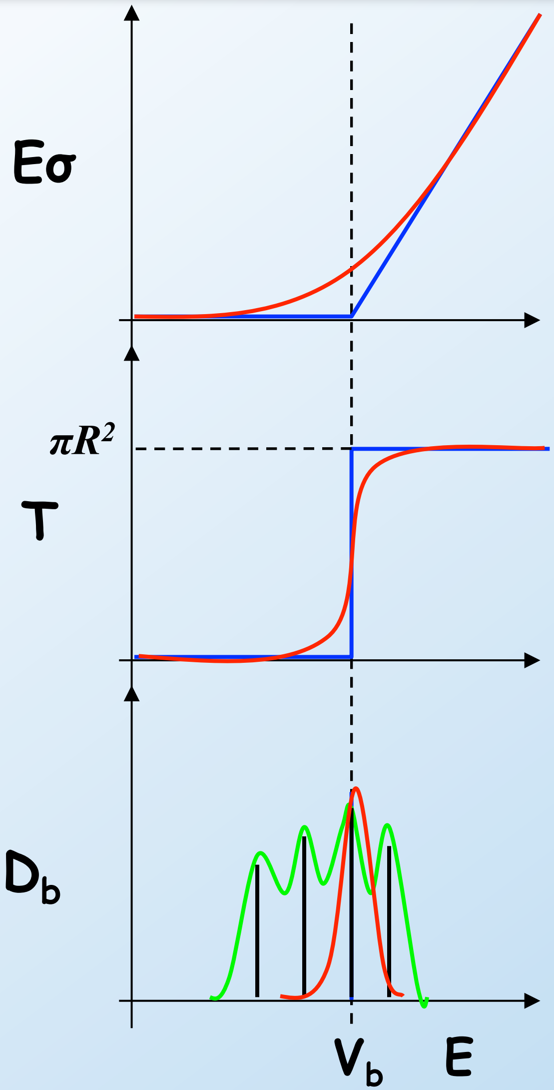

$$\sigma E(E,V_b) = \pi R^2\left(1-\frac{V_b}{E}\right) \qquad , E > V_b$$

$$\sigma E(E,V_b) = 0 \qquad , E < V_b$$

$$\frac{d\left(E\sigma(E,V_b)\right)}{dE} = \pi R^2 \qquad , E > V_b$$

$$\frac{d\left(E\sigma(E,V_b)\right)}{dE} = 0 \qquad , E < V_b$$

$$\frac{d^2\left(E\sigma(E,V_b)\right)}{dE^2} = \pi R^2\delta\left(E\text{-}V_b\right)$$

Fusion Barrier Distribution

- Deformed Nuclei: prolate and oblate

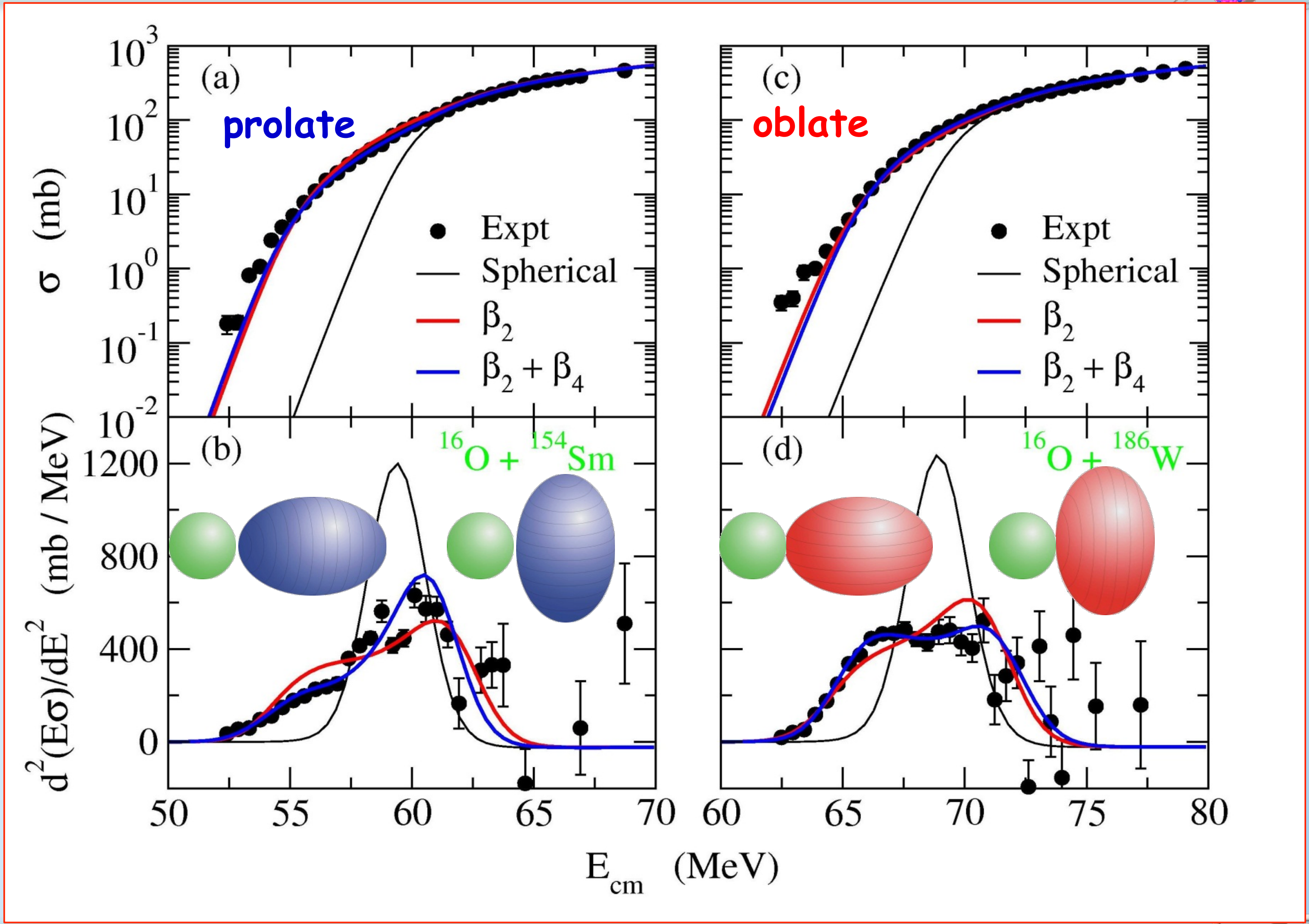

The Statistical Model

- de-excitation of the hot Compound System

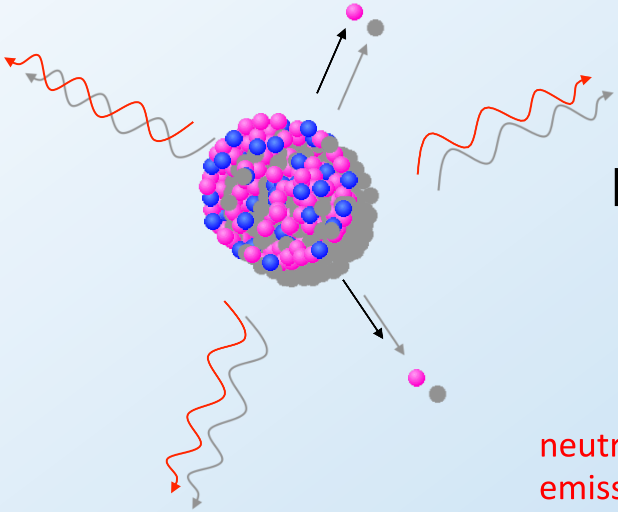

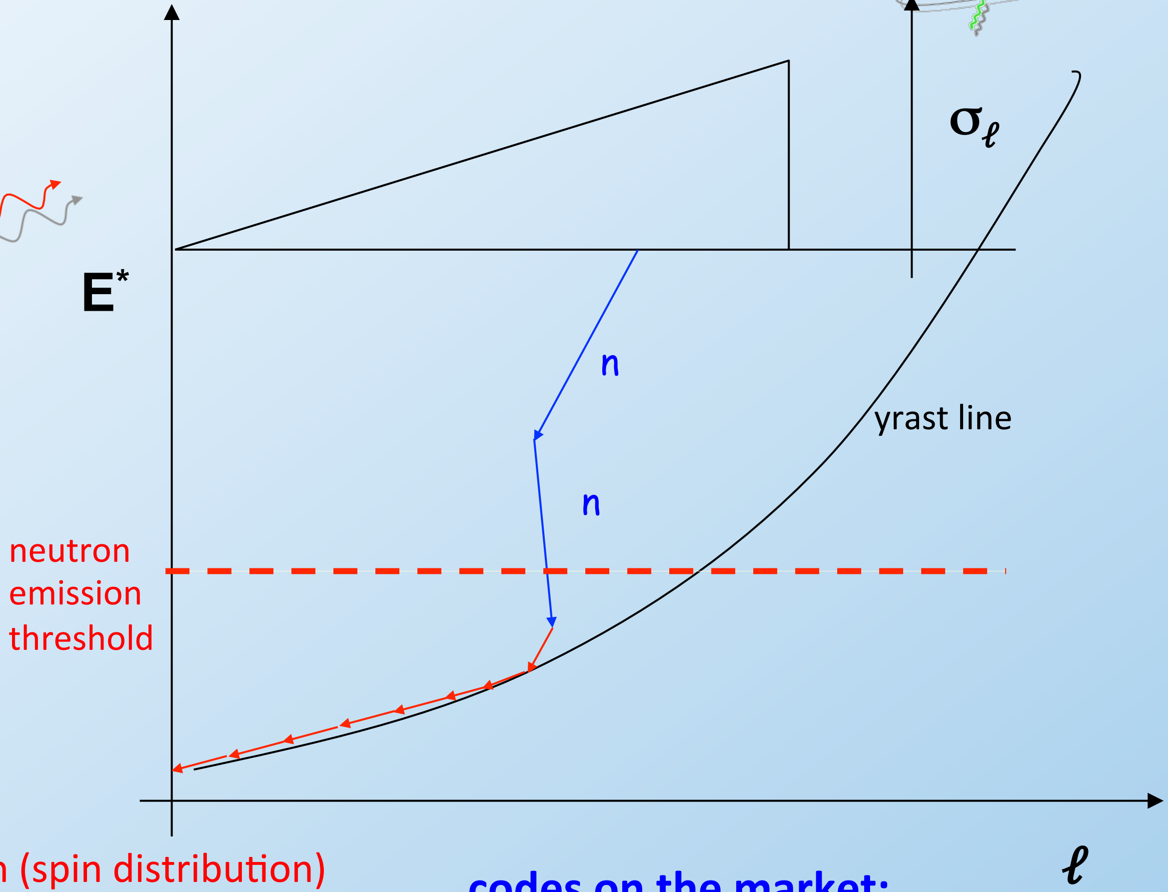

theoretical modeling

- fusion cross section
  e.g. Wong formula
  Partial wave cross section (spin distribution)
- interaction barrier
  e.g. Bass potential
- Particle emission
  Monte-Carlo simulation: particle potential an spectra (theory/exp. data)

codes on the market:

HIVAP, PACE/EVAP, …

Fusion Barrier Distribution

- Partial Wave Cross sections: the CN Spin Distribution

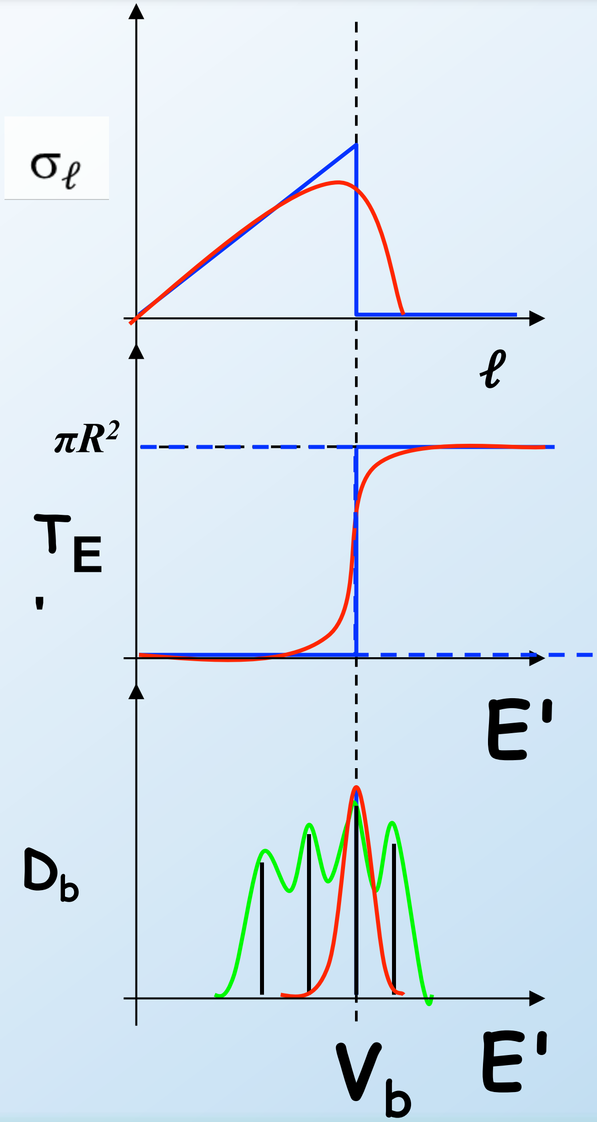

$$\sigma_\ell(E) = T_\ell(E,\ell)(2\ell+1)\pi\bar{\lambda}^2$$

$$\bar{\lambda} = \frac{\hbar}{\sqrt{2\mu E}} \quad \rightarrow \quad \text{de Broglie wave length}$$

$$T_\ell(E,\ell) = \frac{\sigma_\ell(E)}{(2\ell+1)\pi\bar{\lambda}^2}$$

$$\ell \rightarrow E' \quad \text{with} \quad E' = E - E_{rot}, \quad E_{rot}(\ell) = \frac{\ell(\ell+1)}{2\mu R_b^2}$$

$$T_\ell \rightarrow T_{E'}$$

$$T_{E'} = \frac{1}{\pi R_b}\,\frac{d\left(E'\sigma(E',V_b)\right)}{dE'} = \frac{\sigma(E')}{(2\ell+1)\pi\bar{\lambda}^2}$$

$$D_b = \frac{dT_{E'}}{dE'} = \frac{d^2\left(E'\sigma(E,V_b)\right)}{dE'^2} = \pi R^2\delta(E'-V_b)$$

Fusion Dynamics and the Spin Distribution

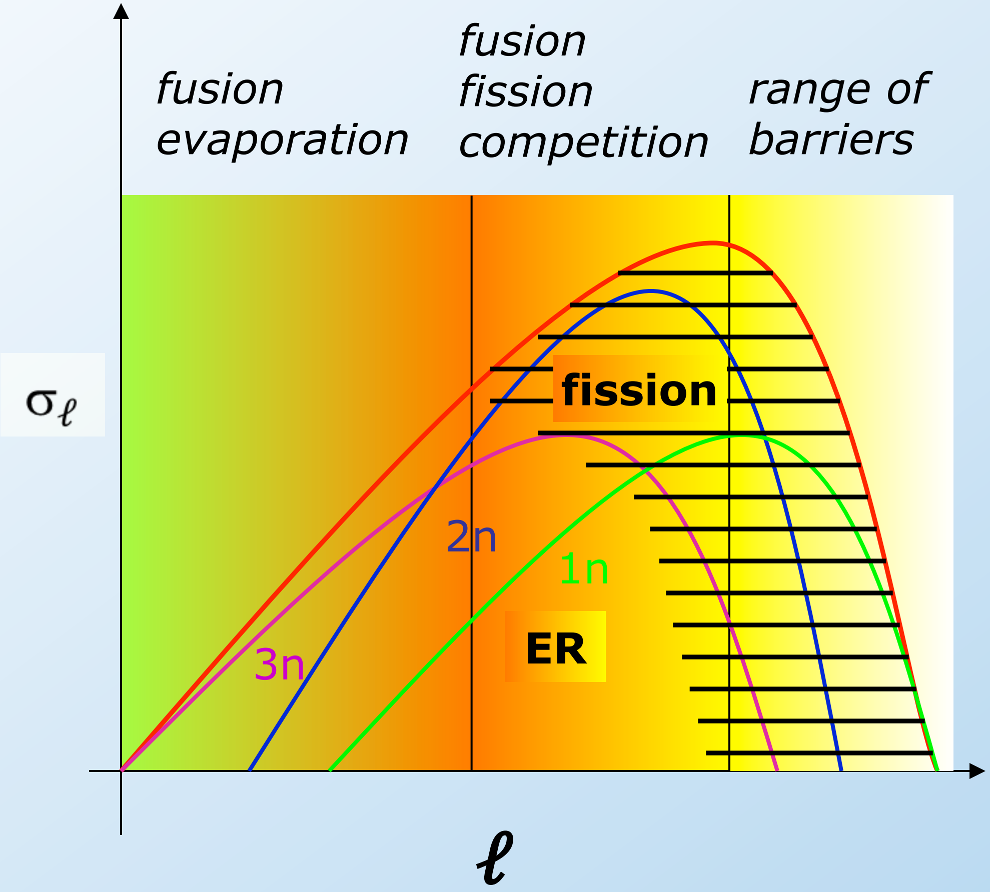

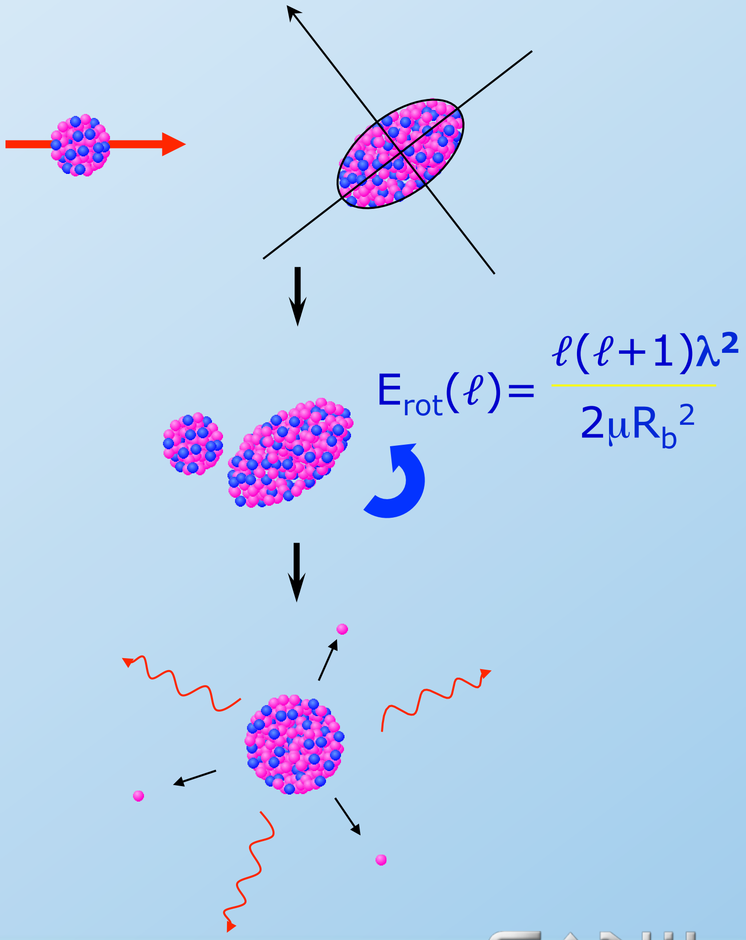

$$E_{rot}(\ell) = \frac{\ell(\ell+1)\lambda^2}{2\mu R_b^2}$$

Fusion Dynamics and the Spin Distribution

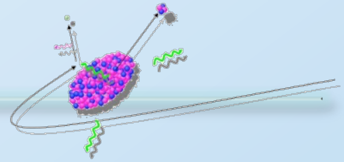

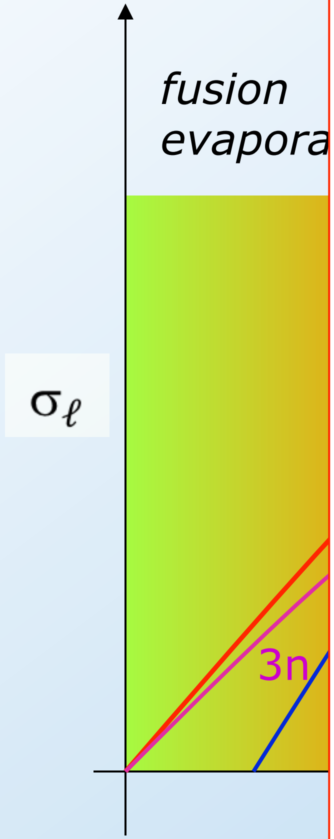

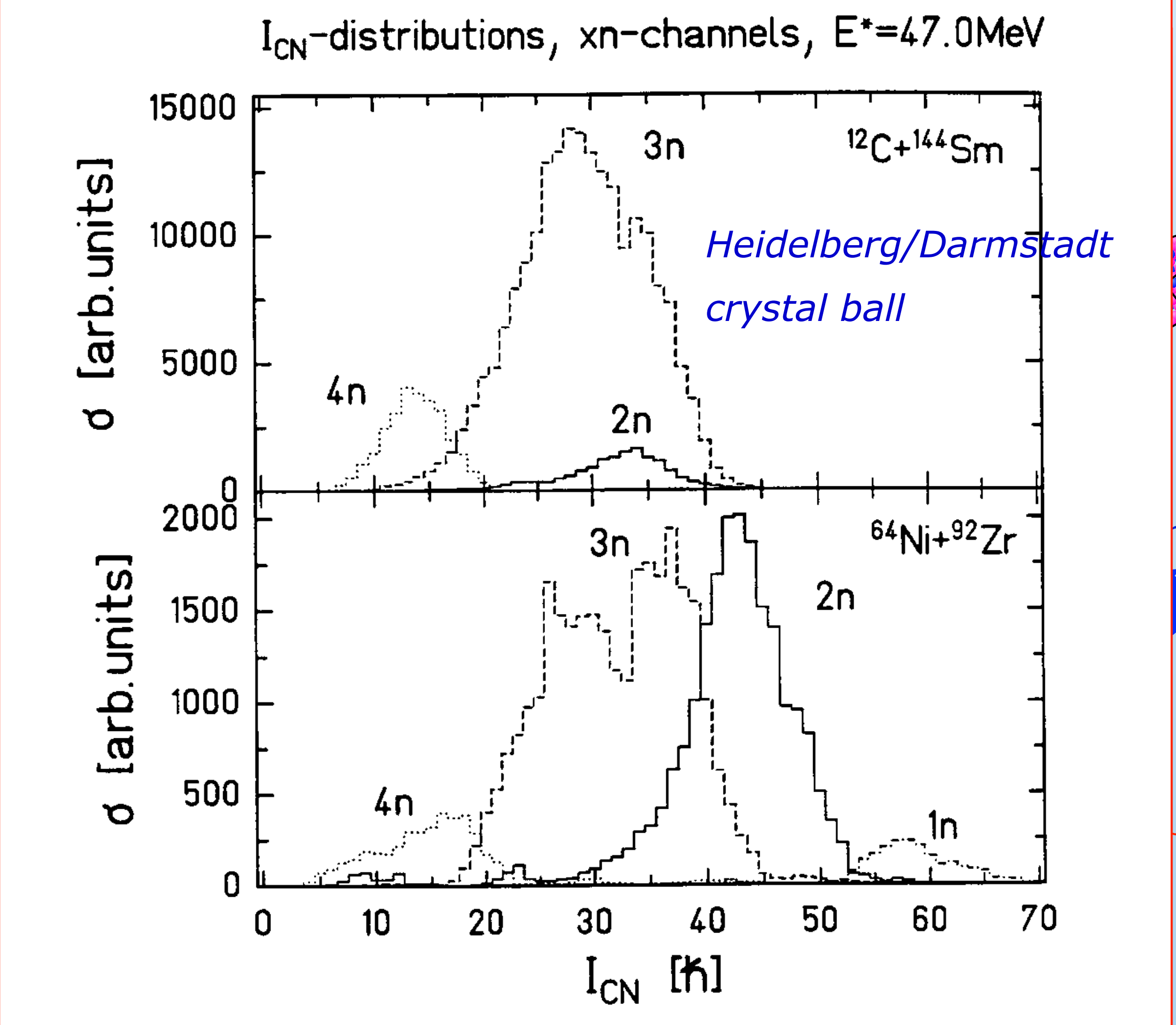

Heidelberg/Darmstadt

crystal ball

Abbildung 4.33. Die I_{CN}-Verteilungen der ungeladenen Kanäle der beiden Eingangskanäle.

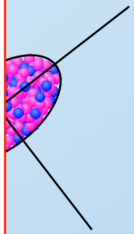

$$\ldots_{rot}(\ell) = \frac{\ell(\ell+1)\lambda^2}{2\mu R_b^{\,2}}$$

Fusion Dynamics and the Spin Distribution

$V = V_{Coulomb} + V_{nuclear} + V_{\ell}$

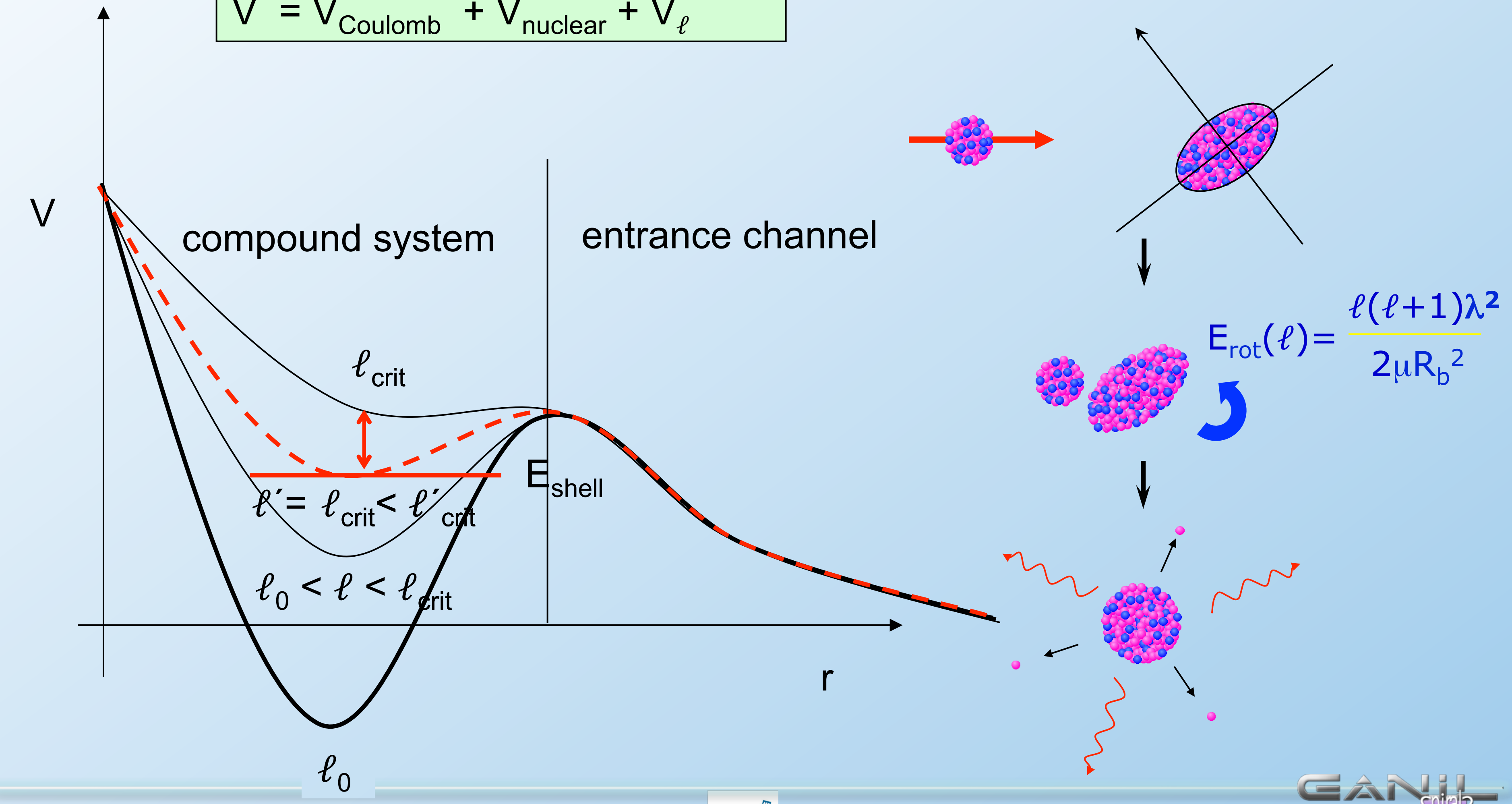

$$E_{rot}(\ell) = \frac{\ell(\ell+1)\lambda^2}{2\mu R_b^2}$$

Fusion-Fission and the Barrier Structure for $^{34}S+^{168}Er \rightarrow ^{202}Po^*$

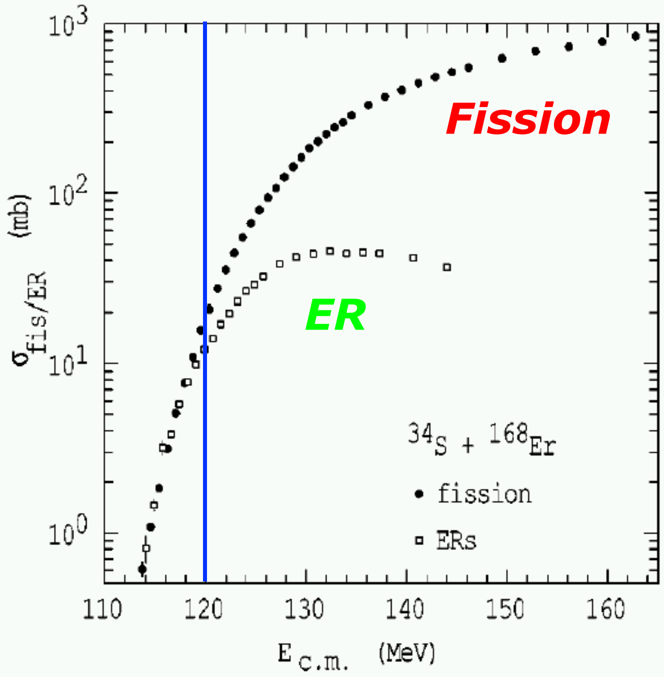

FIG. 2. Fission and ER excitation functions for the $^{34}S+^{168}Er$ reaction. See Secs. II B and II C, for a discussion of the uncertainties on these quantities.

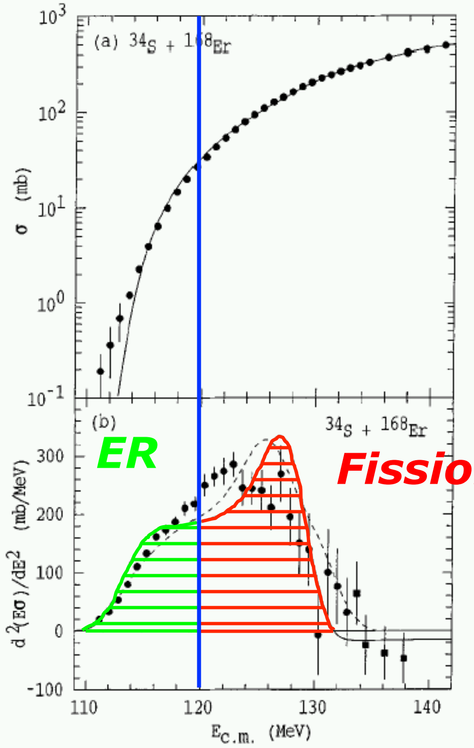

FIG. 4. (a) Measured fusion excitation function compared to a calculation using a geometric model with $\beta_2=0.338$ (solid line). (b) Measured and calculated fusion barrier distributions obtained from the calculation in (a) (solid line) and that from the coupled-channels code CCFULL (dashed line).

C.R. Morton et al., Phys. Rev. C 62 024607

Experimental Approach to the Spin Distribution

- example: GASP, LNL

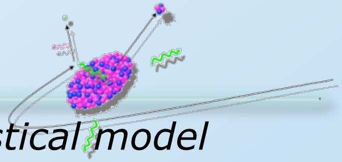

1 *GASP – inner ball (80 BGO-crystals)*

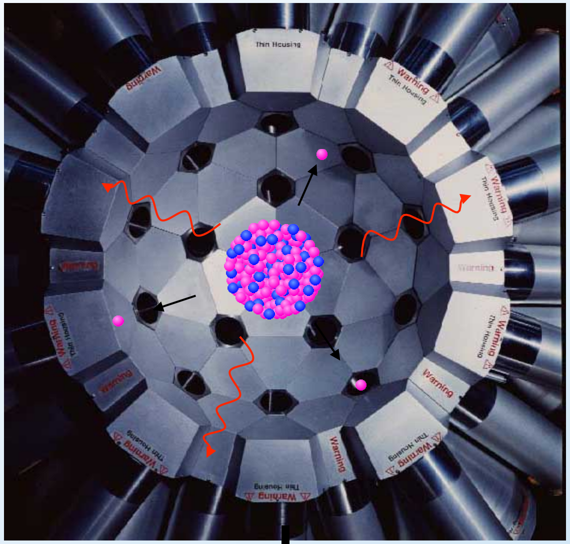

γ-ray fold

GASP ↓ *response function*

$\mathbf{M_\gamma}$

2 *GASP – high resolution Ge-detectors*

↓

$\mathbf{E_\gamma}$

↓

ER identification

3 *statistical model (codes like PACE, EVAP, HIVAP…)*

↓

evaporation parameters

↓

spin removed by particles and statistical γ-rays

$$\ell_{CN} = (\mathbf{M_\gamma} - \mathbf{M_{\gamma s}})\Delta\ell_\gamma + \mathbf{M_{\gamma s}}\Delta\ell_{\gamma s} + \sum_i \mathbf{M_i}\Delta\ell_i + \Delta\ell_{gs/m}\ ; \quad \mathbf{i = p, n, \alpha}$$

Fold Distributions with GASP for ^{64}Ni+^{100}Mo

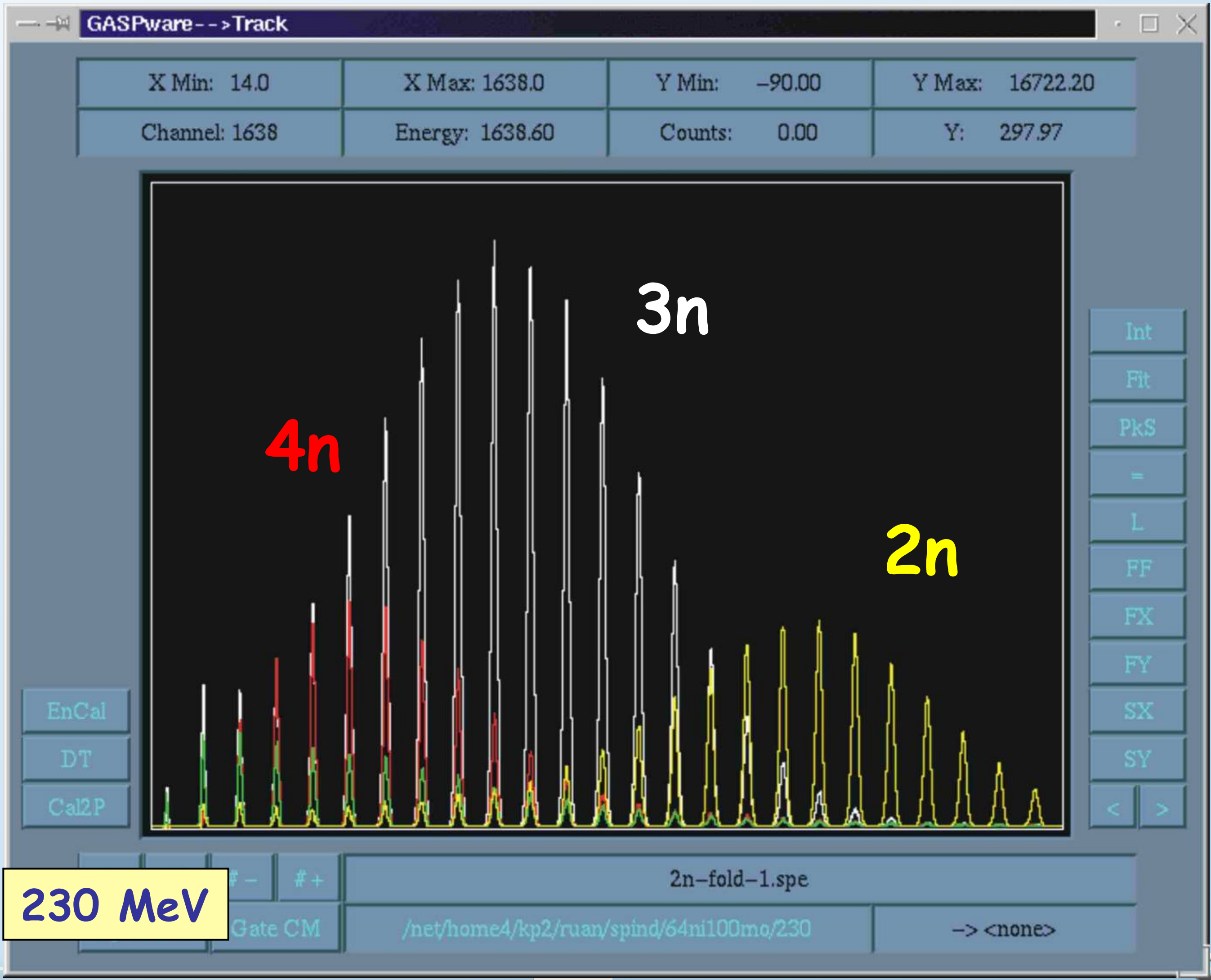

GASPware-->Track

X Min: 14.0
X Max: 1638.0
Y Min: -90.00
Y Max: 16722.20
Channel: 1638
Energy: 1638.60
Counts: 0.00
Y: 297.97

2n-fold-1.spe
/net/home4/kp2/ruan/spind/64ni100mo/230
-> <none>

230 MeV

Fold Distributions with GASP for ^{64}Ni+^{100}Mo

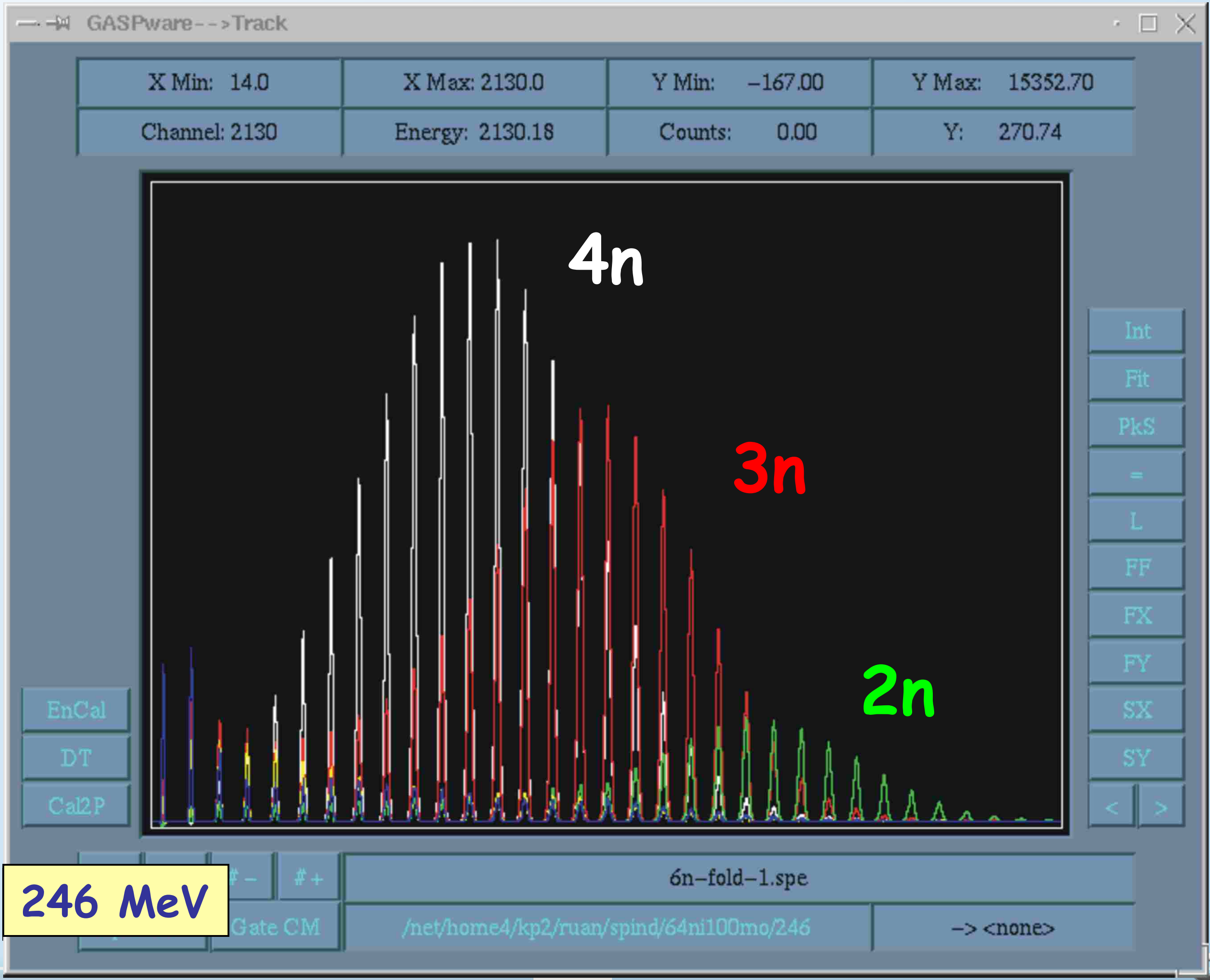

GASPware-->Track

X Min: 14.0 | X Max: 2130.0 | Y Min: −167.00 | Y Max: 15352.70

Channel: 2130 | Energy: 2130.18 | Counts: 0.00 | Y: 270.74

6n−fold−1.spe

/net/home4/kp2/ruan/spind/64ni100mo/246

−> <none>

246 MeV

Fold Distributions with GASP for ^{64}Ni+^{100}Mo

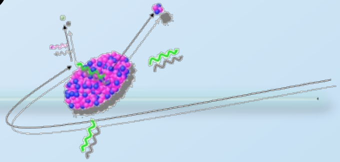

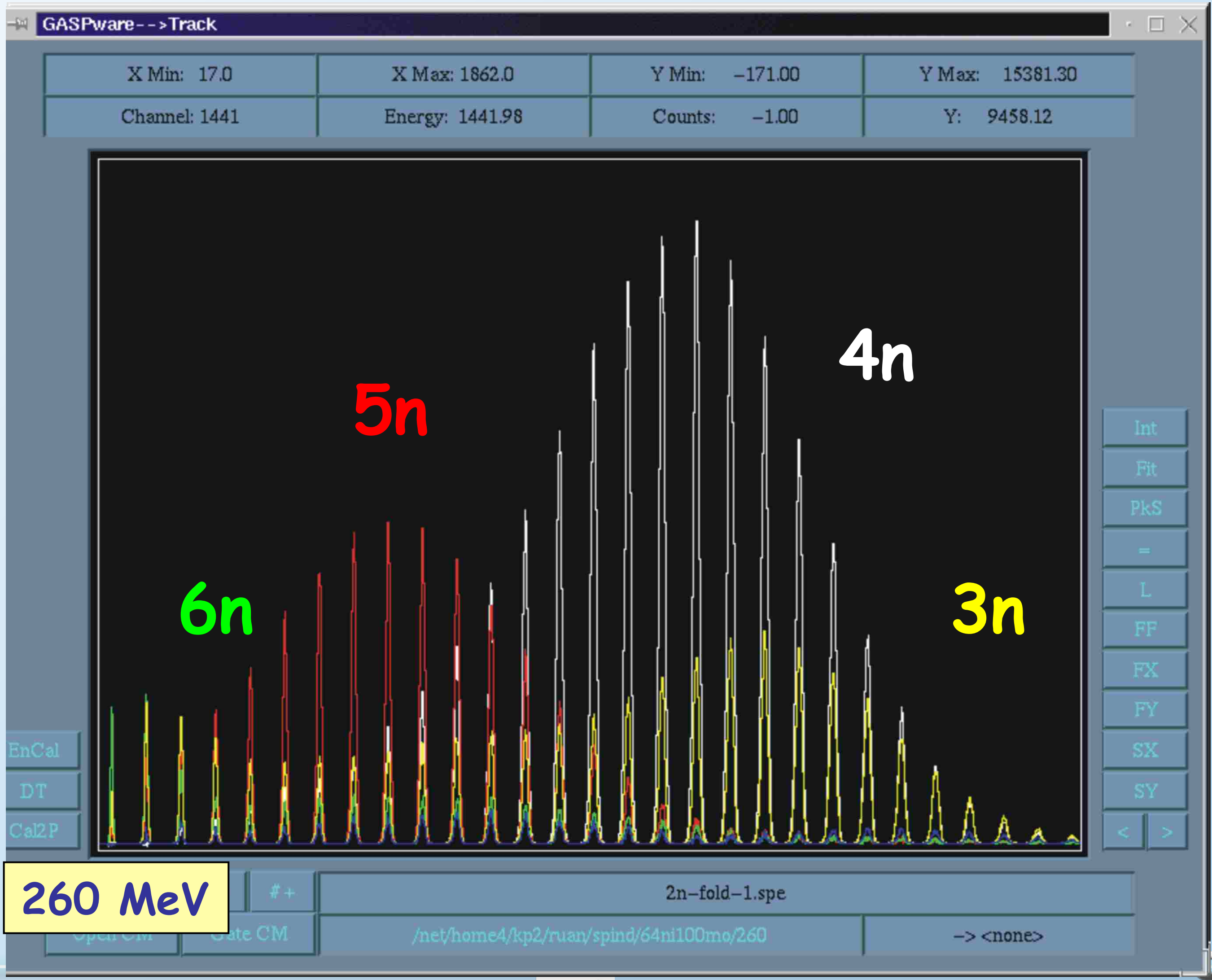

GASPware-->Track

X Min: 17.0 | X Max: 1862.0 | Y Min: –171.00 | Y Max: 15381.30

Channel: 1441 | Energy: 1441.98 | Counts: –1.00 | Y: 9458.12

2n–fold–1.spe

/net/home4/kp2/ruan/spind/64ni100mo/260

–> <none>

260 MeV

Fold Distributions with GASP for ^{64}Ni+^{100}Mo

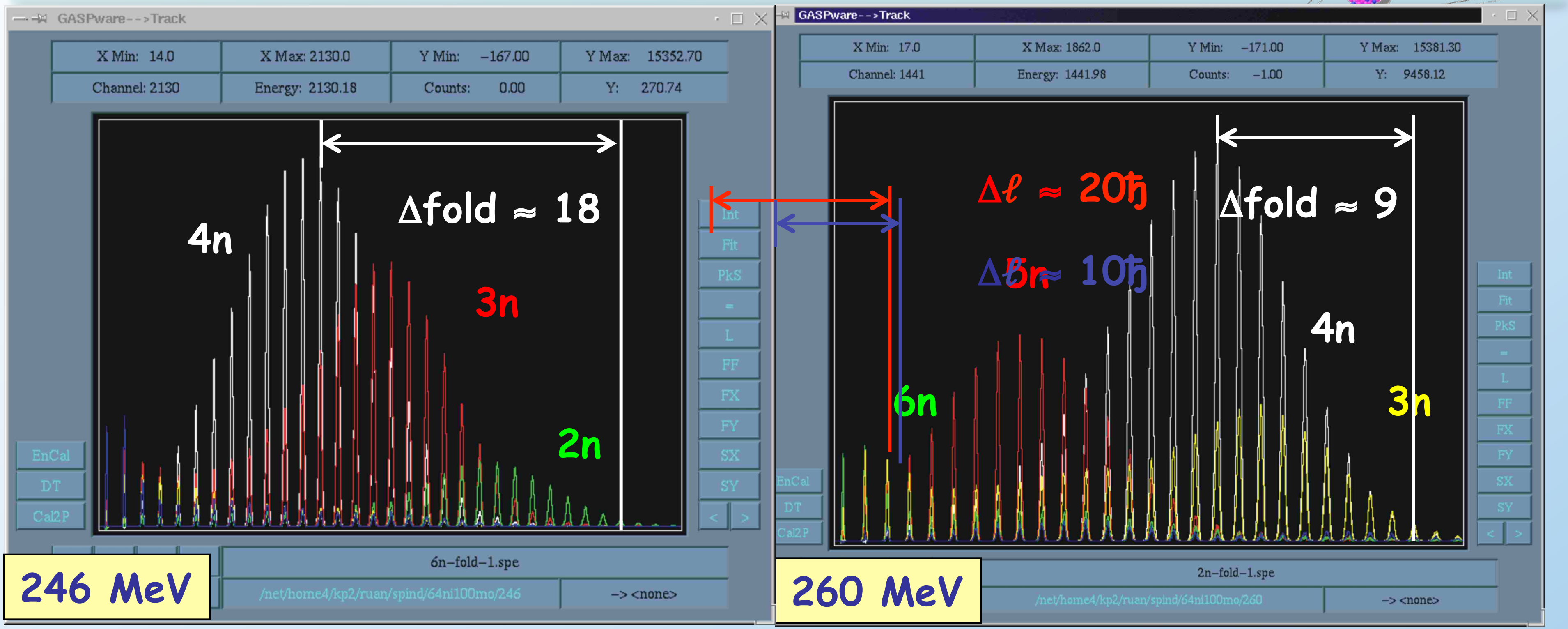

X Min: 14.0
X Max: 2130.0
Y Min: –167.00
Y Max: 15352.70
Channel: 2130
Energy: 2130.18
Counts: 0.00
Y: 270.74
6n–fold–1.spe
/net/home4/kp2/ruan/spind/64ni100mo/246
-> <none>

X Min: 17.0
X Max: 1862.0
Y Min: –171.00
Y Max: 15381.30
Channel: 1441
Energy: 1441.98
Counts: –1.00
Y: 9458.12
2n–fold–1.spe
/net/home4/kp2/ruan/spind/64ni100mo/260
-> <none>

Fold Distributions with GASP for ^{64}Ni+^{100}Mo

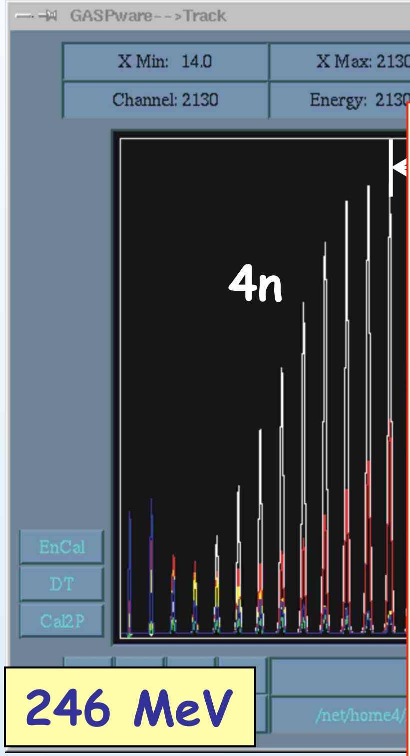

GASPware-->Track

X Min: 14.0
X Max: 2130.0
Y Min: −167.00
Y Max: 15352.70
Channel: 2130
Energy: 2130.18
Counts: 0.00
Y: 270.74

246 MeV

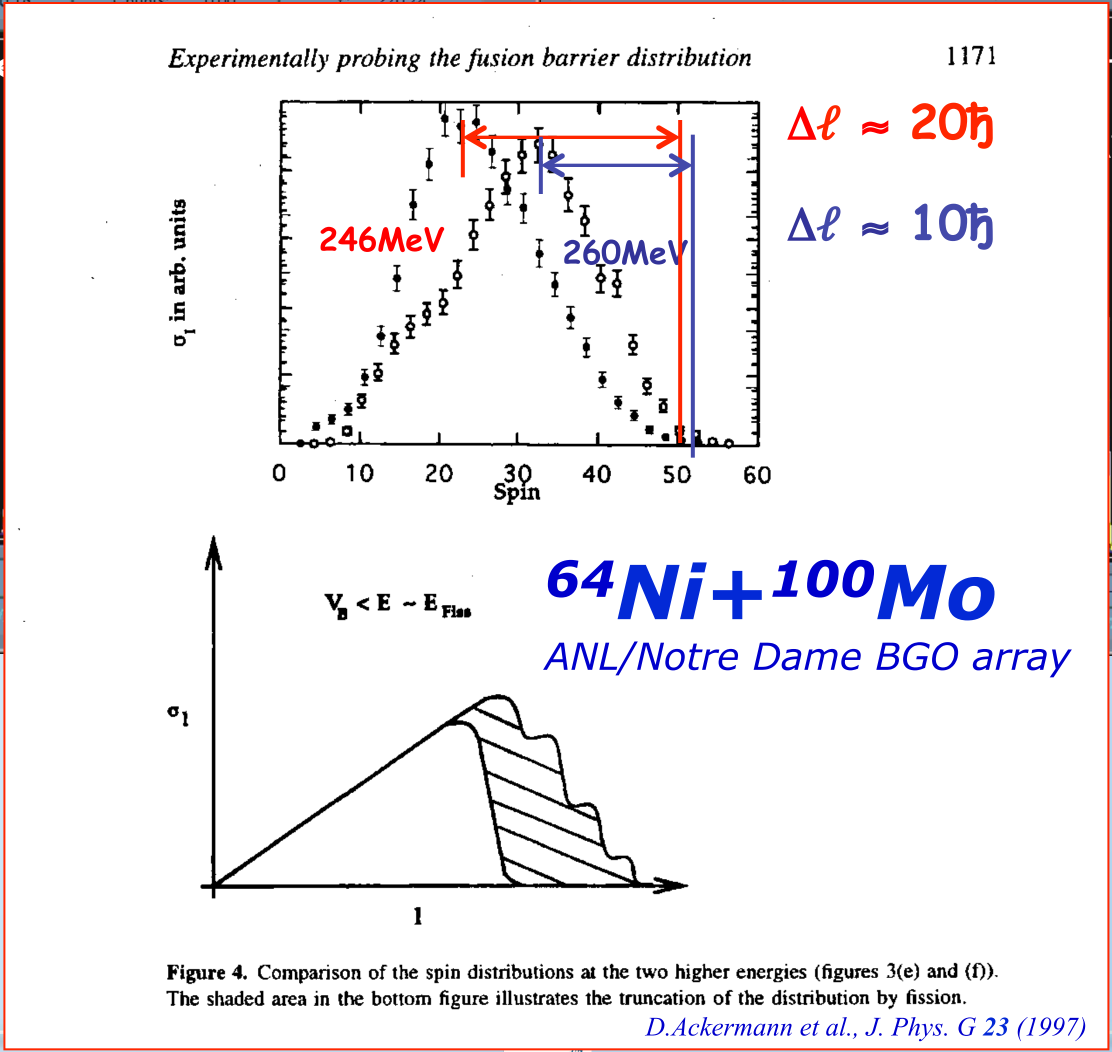

Experimentally probing the fusion barrier distribution 1171

^{64}Ni+^{100}Mo

ANL/Notre Dame BGO array

Figure 4. Comparison of the spin distributions at the two higher energies (figures 3(e) and (f)). The shaded area in the bottom figure illustrates the truncation of the distribution by fission.

D.Ackermann et al., J. Phys. G 23 (1997)

GASPware-->Track

X Min: 17.0
X Max: 1862.0
Y Min: −171.00
Y Max: 15381.30
Channel: 1441
Energy: 1441.98
Counts: −1.00
Y: 9458.12

-1.spe
260
-> <none>

Extraction of the barrier distribution for ^{64}Ni+^{100}Mo

- analysis by Varinderjit Singh, Panjab University, India

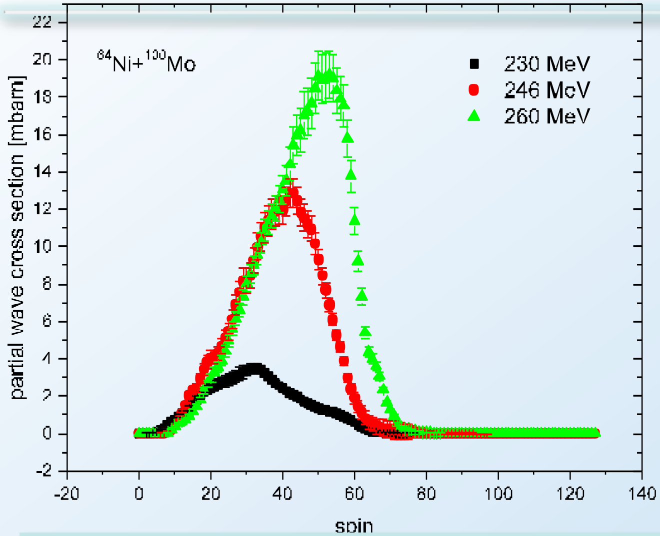

spin ℓ → E‘

with $$E' = E - \frac{\ell(\ell+1)}{2\mu R_b^2}$$

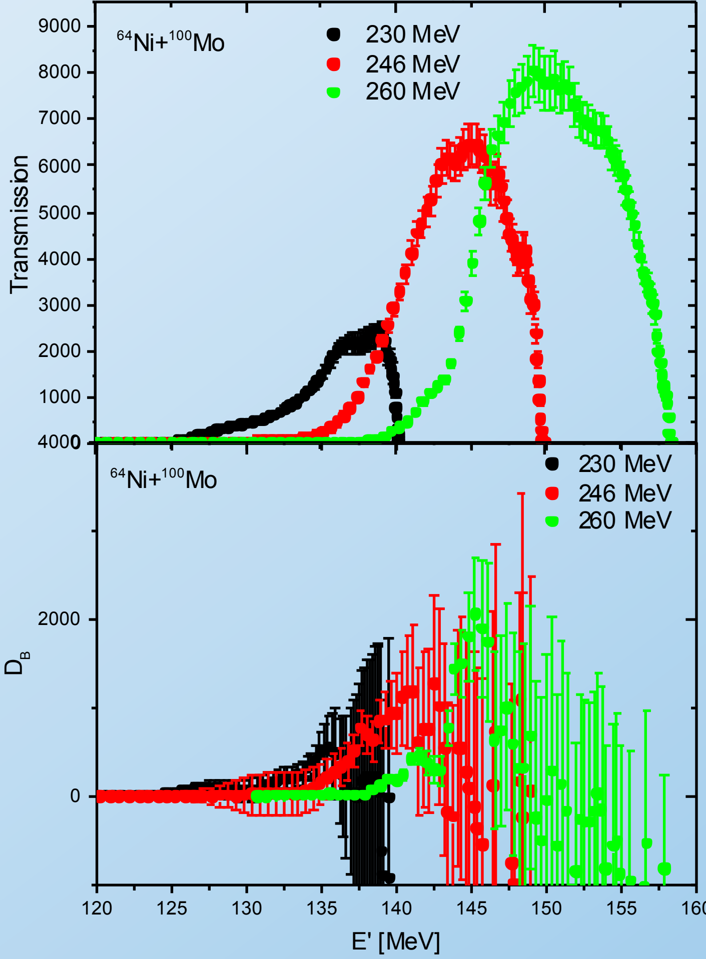

Step wise transformation σ_ℓ to D_b

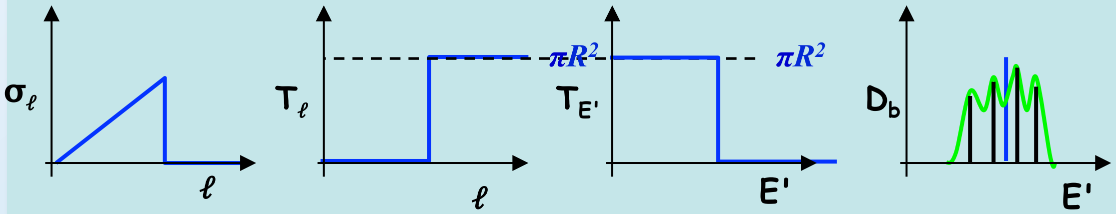

- transmission function T(E‘) (T(ℓ))
- barrier distribution
    - covers large energy range E‘ for one E_{beam}
    - sensitive only for fusion-evaporation
    - fission cut-off leads to truncation at low E‘↔ high ℓ

priliminary – analysis ongoing

Entrance channel effect on ER spin distribution

- G. Mohanto et al., Nucl. Phys. A 890–891 (2012) p. 62–76

Abstract

… **ER gated gamma-multiplicity** was measured for the reaction **^{30}Si+^{170}Er** …

… measured multiplicity distribution was **compared … ^{16}O+^{184}W** and **^{19}F+^{181}Ta** forming the same CN … with **statistical model calculations** … indicate an absence of higher spins in ERs for ^{30}Si+^{170}Er … lowering of spin value is **attributed to non-compound fission**.

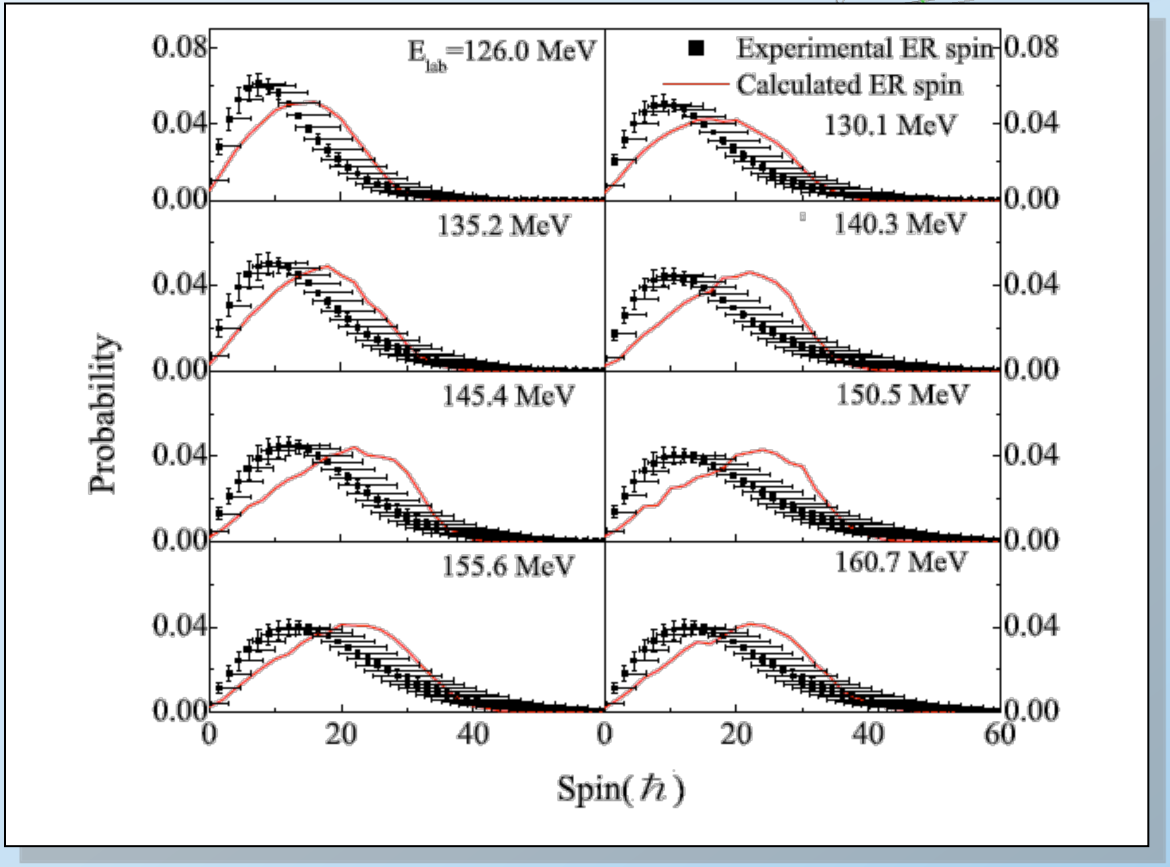

HYRA + T.I.F.R. 4π spin spectrometer at the IUAC, New Delhi

Fig. 11. Calculated and experimentally obtained ER spin distribution for the reaction 30Si+170Er. The experimental ER spin is the spin remaining after particle evaporation. It is obtained by multiplying the gamma-multiplicity by 1.5¯h.

The concept of multiple barriers
– coupling to inelastic channels

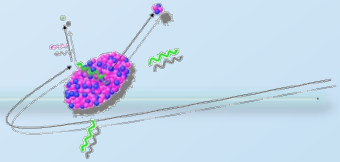

Competing reaction channels modify the interaction barrier

- inelastic excitation of either reaction partner

  vibrational nuclear excitation

  → barrier fluctuations

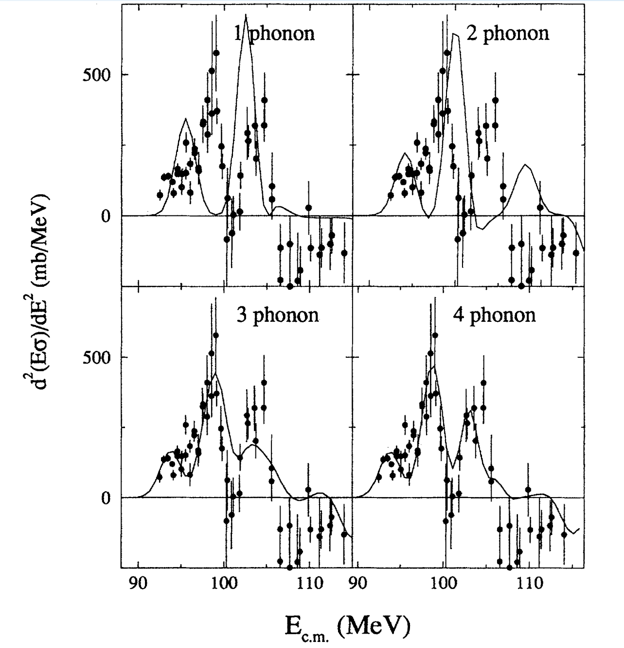

coupling to phonon states

→ collective vibrations

→ convergence after 3-phonon coupling

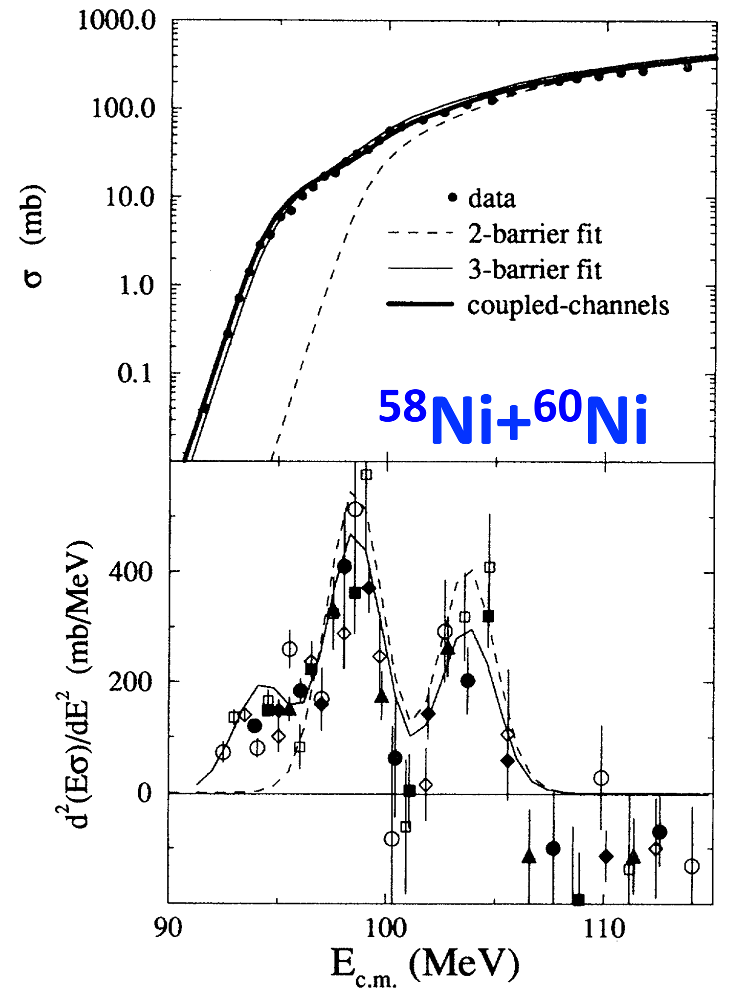

A.M. Strefanini et al., PRL 74 (1995) 864

The concept of multiple barriers
– coupling to inelastic channels

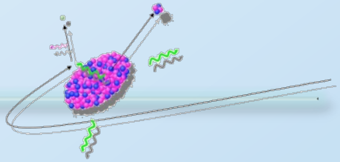

Competing reaction channels modify the interaction barrier

- inelastic excitation of either reaction partner
  vibrational nuclear excitation
  → barrier fluctuations

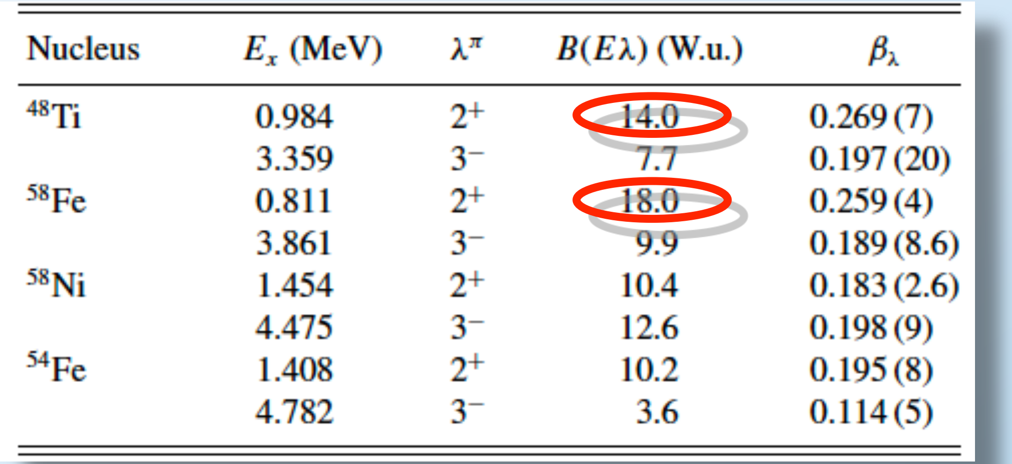

Nucleus	E_x (MeV)	λ^π	$B(E\lambda)$ (W.u.)	β_λ
^{48}Ti	0.984	2^+	14.0	0.269 (7)
	3.359	3^-	7.7	0.197 (20)
^{58}Fe	0.811	2^+	18.0	0.259 (4)
	3.861	3^-	9.9	0.189 (8.6)
^{58}Ni	1.454	2^+	10.4	0.183 (2.6)
	4.475	3^-	12.6	0.198 (9)
^{54}Fe	1.408	2^+	10.2	0.195 (8)
	4.782	3^-	3.6	0.114 (5)

differences in nuclear structure features

→ different behavior far below the barrier

→ fusion is hindered in one of the two systems

→ relevance for astrophysics (discussed later)

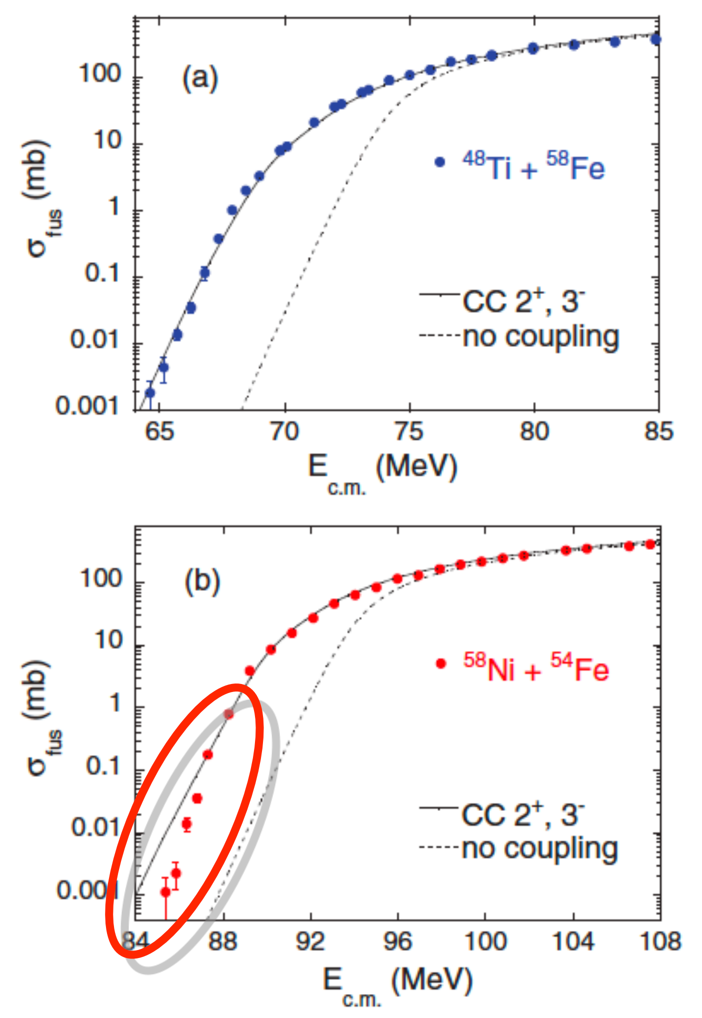

A.M. Strefanini et al., PRC 92 (2015) 064607

The concept of multiple barriers
– coupling to transfer channels

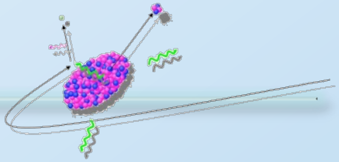

Competing reaction channels modify the interaction barrier

- nucleon transfer between the reaction partners
  proton-neutron ratio is modified
  Q-value effects
  problem: form factor

$$[F(r)]_p = \frac{\beta_p}{3A} R_0 \frac{\partial U_{aA}(r)}{\partial r}$$

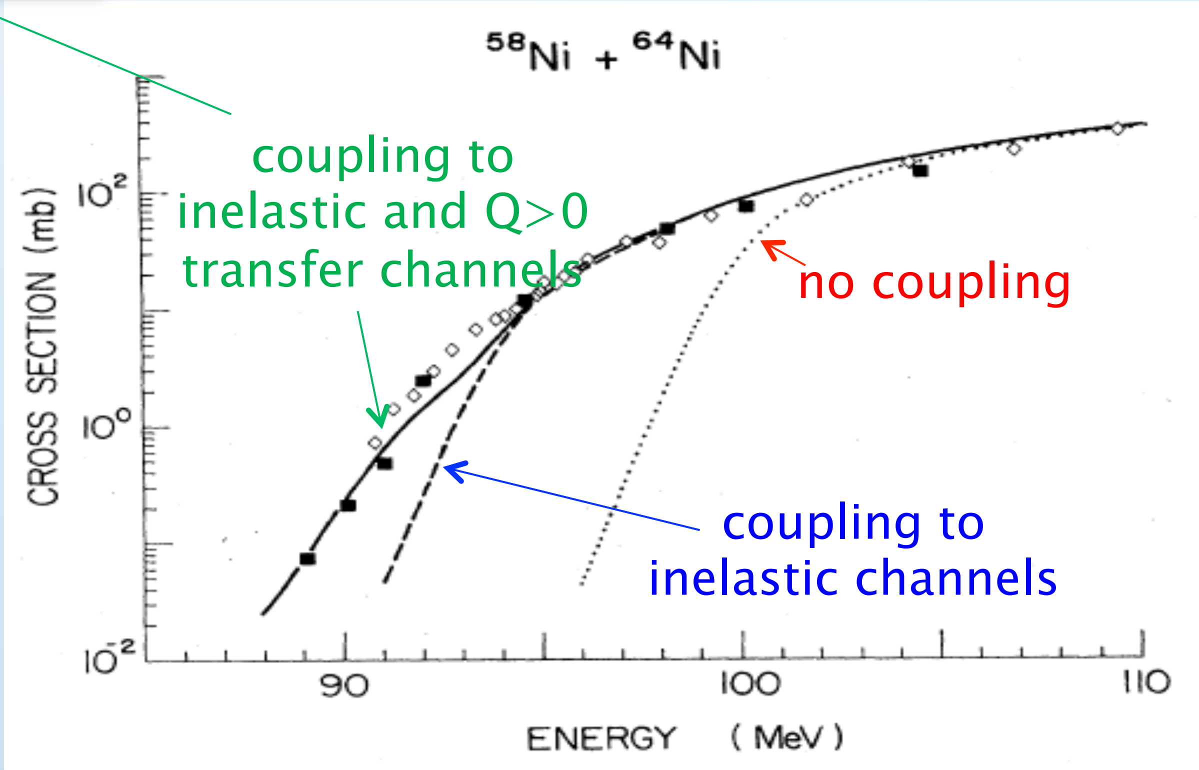

coupling to
inelastic and Q>0
transfer channels

no coupling

coupling to
inelastic channels

R.A.Broglia, C.H.Dasso and S.Landowne, PRC32(1985)1426

The Region of Superheavy Elements

- methods and state of the art

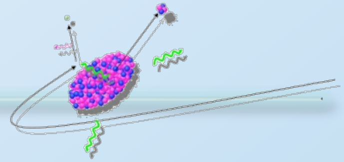

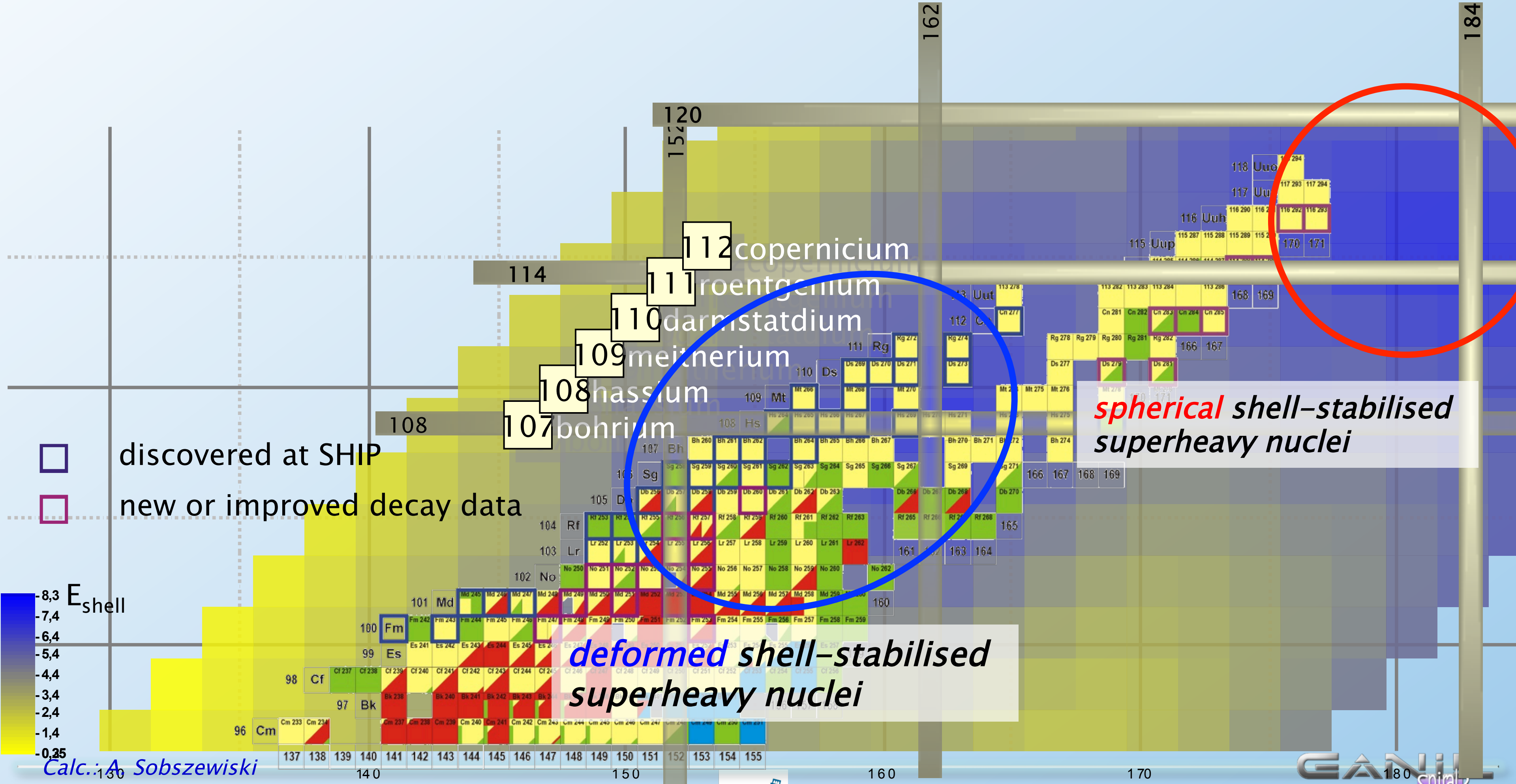

☐ discovered at SHIP

☐ new or improved decay data

spherical shell-stabilised superheavy nuclei

deformed shell-stabilised superheavy nuclei

Calc.: A. Sobszewiski

The Region of Superheavy Elements

- methods and state of the art

0.1 µbarn →

maximum measured cross sections

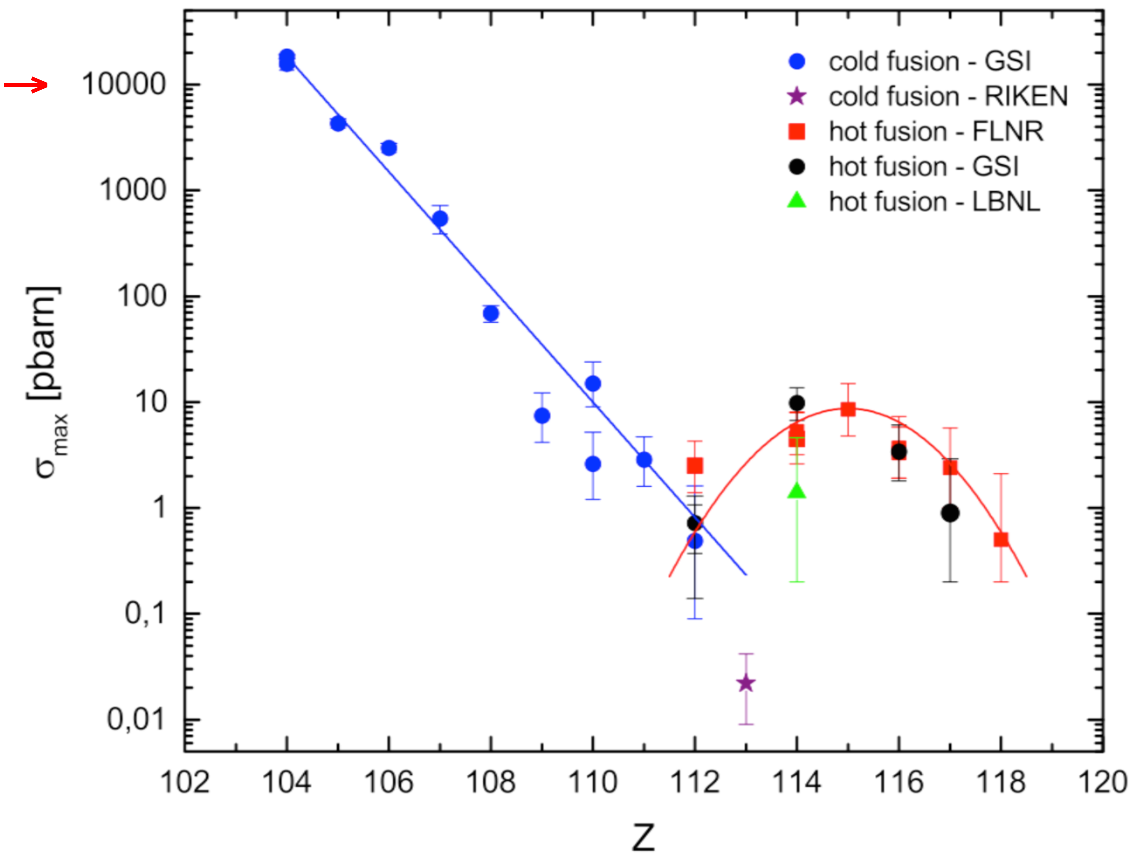

☐ disco

☐ new c

E_{shell}
8,3
7,4
6,4
5,4
4,4
3,4
2,4
1,4
0,25

tabilised
ei

184

130 140 150 160 170 180

137 138 139 140 141 142 143 144 145 146 147 148 149 150 151 152 153 154 155

Calc.: A. Sobszewiski

Fusion/Fission Competition for SHE
- Liquid Drop + Shell Corrections

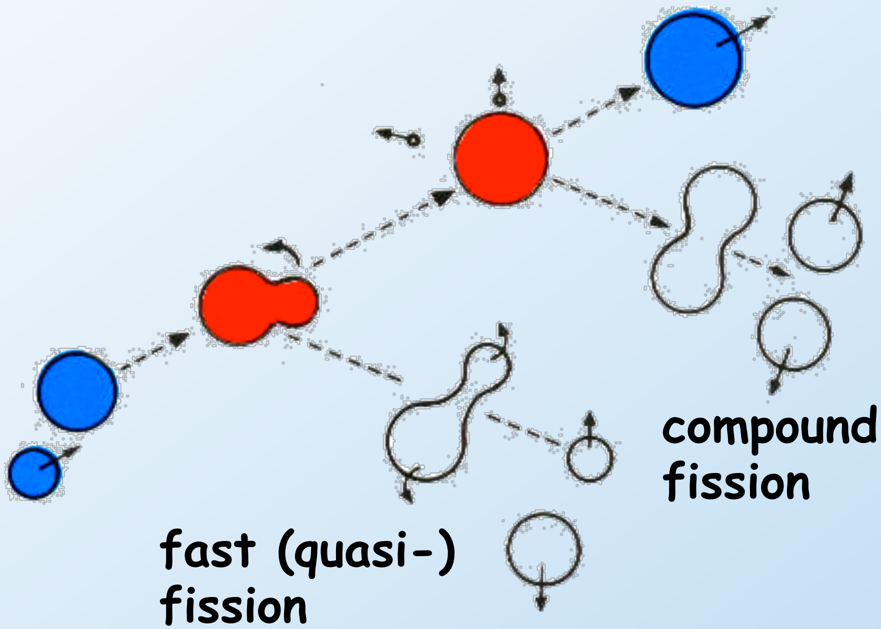

evaporation residue survival

compound fission

fast (quasi-) fission

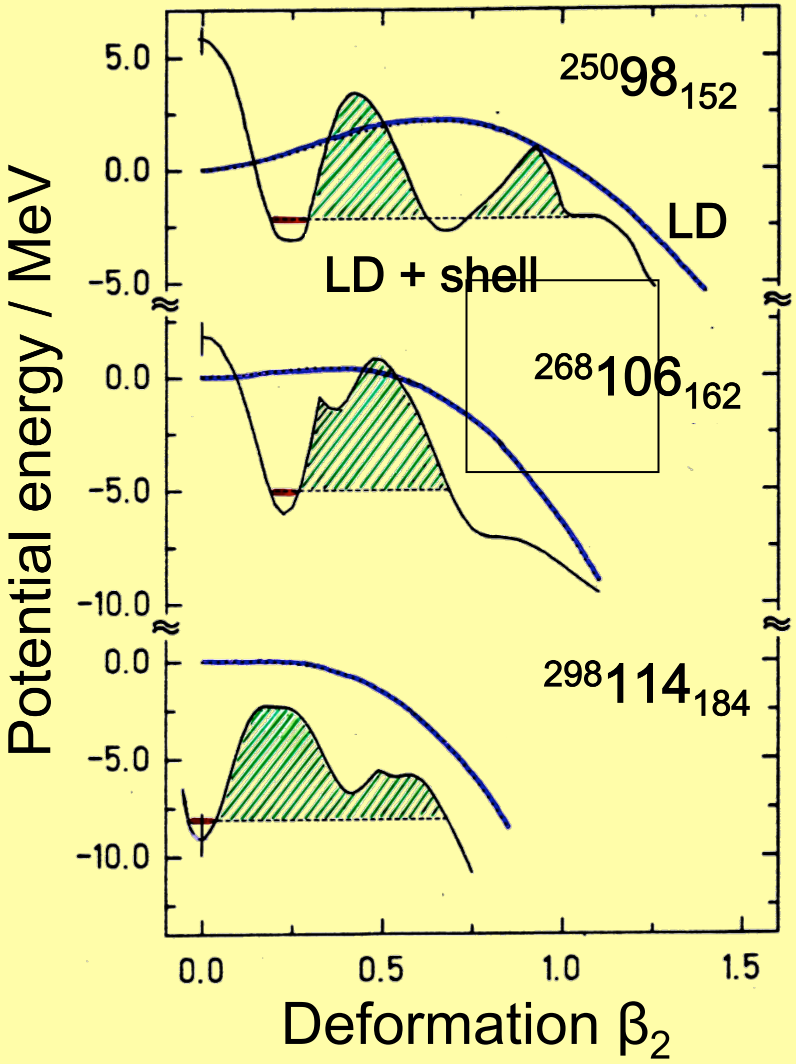

A. Sobiczewski et al.

The (simplified) 2-step process
- Fusion - Evaporation

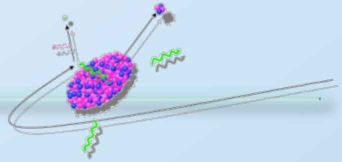

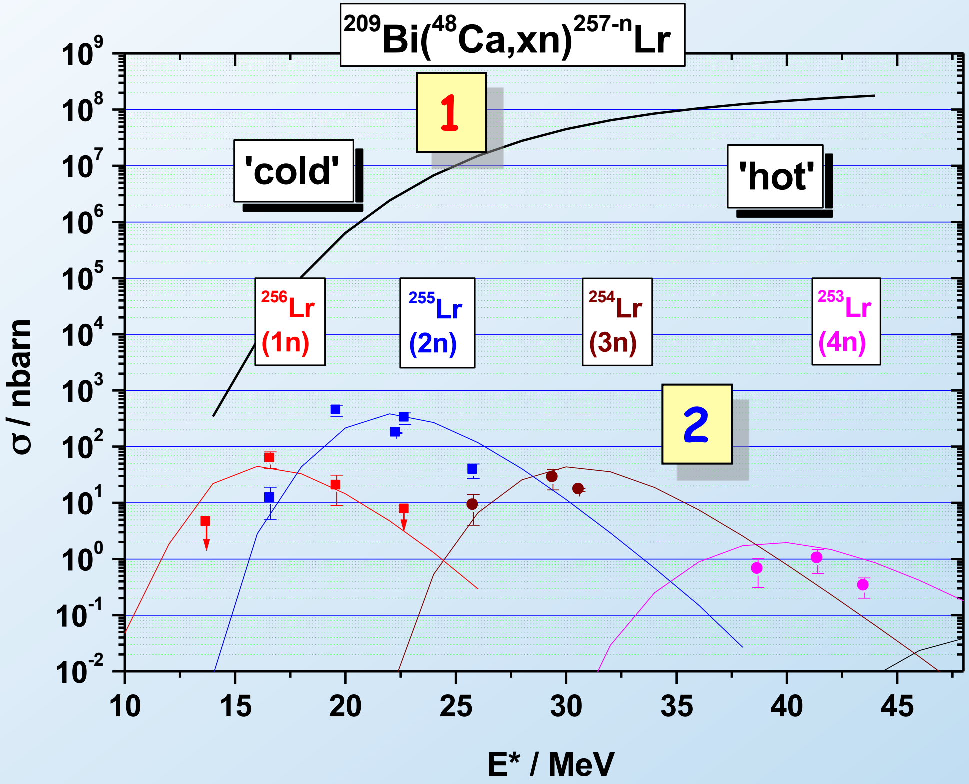

F.P.Heßberger 2.5.2005

1. **compound nucleus (CN) formation**

   - entrance channel properties

   coupling to competing channels:
   nuclear structure, deformation, …

2. **Evaporation residue (ER) formation**

   - surviving de-excitation

   competition
   fission-neutron emission:

Γ_n/Γ_f

Γ_n: n-emission probability
Γ_f: fission probability

Excitation functions for Z≥104

- cross section as a function of the E*

- after subtraction of $E_{bin}(xn)$ maxima coincide

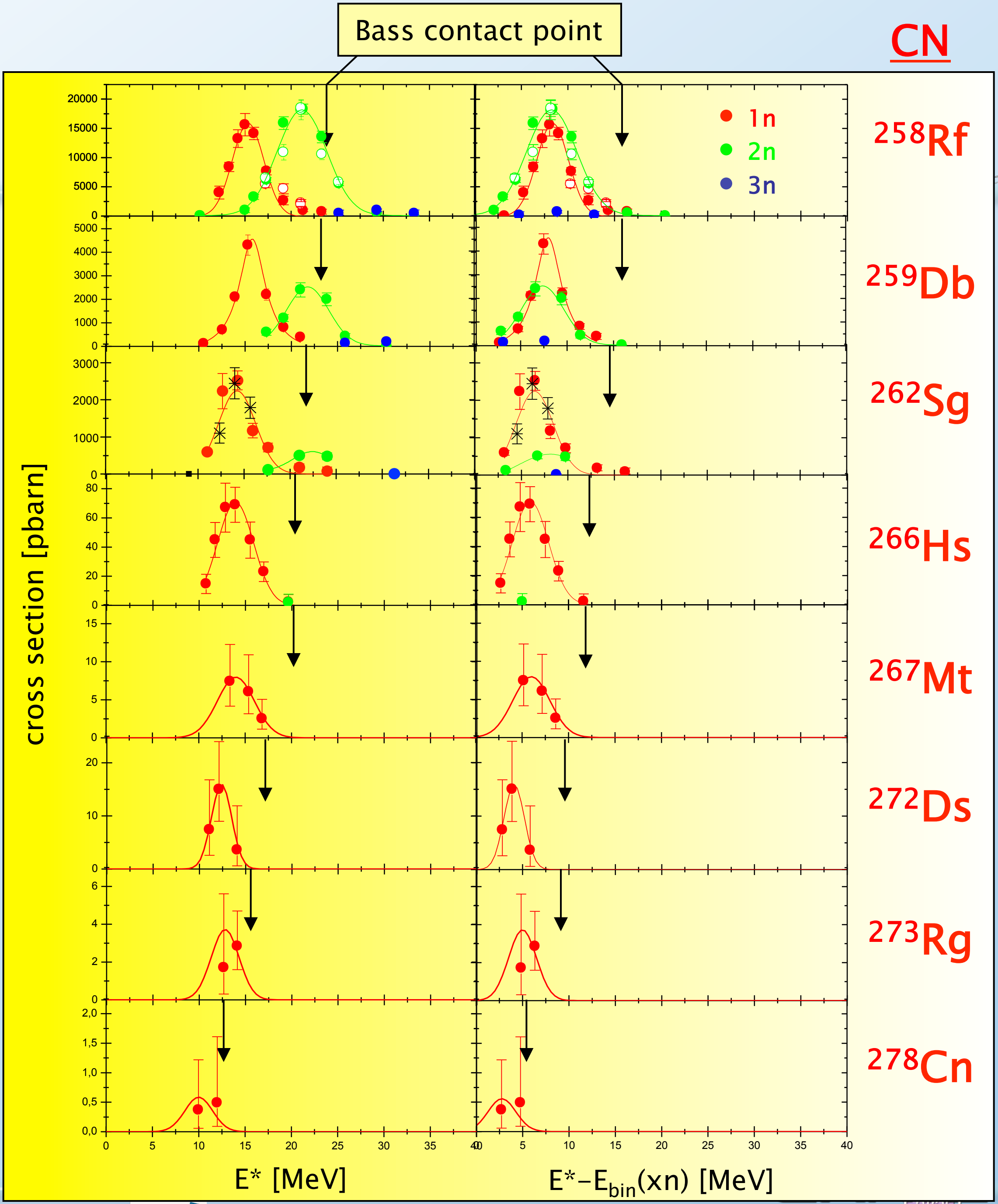

Synthesis and Identification of SHE at SHIP

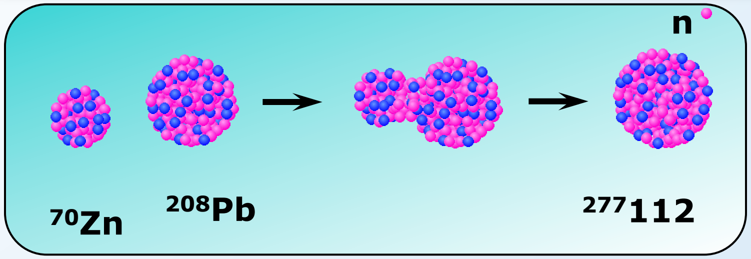

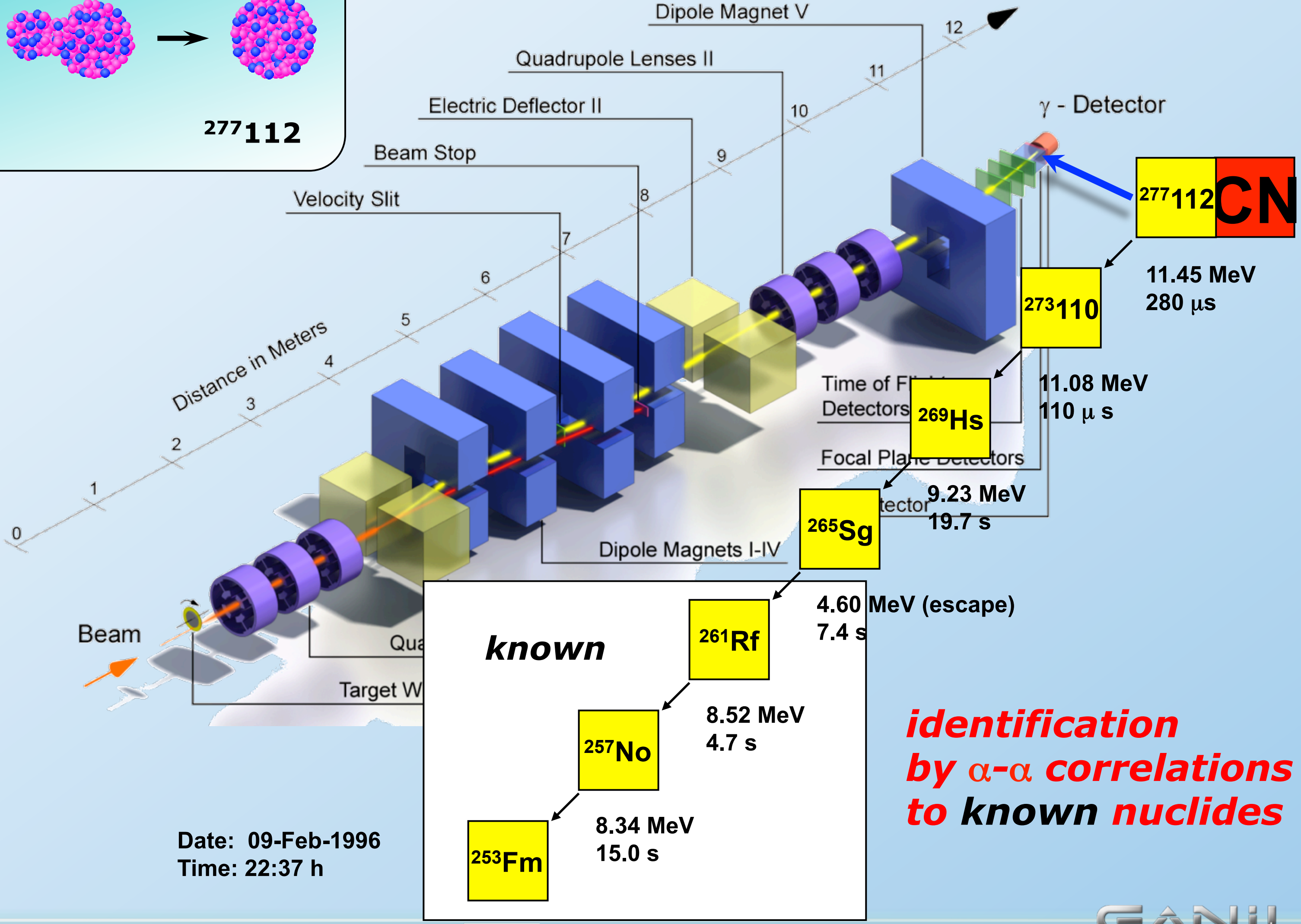

Date: 09-Feb-1996
Time: 22:37 h

kinematic separation in flight

identification by α-α correlations to known nuclides

ER-α Correlation method

- Example: $^{58}Fe + ^{209}Bi \rightarrow ^{266}Mt + 1n$

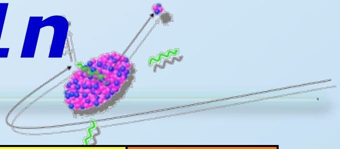

Si (STOP) detector

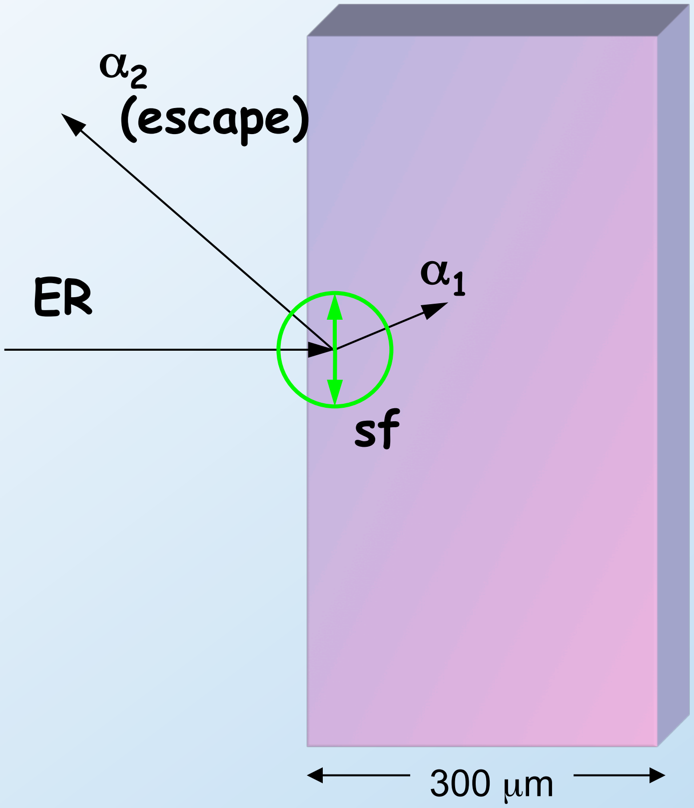

date: August 29th 1982
time: 16:10 h

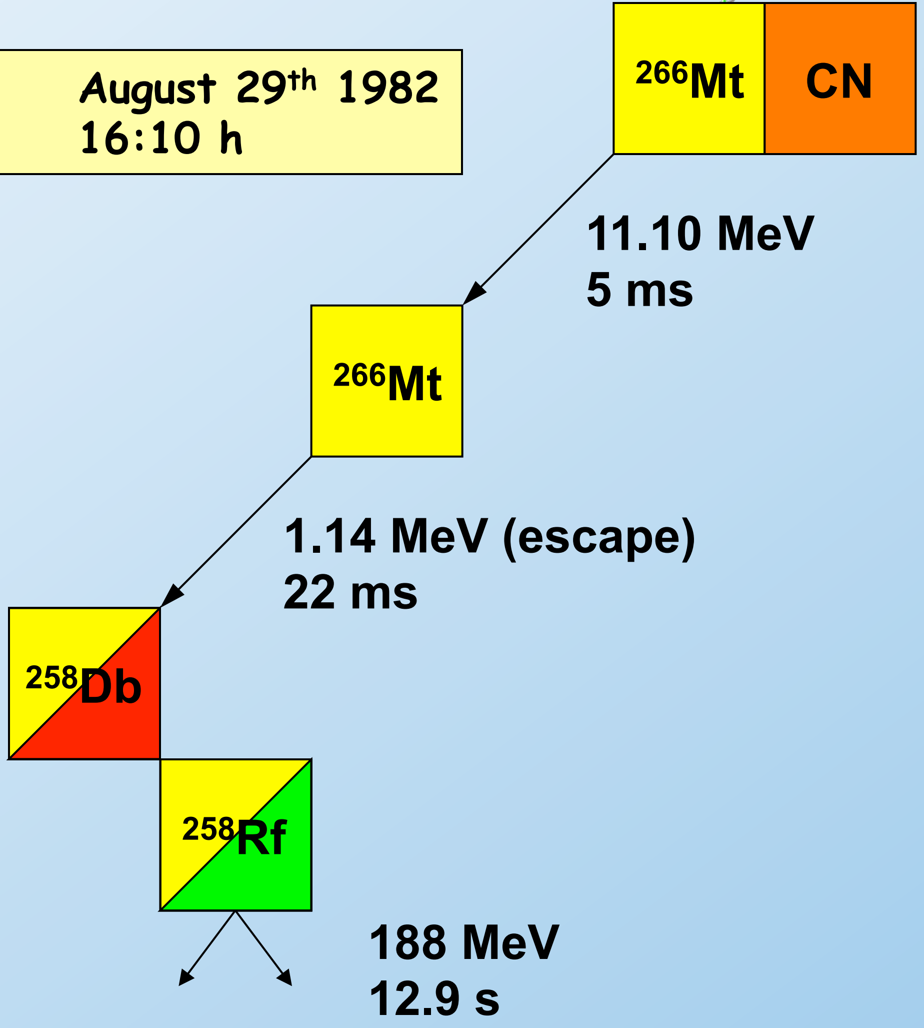

Revelation of escape α's

- "Backward Box" SI detector array

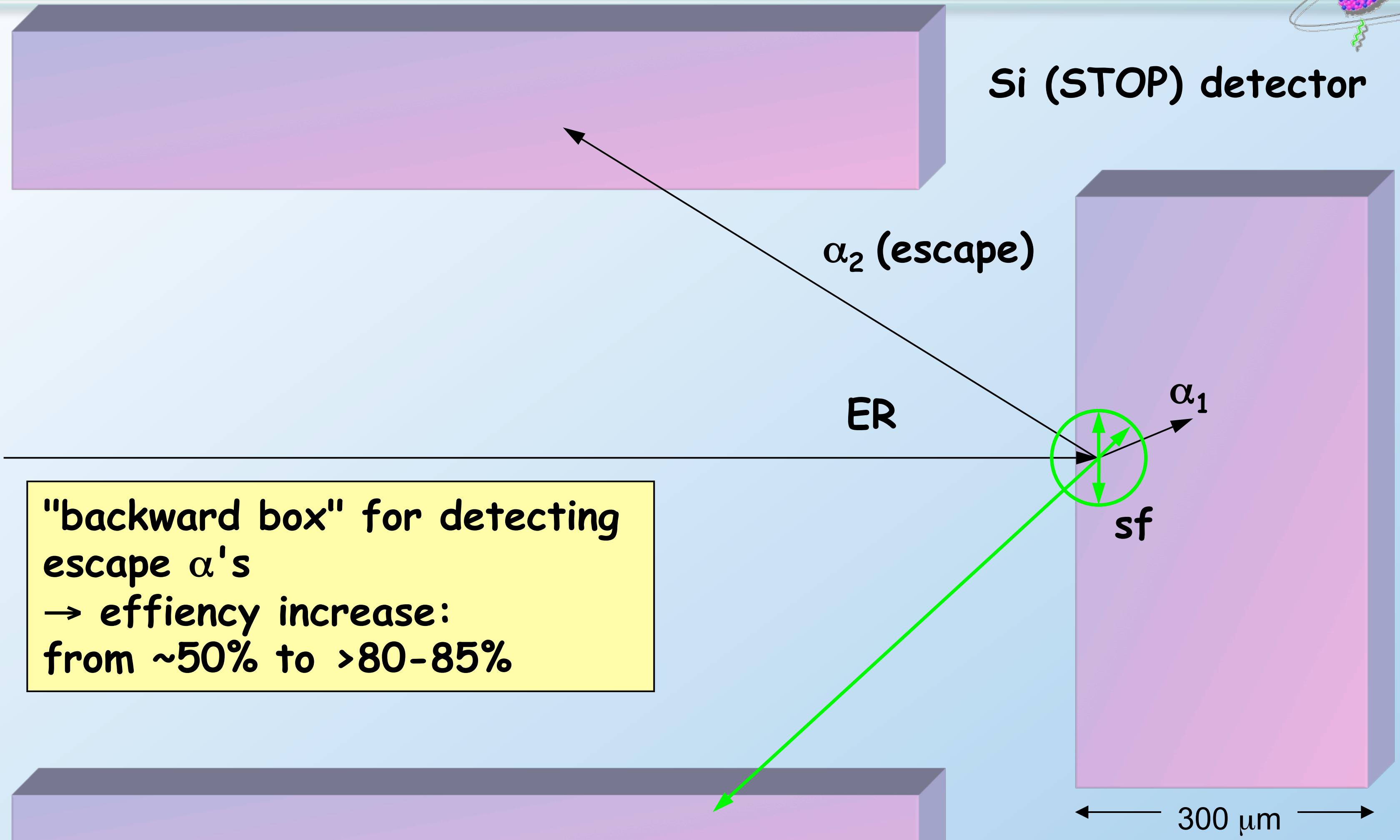

"backward box" for detecting escape α's
→ effiency increase:
from ~50% to >80-85%

"Hot Fusion" Studies

- ^{48}Ca (et al.) Induced Reactions on Actinide Targets

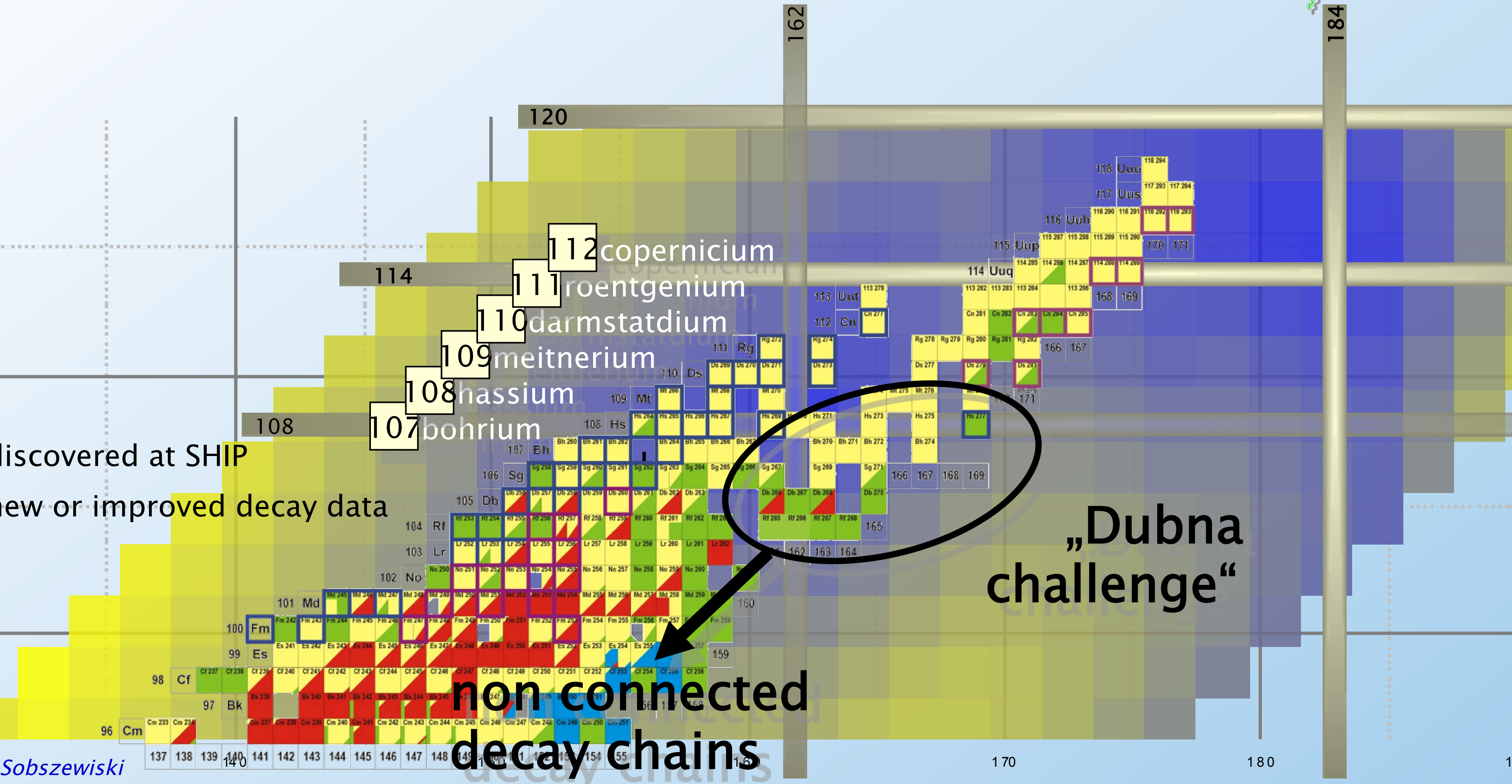

„Dubna challenge“

non connected decay chains

Comparison with FLNR Results

- ^{48}Ca+^{244}Pu→ ^{288}114+4n

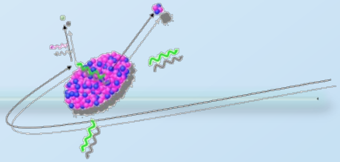

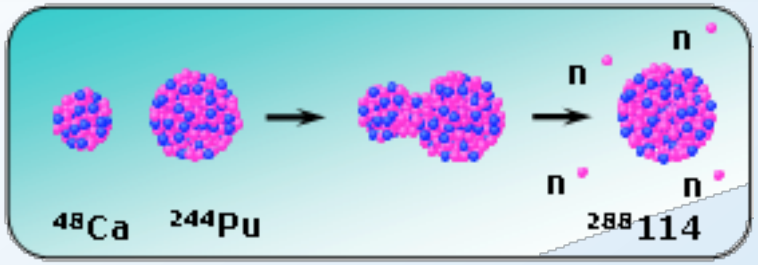

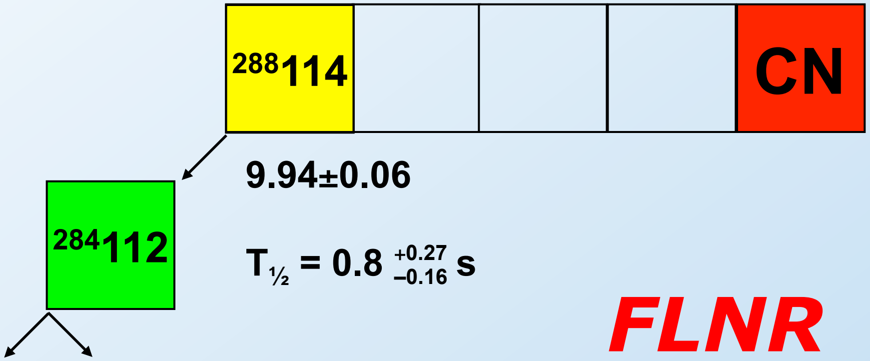

9.94±0.06

$T_{1/2} = 0.8^{+0.27}_{-0.16}$ s

FLNR

216^{+30}_{-15} MeV

$T_{1/2} = 97^{+31}_{-19}$ ms

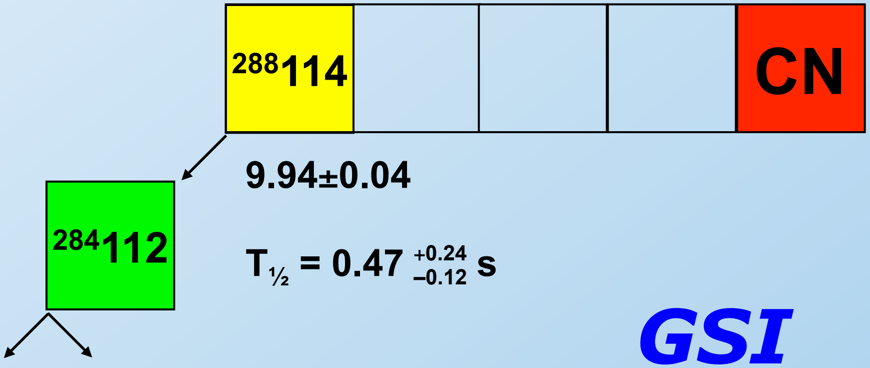

9.94±0.04

$T_{1/2} = 0.47^{+0.24}_{-0.12}$ s

GSI

$T_{1/2} = 101^{+50}_{-25}$ ms

$\sigma_{max} = 9.8^{+3.9}_{-3.1}$ pbarn

a total of 9 chains at TASCA

Yu.Ts. Oganessian, J. Phys. G 34 (2007) R165

Ch. Düllmann et al., Phys. Rev. Lett. 104 (2010) 252701

Comparison with FLNR Results

- ^{48}Ca+^{244}Pu→ ^{289}114+3n

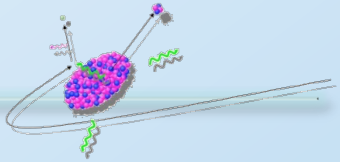

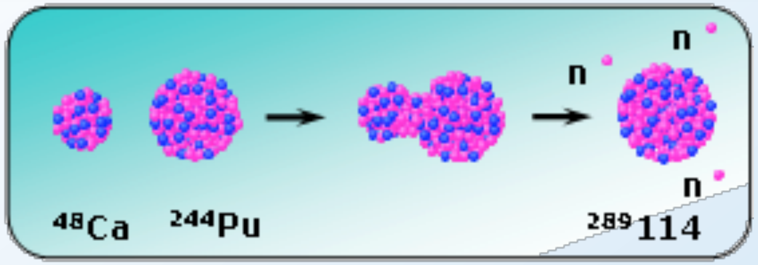

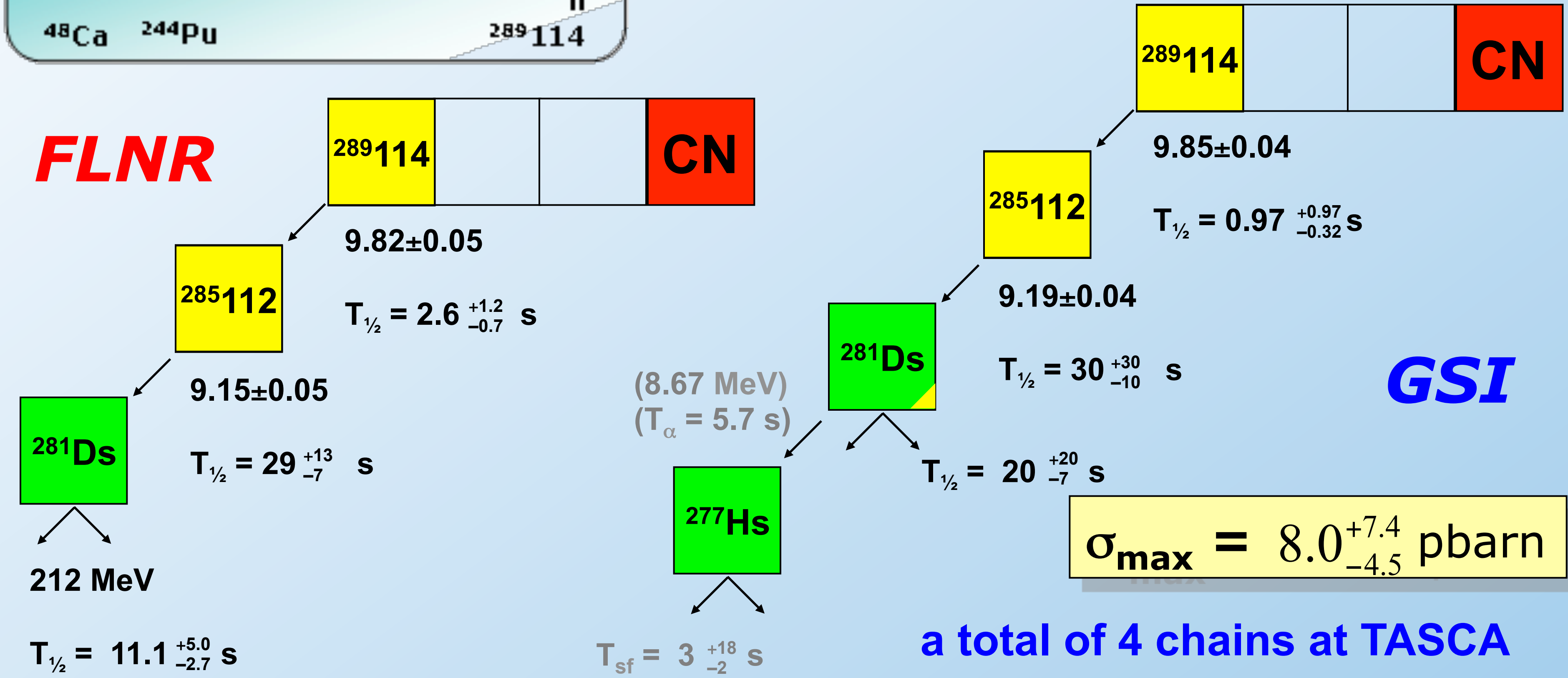

FLNR

^{289}114 | CN

9.82±0.05

$T_{1/2}$ = 2.6 $^{+1.2}_{-0.7}$ s

^{285}112

9.15±0.05

$T_{1/2}$ = 29 $^{+13}_{-7}$ s

^{281}Ds

212 MeV

$T_{1/2}$ = 11.1 $^{+5.0}_{-2.7}$ s

GSI

^{289}114 | CN

9.85±0.04

$T_{1/2}$ = 0.97 $^{+0.97}_{-0.32}$ s

^{285}112

9.19±0.04

$T_{1/2}$ = 30 $^{+30}_{-10}$ s

^{281}Ds

(8.67 MeV)
(T_{α} = 5.7 s)

$T_{1/2}$ = 20 $^{+20}_{-7}$ s

^{277}Hs

T_{sf} = 3 $^{+18}_{-2}$ s

$$\sigma_{max} = 8.0^{+7.4}_{-4.5} \text{ pbarn}$$

a total of 4 chains at TASCA

Yu.Ts. Oganessian, J. Phys. G 34 (2007) R165

Ch. Düllmann et al., Phys. Rev. Lett. 104 (2010) 252701

The "Dubna Challenge"
- ^{48}Ca + ^{248}Cm → ^{296}116* at GSI

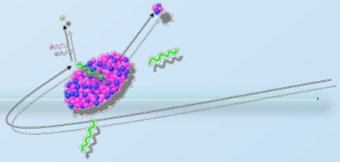

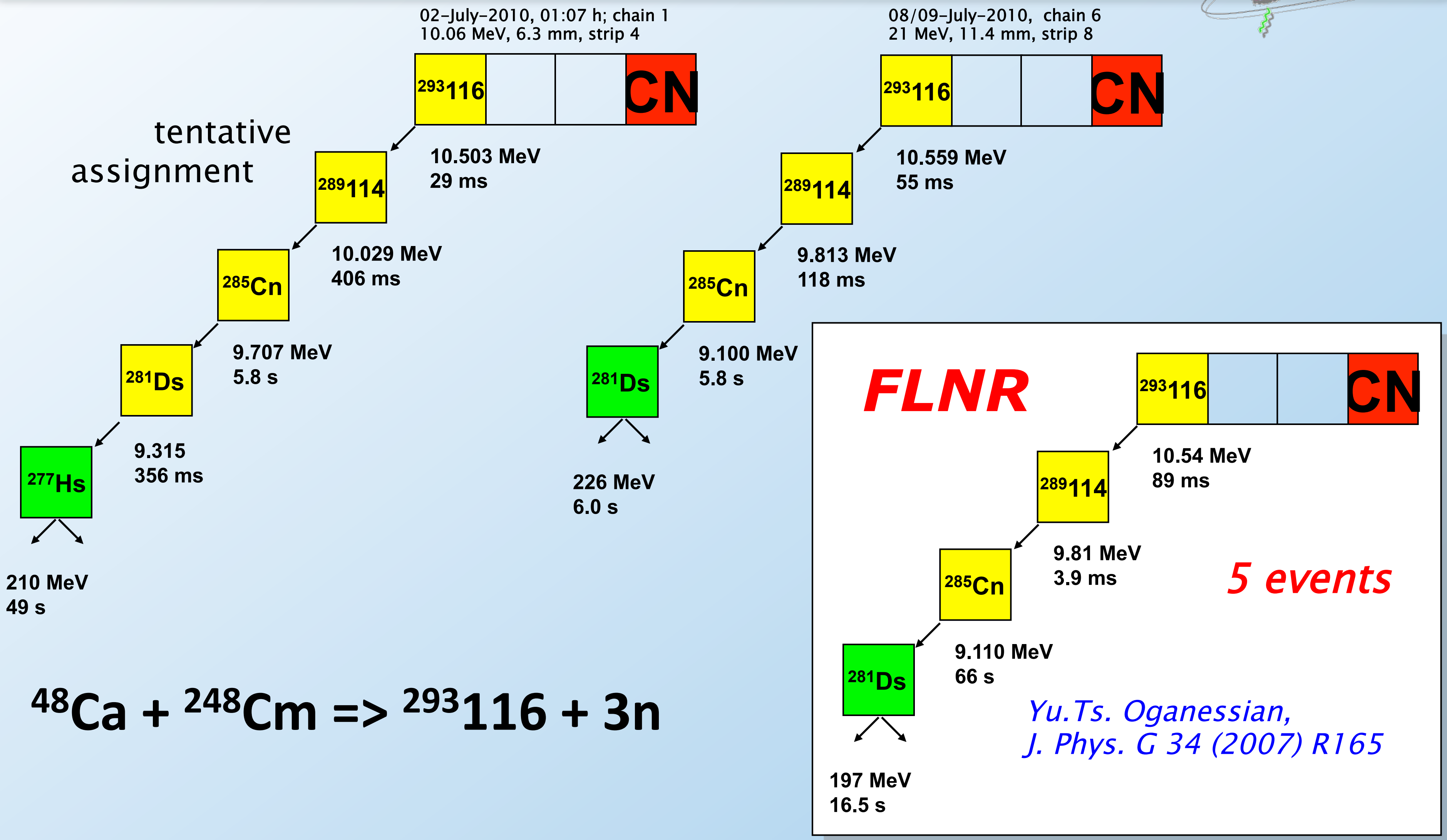

02–July–2010, 01:07 h; chain 1
10.06 MeV, 6.3 mm, strip 4

tentative assignment

^{293}116 | CN

10.503 MeV
29 ms

^{289}114

10.029 MeV
406 ms

^{285}Cn

9.707 MeV
5.8 s

^{281}Ds

9.315
356 ms

^{277}Hs

210 MeV
49 s

08/09–July–2010, chain 6
21 MeV, 11.4 mm, strip 8

^{293}116 | CN

10.559 MeV
55 ms

^{289}114

9.813 MeV
118 ms

^{285}Cn

9.100 MeV
5.8 s

^{281}Ds

226 MeV
6.0 s

FLNR

^{293}116 | CN

10.54 MeV
89 ms

^{289}114

9.81 MeV
3.9 ms

^{285}Cn

9.110 MeV
66 s

^{281}Ds

197 MeV
16.5 s

5 events

Yu.Ts. Oganessian,
J. Phys. G 34 (2007) R165

$$^{48}\mathrm{Ca} + {}^{248}\mathrm{Cm} \Rightarrow {}^{293}116 + 3n$$

The "Dubna Challenge"

- ^{48}Ca + ^{248}Cm → ^{296}116* at GSI

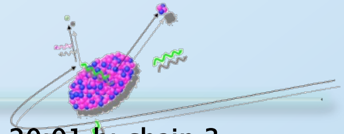

02–July–2010, 01:57 h; chain 2
8.96 MeV, 10.4 mm, strip 4

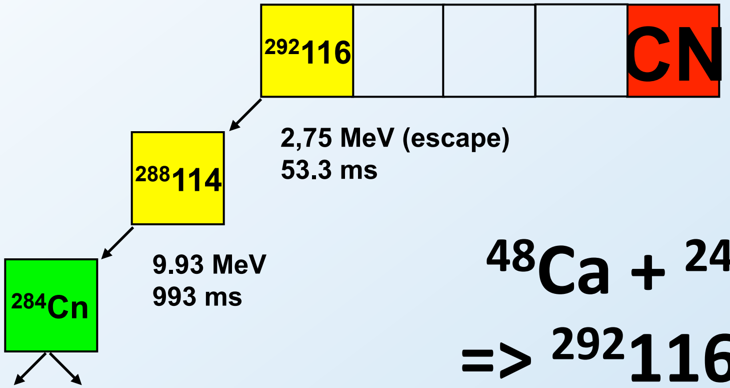

2,75 MeV (escape)
53.3 ms

9.93 MeV
993 ms

03–July–2010, 20:01 h; chain 3
18 MeV, 27.4 mm, strip 2

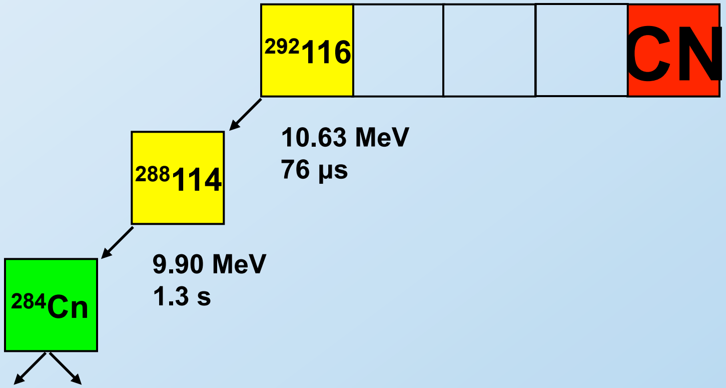

10.63 MeV
76 μs

9.90 MeV
1.3 s

^{48}Ca + ^{248}Cm
=> ^{292}116 + 4n

172
50 m

197 MeV
269 ms

28

195
121 ms

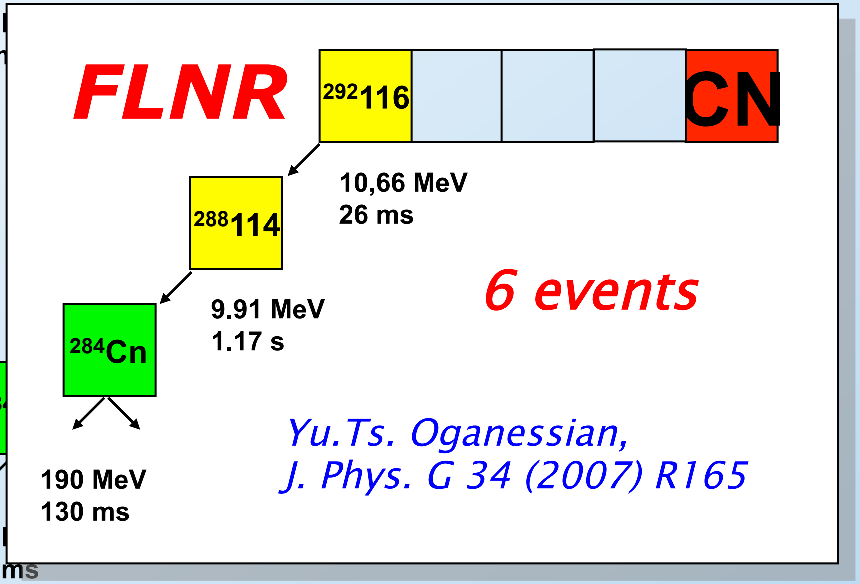

FLNR

10,66 MeV
26 ms

9.91 MeV
1.17 s

190 MeV
130 ms

6 events

Yu.Ts. Oganessian,
J. Phys. G 34 (2007) R165

07–July–2010, 09:01 h; chain 5
21 MeV, 28 mm, strip 12

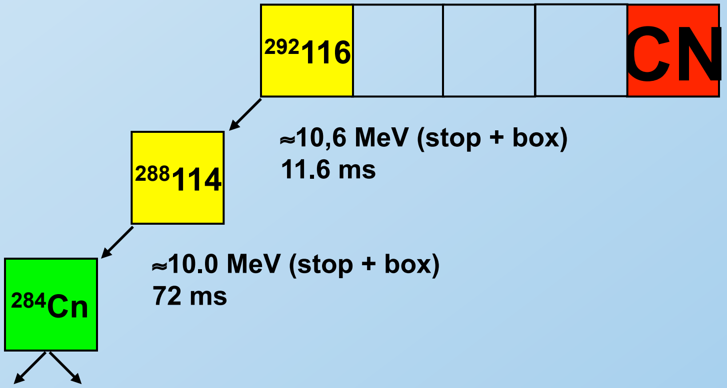

≈10,6 MeV (stop + box)
11.6 ms

≈10.0 MeV (stop + box)
72 ms

185 MeV
25 ms

The "Dubna Challenge"
- ^{48}Ca + ^{248}Cm $\rightarrow$ ^{296}116* at GSI

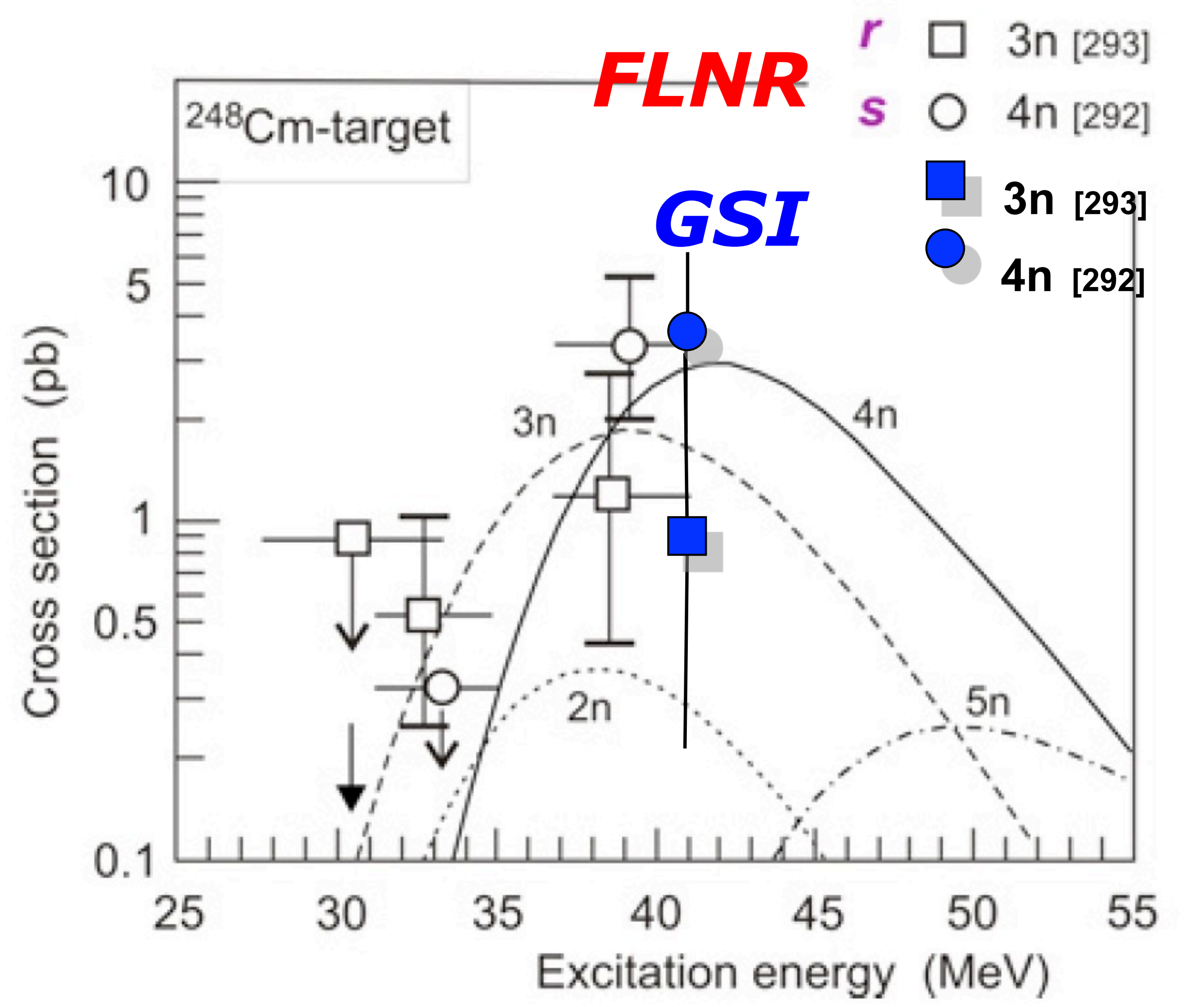

Yu.Ts. Oganessian, J. Phys. G 34 (2007) R165

V. Zagrebaev @FUSHE 2012

Cross Section Predictions and their Validity

**Predictive power
of theory
for hot fusion reactions**

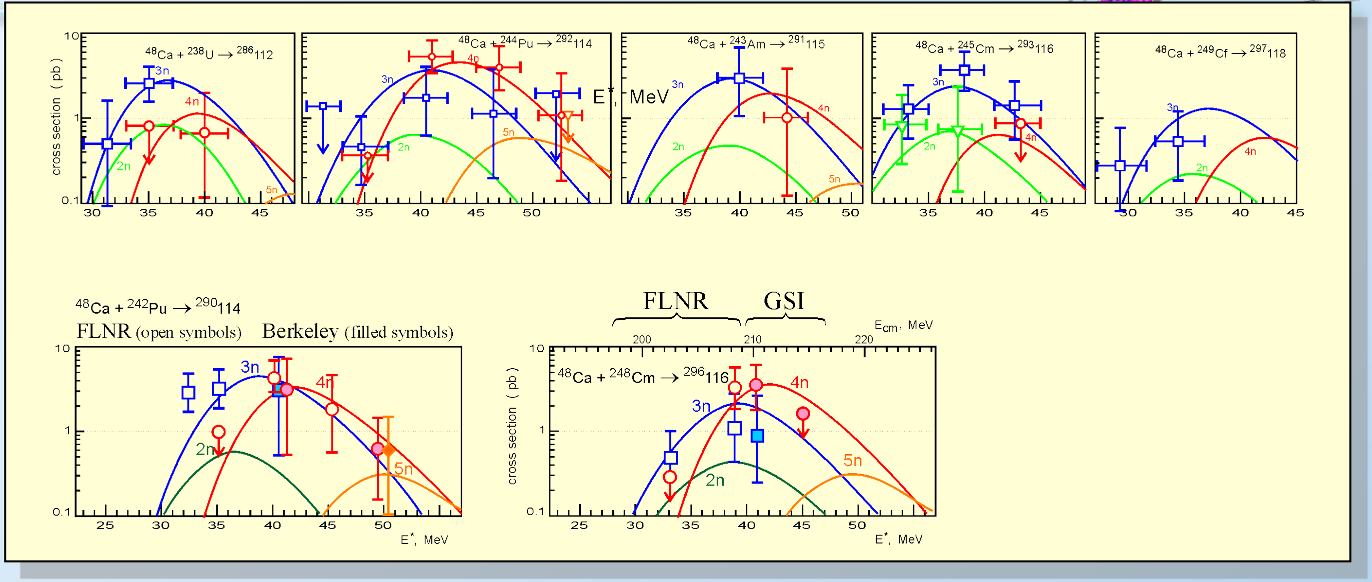

**looks quite impressive,
but…**

Synthesis of SHE
in **fusion reactions**
(theoretical problems
to be solved)

1. **Capture (contact) reaction stage**

   standard CC calculation:

   → no problems with predictions of capture cross sections (within factor 2 or 3)

2. **CN formation stage**

   two-center shell model and transport equations:

   - explicit potential energy surface?
   - appropriate degrees of freedom and equations of motion?
   - nuclear viscosity?
   - nucleon transfer rate?

   → uncertainty factor may vary from 10 to 1000

3. **Cooling stage**

   standard Statistical Model calculation:

   - collective enhancement factor in level density?
   - damping of shell corrections and fission barrier?
   - unknown fission barriers for SH nuclei?

   → uncertainty factor is about 10

(2 or 3) × 10 to 1000 × 10 = ?!!!

Confirmation of FLNR Results

- Summary

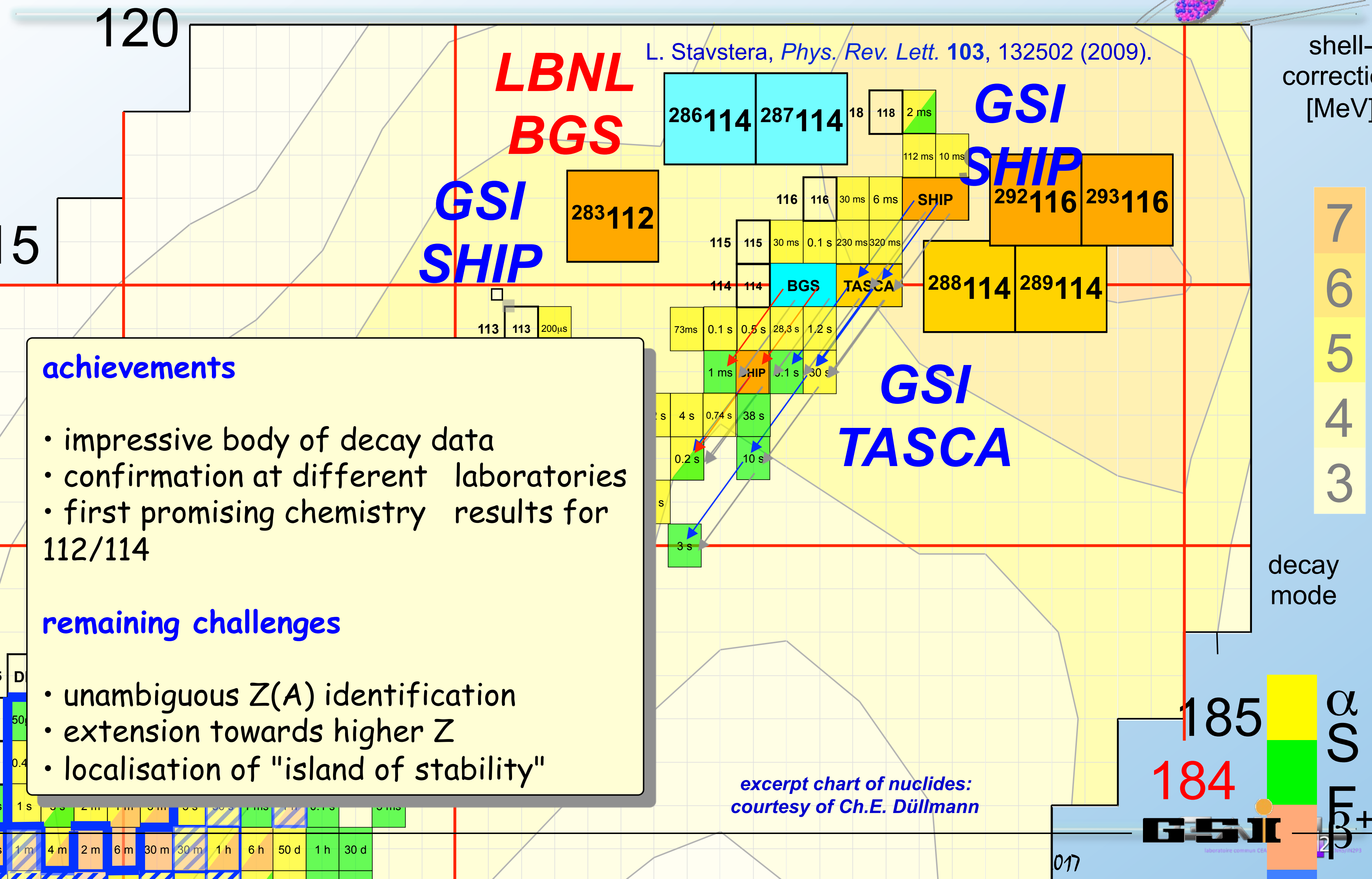

L. Stavstera, *Phys. Rev. Lett.* **103**, 132502 (2009).

achievements

- impressive body of decay data
- confirmation at different laboratories
- first promising chemistry results for 112/114

remaining challenges

- unambiguous Z(A) identification
- extension towards higher Z
- localisation of "island of stability"

excerpt chart of nuclides: courtesy of Ch.E. Düllmann

Hunt for the heaviest

- towards element 119,120 at SHIP and TASCA

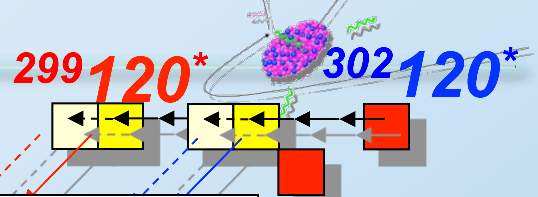

SHIP

1. $^{64}Ni + ^{238}U \rightarrow ^{302}120^*$ 2007/2008

   120 days / σ_{lim} < 0.09 pbarn

2. $^{54}Cr + ^{24}$

   36 days

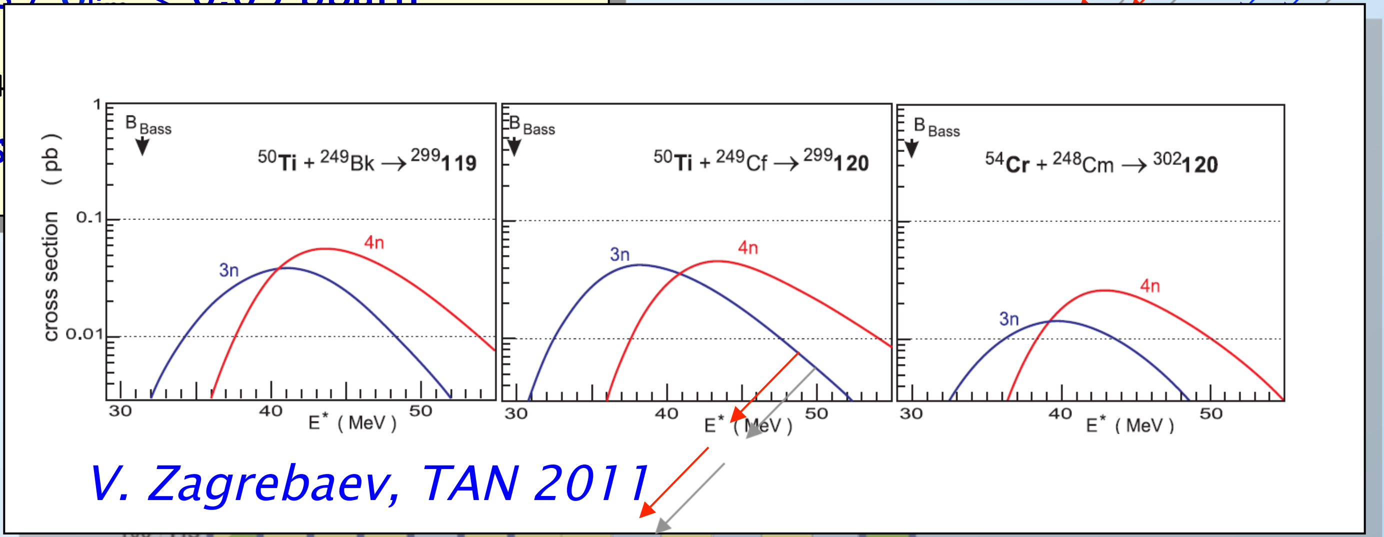

V. Zagrebaev, TAN 2011

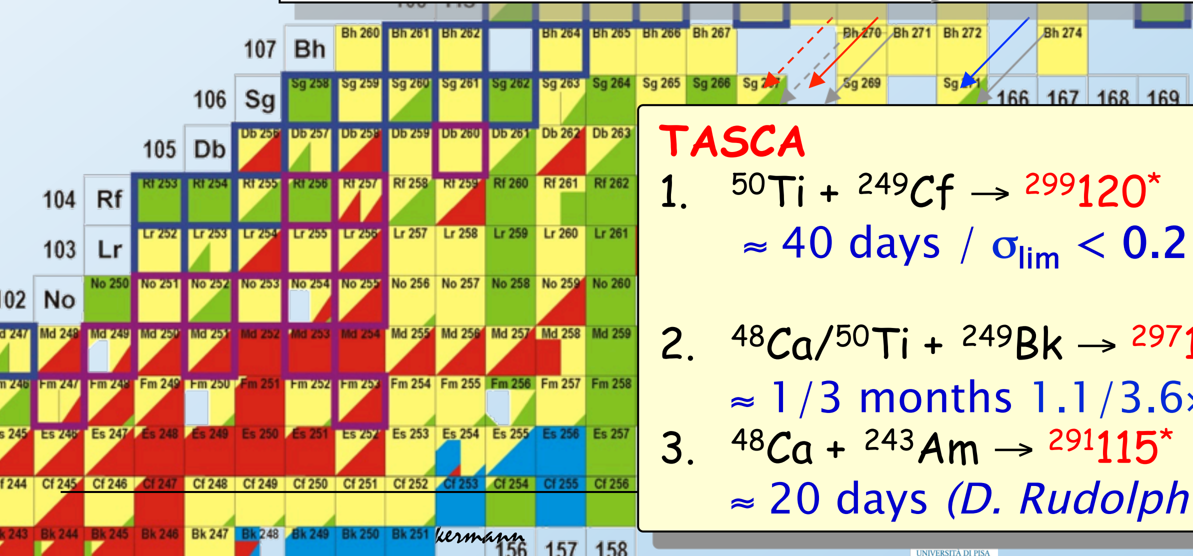

TASCA

1. $^{50}Ti + ^{249}Cf \rightarrow ^{299}120^*$ August-October 2011

   ≈ 40 days / σ_{lim} < 0.2 pbarn

2. $^{48}Ca/^{50}Ti + ^{249}Bk \rightarrow ^{297}117^*/^{299}119^*$ April-October 2012

   ≈ 1/3 months $1.1/3.6 \times 10^{19}$ projectiles on target

3. $^{48}Ca + ^{243}Am \rightarrow ^{291}115^*$ November 2012

   ≈ 20 days *(D. Rudolph et al. – charateristic X-rays)*

Hunt for the heaviest

- towards element 119,120 at SHIP and TASCA

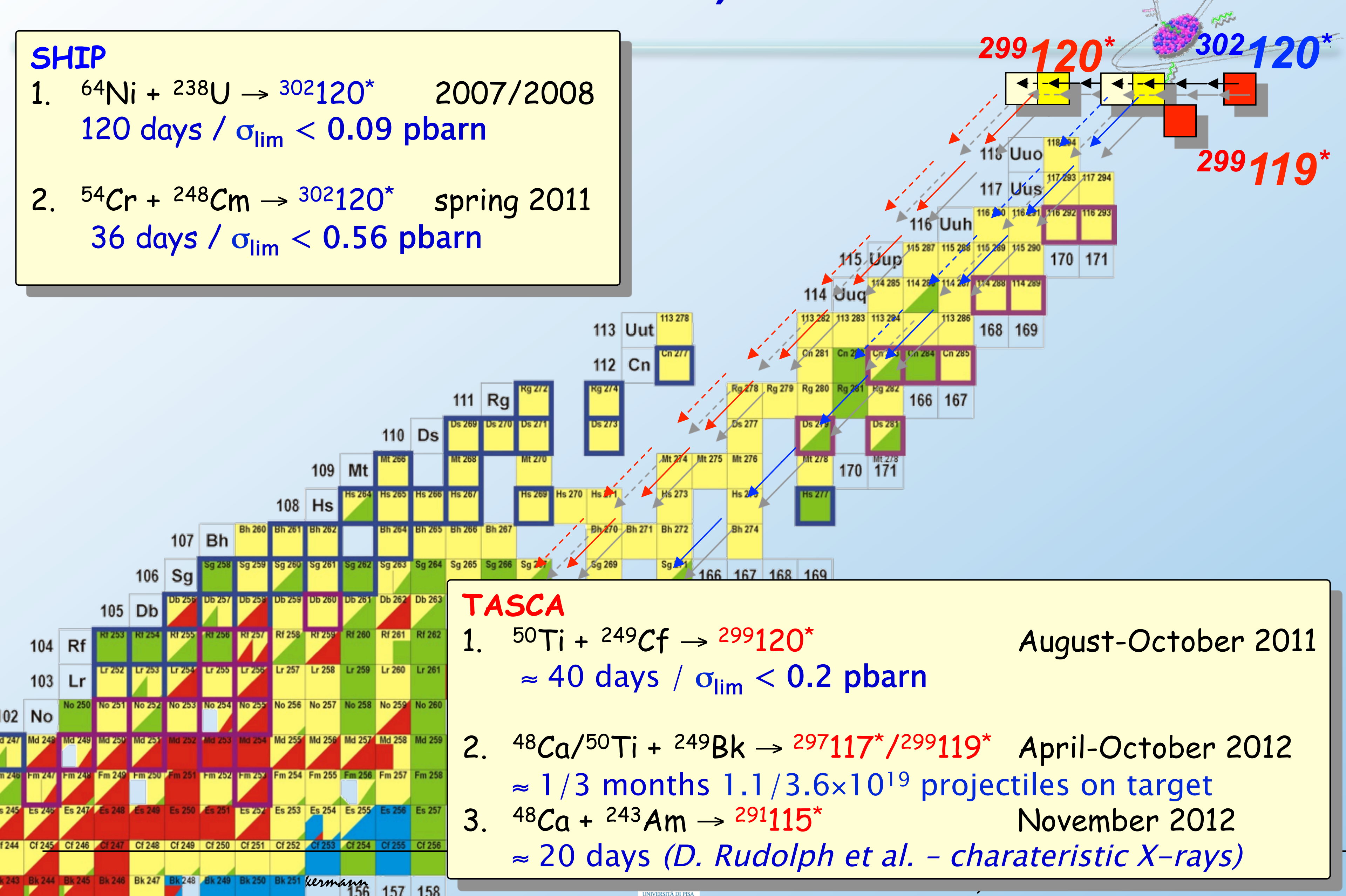

SHIP

1. ^{64}Ni + ^{238}U → ^{302}120* 2007/2008

   120 days / σ_{lim} < 0.09 pbarn

2. ^{54}Cr + ^{248}Cm → ^{302}120* spring 2011

   36 days / σ_{lim} < 0.56 pbarn

TASCA

1. ^{50}Ti + ^{249}Cf → ^{299}120* August-October 2011

   ≈ 40 days / σ_{lim} < 0.2 pbarn

2. ^{48}Ca/^{50}Ti + ^{249}Bk → ^{297}117*/^{299}119* April-October 2012

   ≈ 1/3 months 1.1/3.6×10^{19} projectiles on target

3. ^{48}Ca + ^{243}Am → ^{291}115* November 2012

   ≈ 20 days *(D. Rudolph et al. – charateristic X-rays)*

Hunt for the heaviest
- towards element 119,120 at SHIP and TASCA

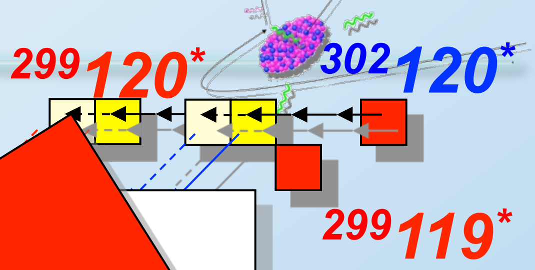

SHIP

1. ^{64}Ni + ^{238}U → ^{302}120* 2007/2008
   120 days / σ < 0.09 pbarn

2. ^{54}Cr + 24
   36 days

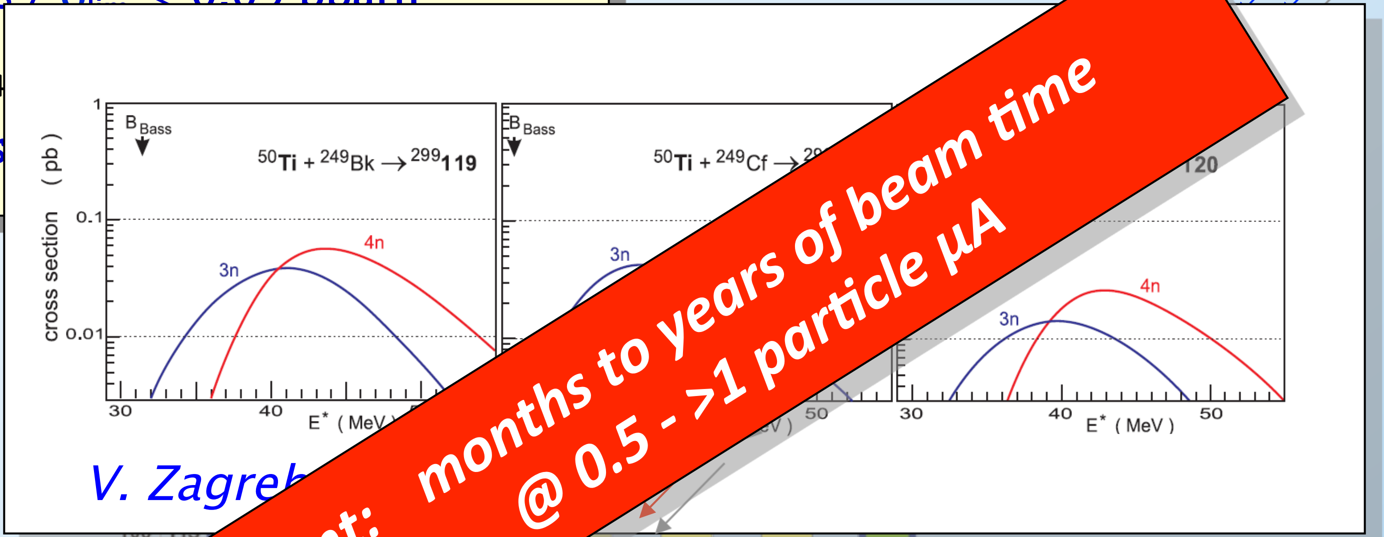

V. Zagreb

Requirement: months to years of beam time @ 0.5 - >1 particle μA

TASCA

1. ^{50}Ti + ^{249}Cf → ^{299}120* August-October 2011
   ≈ 40 days / σ_{lim} < 0.2 pbarn

2. ^{48}Ca/^{50}Ti + ^{249}Bk → ^{297}117*/^{299}119* April-October 2012
   ≈ 1/3 months 1.1/3.6×10^{19} projectiles on target

3. ^{48}Ca + ^{243}Am → ^{291}115* November 2012
   ≈ 20 days *(D. Rudolph et al. – charateristic X-rays)*

Multi nucleon transfer as a tool to study n-rich species
- Reaction dynamics

D. Ackermann, L. Corradi, E. Fioretto, D. Montanari, G. Montagnoli,
G. Pllatolo, F. Scarlassara, A.M. Stefanini, S. Szilner

investigation of transfer reaction dynamics

- n rich projectiles favor p pick-up/n stripping (light partner)
    - ➢ caution: n evaporation and (transfer induced) fission shifts towards stability

instrumental requirements:

- large acceptance magnetic (tracking) spectrometer (PRISMA/VAMOS type)
    - ➢ also in coincidence with particle and γ detector arrays
- detection of the heavy partner → high spatial and energy resolution (PRISMA:
    - Δx,Δy ≈ 1mm
    - $\Delta\theta_{in}$ ≈ 1°
    - ΔE ≈ 1%)

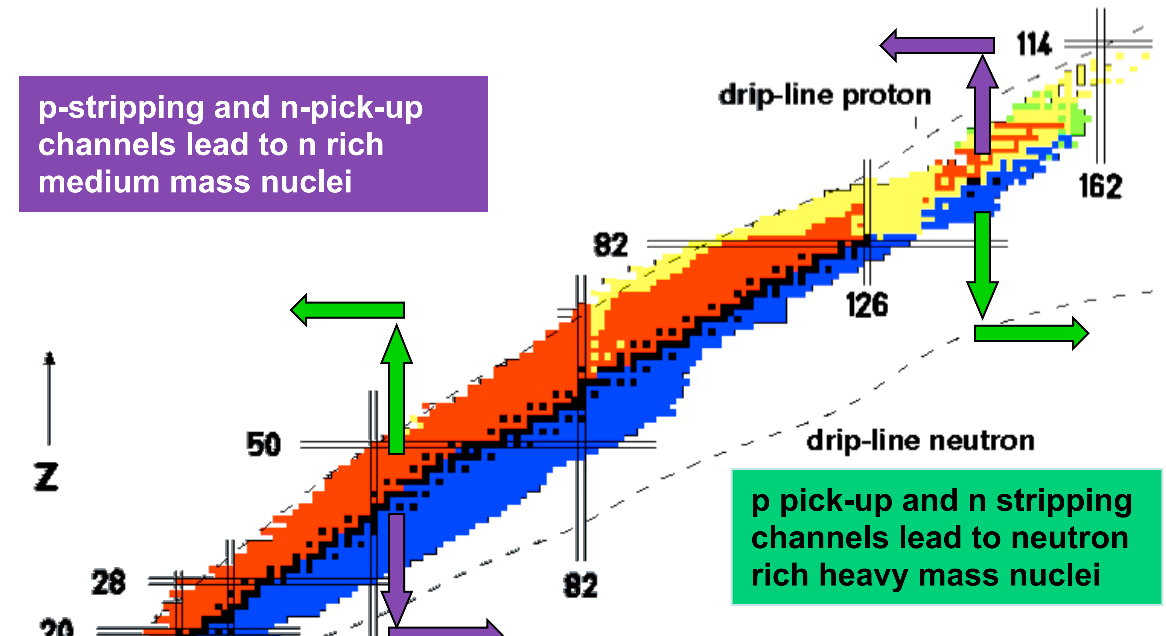

p-stripping and n-pick-up channels lead to n rich medium mass nuclei

p pick-up and n stripping channels lead to neutron rich heavy mass nuclei

PRISMA@LNL

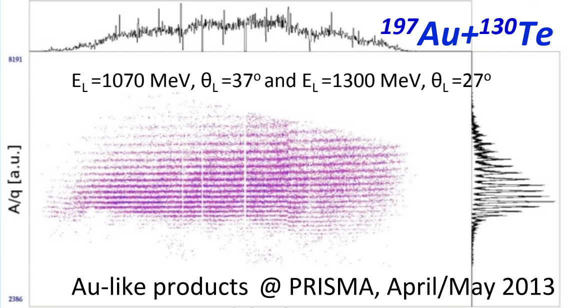

$^{197}Au+^{130}Te$

E_L=1070 MeV, θ_L=37° and E_L=1300 MeV, θ_L=27°

Au-like products @ PRISMA, April/May 2013

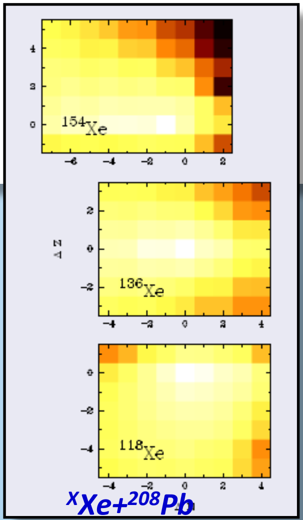

$^{x}Xe+^{208}Pb$

C.H. Dasso, G. Pollarolo, A. Winther, PRL73 (1994) 1907;

L. Corradi, G. Pollarolo, S. Szilner, J. of Phys. G 36 (2009) 113101

Multi nucleon transfer as a tool to study n-rich species

- research topics ...

D. Ackermann, L. Corradi, E. Fioretto, D. Montanari, G. Montagnoli,
G. Pllatolo, F. Scarlassara, A.M. Stefanini, S. Szilner

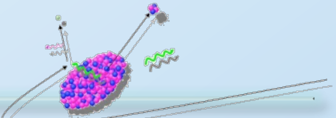

- **competitive with fragmentation – where and to what extent?**
- **complementarity**

J. Benlliure et al., Phys.Rev.C78 (2008) 054605

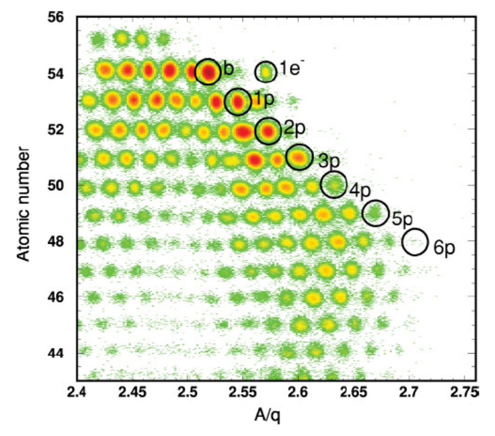

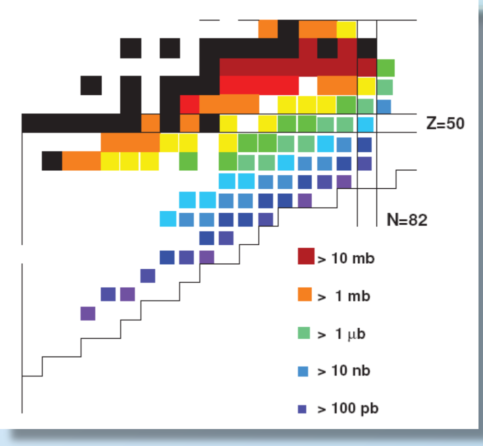

Fragmentation reactions of Xe isotopes at 1 A GeV on light targets

- **production and nuclear structure of n-rich species (actinides, Z=82, N=126)**

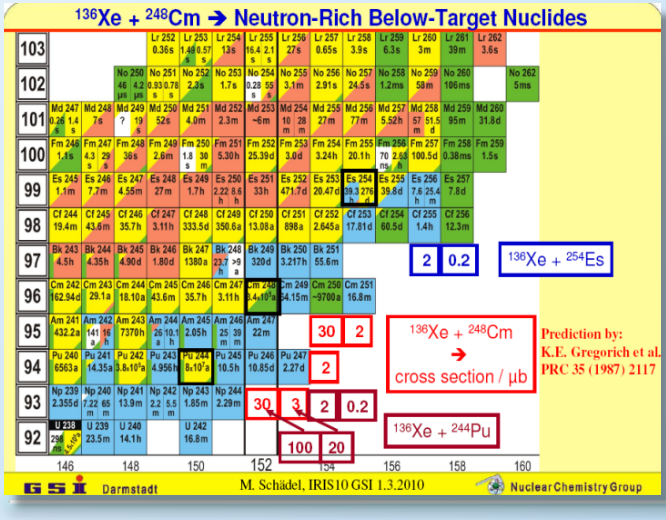

^{136}Xe + ^{248}Cm ➔ Neutron-Rich Below-Target Nuclides

	146		148		150		152		154		156		158		160
103				Lr 252 0.36s	Lr 253 1.49 s 0.57 s	Lr 254 13s	Lr 255 16.4 s 2.1 s	Lr 256 27s	Lr 257 0.65s	Lr 258 3.9s	Lr 259 6.3s	Lr 260 3m	Lr 261 39m	Lr 262 3.6s	
102			No 250 46 µs 4.2 µs	No 251 0.93 s 0.78 s	No 252 2.3s	No 253 1.7s	No 254 0.28 s 55 s	No 255 3.1m	No 256 2.91s	No 257 24.5s	No 258 1.2ms	No 259 58m	No 260 106ms		No 262 5ms
101	Md 247 0.26 s 1.4 s	Md 248 7s	Md 249 ? 19 s	Md 250 52s	Md 251 4.0m	Md 252 2.3m	Md 253 ~6m	Md 254 10 m 28 m	Md 255 27m	Md 256 77m	Md 257 5.52h	Md 258 57 m 51.5 d	Md 259 95m	Md 260 31.8d	
100	Fm 246 1.1s	Fm 247 4.3 s 29 s	Fm 248 36s	Fm 249 2.6m	Fm 250 1.8 s 30 m	Fm 251 5.30h	Fm 252 25.39d	Fm 253 3.0d	Fm 254 3.24h	Fm 255 20.1h	Fm 256 70 ns 2.63 h	Fm 257 100.5d	Fm 258 0.38ms	Fm 259 1.5s	
99	Es 245 1.1m	Es 246 7.7m	Es 247 4.55m	Es 248 27m	Es 249 1.7h	Es 250 2.22 h 8.6 h	Es 251 33h	Es 252 471.7d	Es 253 20.47d	Es 254 39.3 h 276 d	Es 255 39.8d	Es 256 7.6 h 25.4 m	Es 257 7.8d		
98	Cf 244 19.4m	Cf 245 43.6m	Cf 246 35.7h	Cf 247 3.11h	Cf 248 333.5d	Cf 249 350.6a	Cf 250 13.08a	Cf 251 898a	Cf 252 2.645a	Cf 253 17.81d	Cf 254 60.5d	Cf 255 1.4h	Cf 256 12.3m		
97	Bk 243 4.5h	Bk 244 4.35h	Bk 245 4.90d	Bk 246 1.80d	Bk 247 1380a	Bk 248 23.7 h >9 a	Bk 249 320d	Bk 250 3.217h	Bk 251 55.6m			2	0.2		
96	Cm 242 162.94d	Cm 243 29.1a	Cm 244 18.10a	Cm 245 43.6m	Cm 246 35.7h	Cm 247 3.11h	Cm 248 3.4×10^5a	Cm 249 64.15m	Cm 250 ~9700a	Cm 251 16.8m					
95	Am 241 432.2a	Am 242 141 a 16 h	Am 243 7370h	Am 244 26 a 10.1 h	Am 245 2.05h	Am 246 25 m 39 m	Am 247 22m		30	2					
94	Pu 240 6563a	Pu 241 14.35a	Pu 242 3.8×10^5a	Pu 243 4.956h	Pu 244 8×10^7a	Pu 245 10.5h	Pu 246 10.85d	Pu 247 2.27d	2						
93	Np 239 2.355d	Np 240 7.22 m 65 m	Np 241 13.9m	Np 242 2.2 m 5.5 m	Np 243 1.85m	Np 244 2.29m	30	3	2	0.2					
92	U 238 298 ns 4.5×10^9a	U 239 23.5m	U 240 14.1h		U 242 16.8m			100	20						

^{136}Xe + ^{254}Es

^{136}Xe + ^{248}Cm ➔ cross section / µb

^{136}Xe + ^{244}Pu

Prediction by: K.E. Gregorich et al. PRC 35 (1987) 2117

GSI Darmstadt M. Schädel, IRIS10 GSI 1.3.2010 Nuclear Chemistry Group

- **population of high-A/high-Z in the tail of the transfer mass distribution**

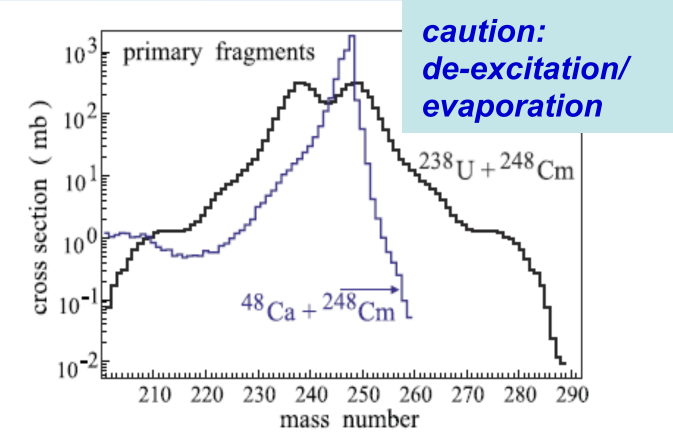

caution: de-excitation/ evaporation

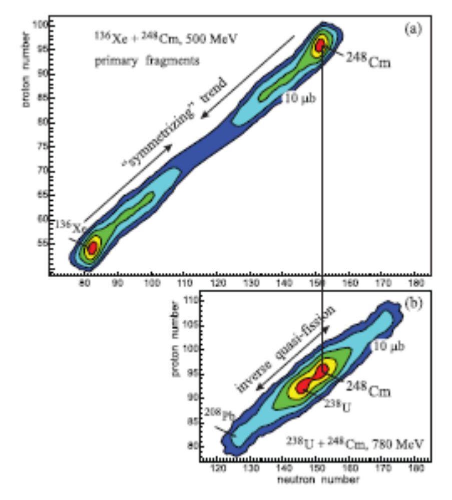

V.I. Zagrebaev and W. Greiner, Phys.Rev.C87 (2013) 034608

Fusion in astrophysics

- stellar nucleo-synthesis

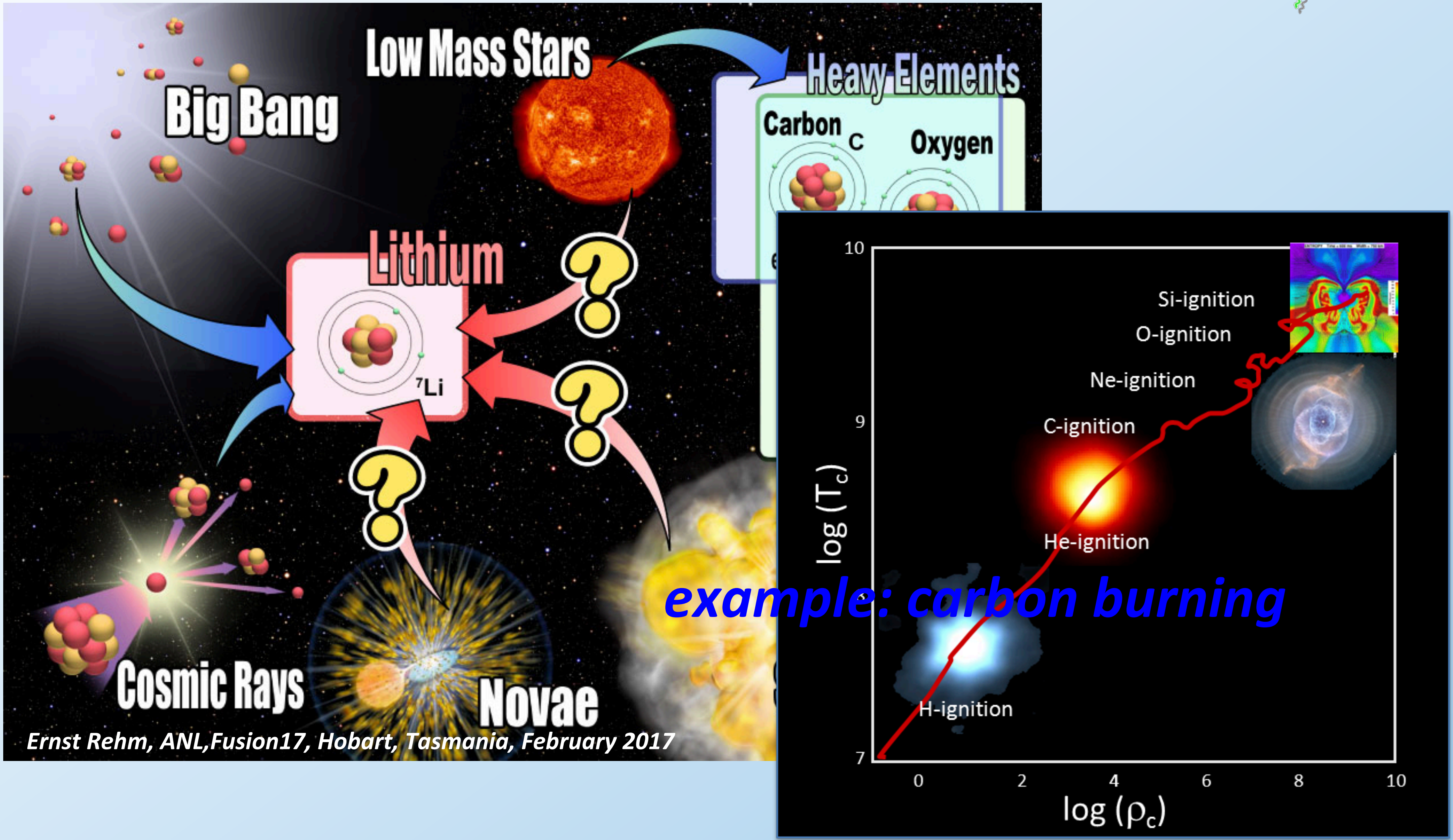

Ernst Rehm, ANL,Fusion17, Hobart, Tasmania, February 2017

example: carbon burning

Fusion in astrophysics

- stellar nucleo-synthesis

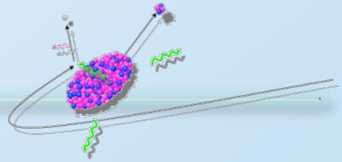

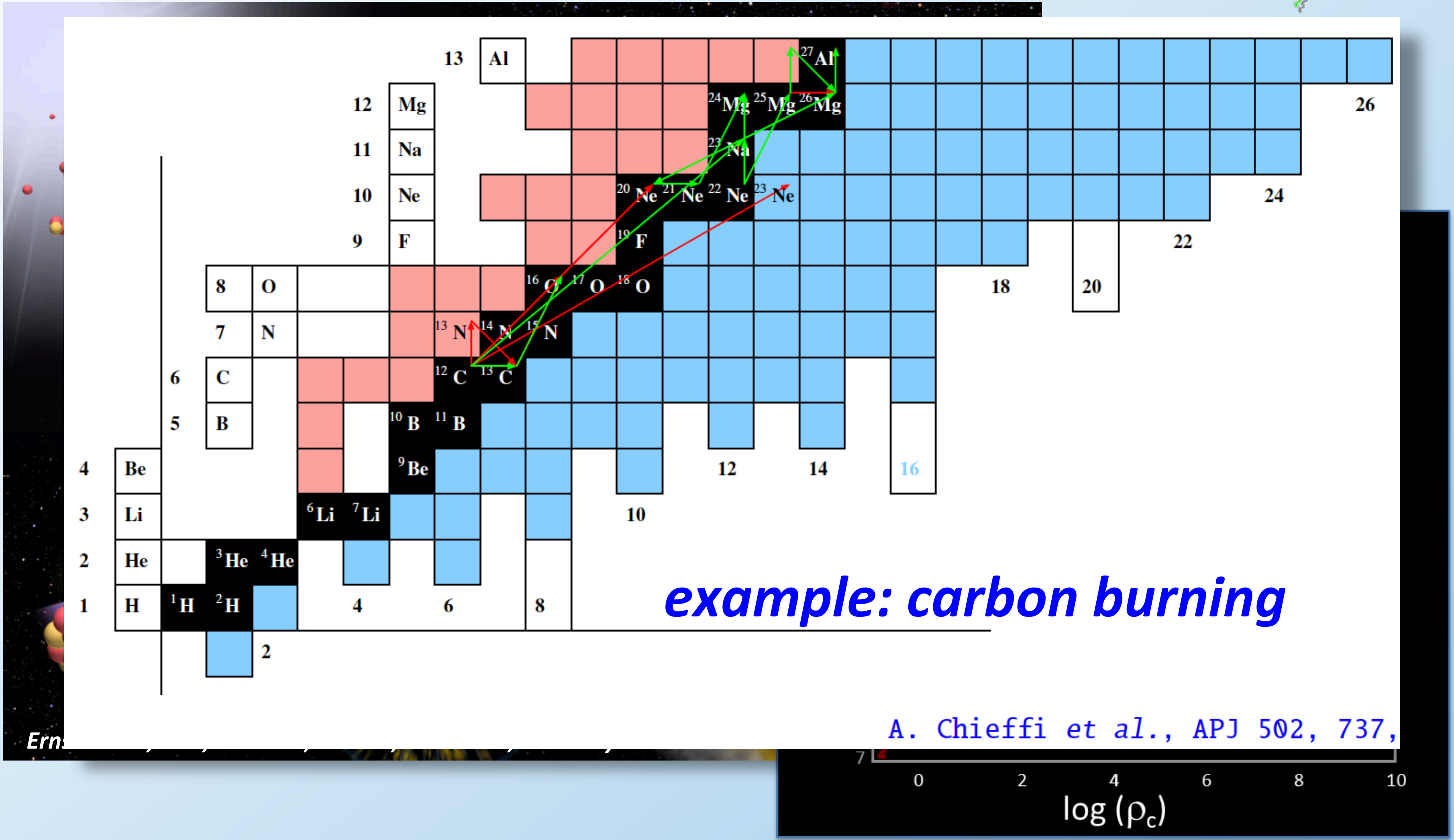

example: carbon burning

A. Chieffi *et al.*, APJ 502, 737,

Fusion in astrophysics

- fusion hindrance far below the barrier

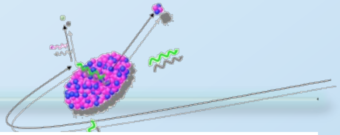

fusion cross section and the astrophysical S factor

$$\sigma(E) = \frac{1}{E} e^{-2\pi\eta} S(E)$$

Sommerfeld parameter $\eta = Z_1 Z_2 \frac{e^2}{\hbar\omega}$

$$S(E) = E\sigma(E)e^{2\pi\eta}$$

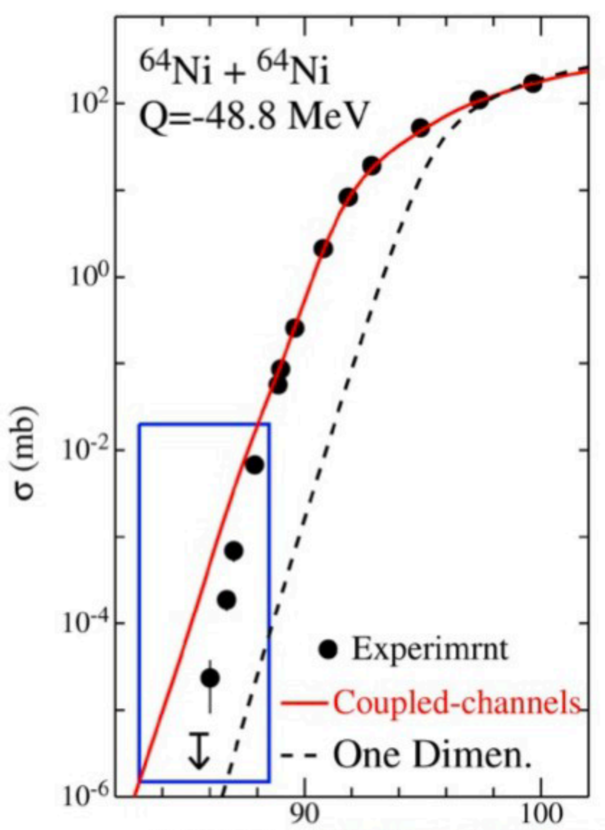

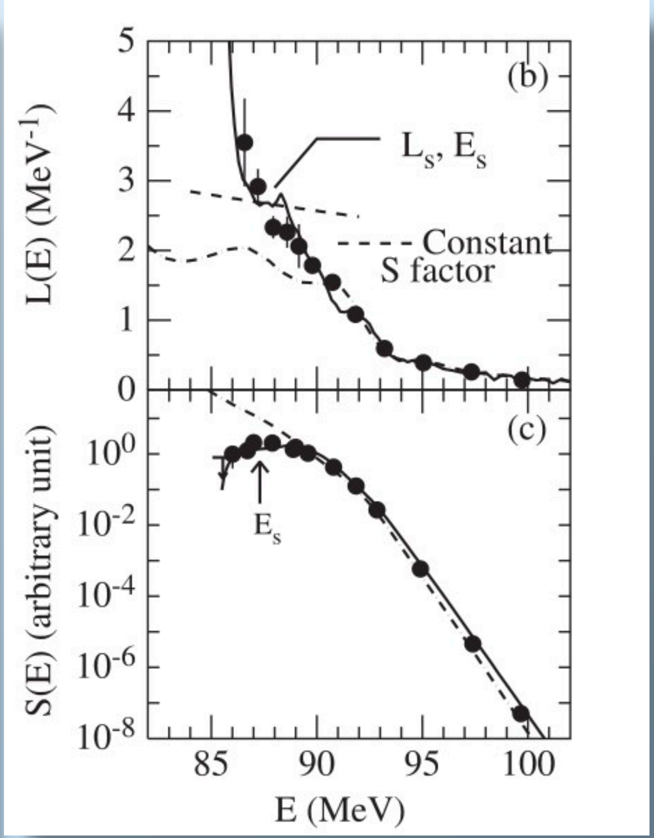

Logarithmic derivative for a constant S factor:

$$\frac{dS}{dE} = S\left[L - \frac{\pi\eta}{E}\right] = 0 \quad \Rightarrow \quad L_{CS}(E) = \frac{\pi\eta}{E}$$

Jiang, C. L., et al., 2004, Phys. Rev. Lett. 93, 012701

Fusion in astrophysics

- hindrance and reaction rates

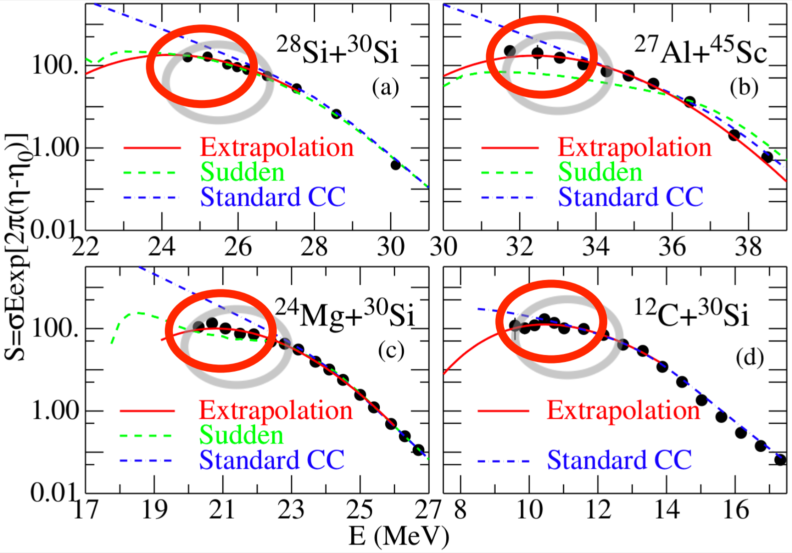

fusion cross section and the astrophysical S factor

$$\sigma(E) = \frac{1}{E} e^{-2\pi\eta} S(E)$$

Sommerfeld parameter

$$\eta = Z_1 Z_2 \frac{e^2}{\hbar\omega}$$

$$S(E) = E\sigma(E) e^{2\pi\eta}$$

systematics of max. S energy E_s

→ purely empirical!

... physics behind ?!

F. Galtarossa, Ph.D. - Univ. di Padova/LNL Legnaro

C.L. Jiang, et al., Phys. Rev. C 78, 017601 (2008).

C.L. Jiang, et al., Phys. Rev. C 81 024611, (2009).

C.L. Jiang, et al., Phys. Rev. Lett. 113 022701 (2014).

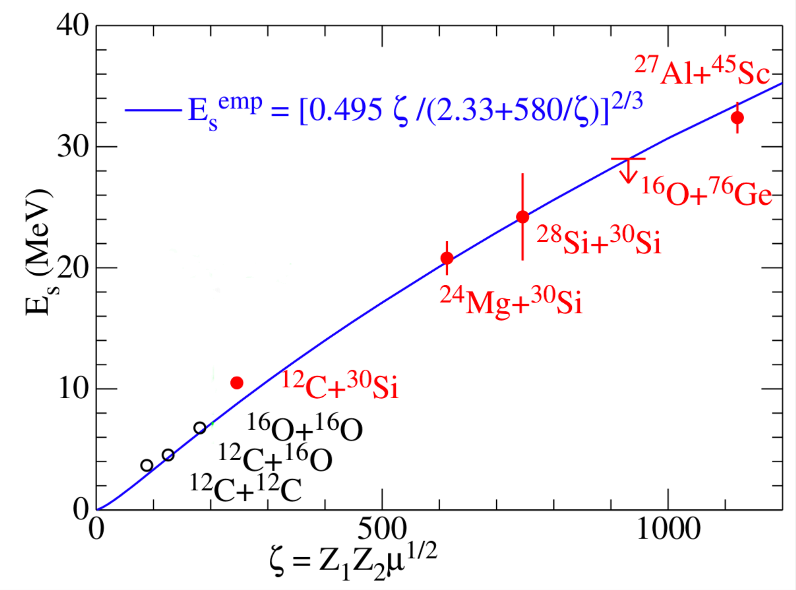

Competition between different decay modes

- partial decay times → global decay times

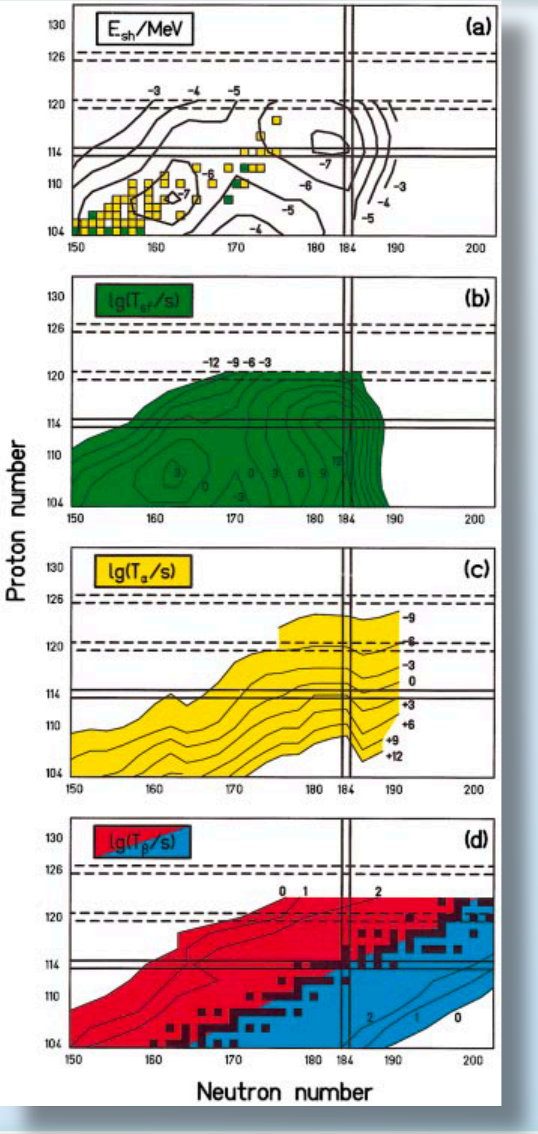

The predicted values (microscopic/macroscopic model Approach) in (a), (b), and (c) are from Smolanczuk and Sobiczewski (1995a, 1995b) and Smolanczuk (1997, 1998), and in (d) from Mö ller et al. (1995a, 1995b)

References in:

S. Hofmann and G. Münzenberg, Reviews of Modern Physics, Vol. 72, No. 3, July 2000

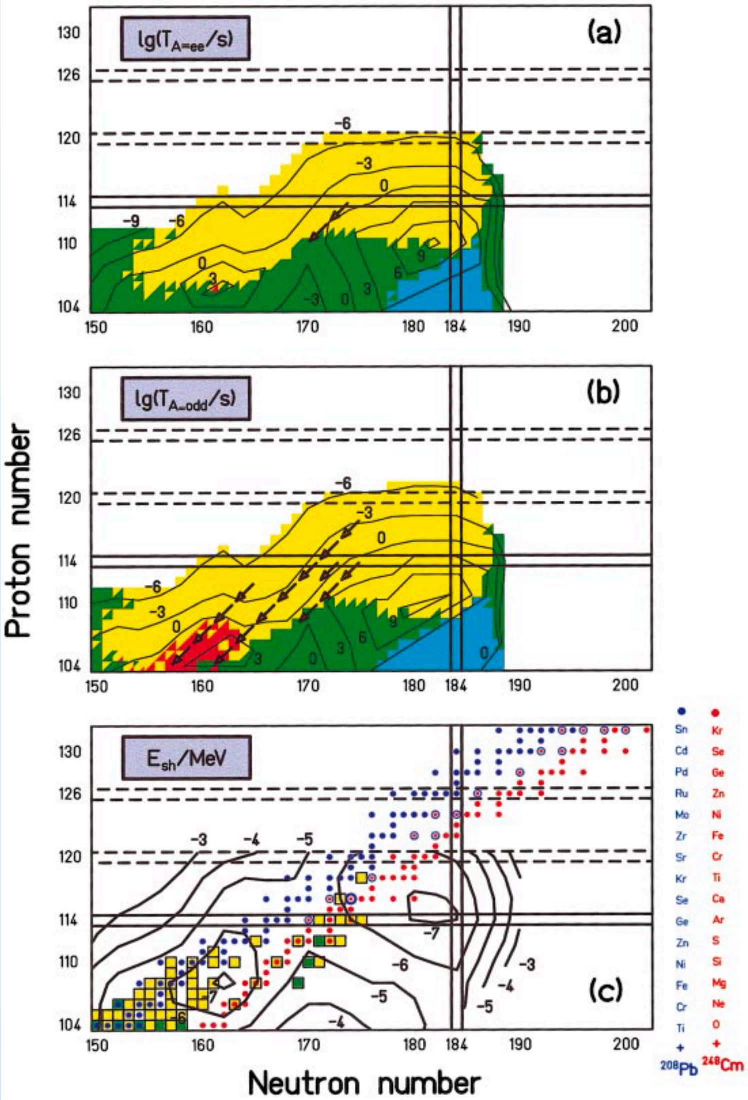

Literature

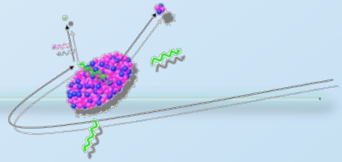

Books:

Nuclear Reactions With Heavy Ions,
R. Bass, Springer-Verlag, Berlin-Heidelberg-New York 1980

The Elements beyond Uranium
G.T. Seaborg and W.D. Loveland, John Wiley and Sons Inc., New York 1990

On beyond Uranium
Sigurd Hofmann, Science Spectra Book Series, Taylor & Francis, London/New York, 2002

The Chemistry of Superheavy Elements
Matthias Schädel, Kluwer Academic Publishers, Dorrecht, Boston

Review papers:

Recent developments in heavy-ion fusion reactions
B. B. Back,* H. Esbensen, C. L. Jiang, and K. E. Rehm,Rev. Mod. Phys 86 (2014) 317

Multinucleon transfer processes in heavy-ion reactions
L. Corradi, G. Pollarolo and S. Szilner, J. of Phys. G 36, 113101 (2009)

Nuclear structure features of very heavy and superheavy nuclei—tracing quantum mechanics towards the 'island of stability'
D. Ackermann and Ch. Theisen, Phys. Scr. 92 (2017) 083002

Take home questions lecture 1

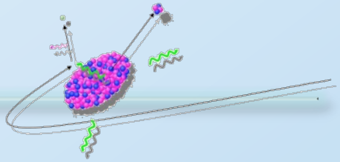

Lecture 1 – Reaction mechanism and SHE production

- Components of the potential in heavy ion collisions
- How does a prolate deformation influence the subbarrier fusion cross section?
- What is the equivalent to the barrier distribution in the partial wave picture?
- How are the magic numbers generated by nature?
- What governs the production of heavy nuclei?
- Which two types of models are used to describe heavy nuclei and what are the main features?